JOURNAL OF MATHEMATICAL SCIENCES AND MODELLING

ISSN: 2636-8692

VOLUME IV
ISSUE I

VOLUME IV ISSUE I
ISSN 2636-8692

April 2021
http://dergipark.gov.tr/jmsm

JOURNAL OF MATHEMATICAL SCIENCES AND MODELLING

Editors

Editorial Board of Journal of Mathematical Sciences and Modelling

Contents

Journal of Mathematical Sciences and Modelling, 4 (1) (2021) 1-6
Research Article

Journal of Mathematical Sciences and Modelling

Journal Homepage: www.dergipark.gov.tr/jmsm
ISSN 2636-8692
DOI: http://dx.doi.org/10.33187/jmsm.815125

Kinematics of Supination and Pronation with Stewart Platform

Bülent Karakaş[1] and Şenay Baydaş[2*]

[1]*Department of Business Administration, Faculty of Economics and Administrative Science, Van Yuzuncu Yil University, Van, Turkey*
[2]*Department of Mathematics, Faculty of Science, Van Yuzuncu Yil University, Van, Turkey*
[*]*Corresponding author*

Article Info

Keywords: *Artificial intelligence, Kinematics, Modelling, Pronation, Stewart platform, Supination.*
2010 AMS: *53A04, 53A17, 57R25.*
Received: *22 October 2020*
Accepted: *12 March 2021*
Available online: *30 April 2021*

Abstract

This paper presents kinematics form of pronation and supination movement. The algorithm of Stewart platform motion can be used to create a new motion of supination (or pronation) motion. Pronation motion can be taken as Stewart motion which has not any rotation on x-axis and y-axis. In this case, pronation motion has only one parameter. Supination movement creates a helix curve. Additionally, the correlation between rotation angle and extension is 1. This allows us to use artificial intelligence in pronation motion. In this article, the algorithm and Matlab applications of pronation motion are given in the concepts of artificial intelligence approach. This is a new and important approach.

1. Stewart platform

A Stewart platform is called a form of manipulator with six degrees of freedom, which allows one to provide a given position and orientation of the surface in the vicinity of any point of the platform on its three cartesian coordinates and projections of the unit normal vector [1]. A mathematical model of the mechanism of movement of an undeformed platform with six degrees of freedom is proposed [2].
The Stewart platform consists of two rigid frames connected by 6 variable length legs. The base is considered to be the reference frame work, with orthogonal axes x, y, z. The platform has 6 degrees of freedom with respect to the base. The origin of the platform coordinates can be defined by 3 translational displacements with respect to the base, one for each axis [3, 4].
Three angular displacements then define the orientation of the platform with respect to the base. A set of Euler angles is used in the following sequence:
1. Rotate an angle ψ (yaw) around the z-axis,
2. Rotate an angle θ(pitch) around the y-axis,
3. Rotate an angle φ (roll) around the x-axis.

$$P = i'x' + j'y' + k'z' = ix + jy + kz$$

$$\begin{aligned} x &= OA - BC = x'\cos\psi - y'\sin\psi \\ y &= AB + PC = x'\sin\psi + y'\cos\psi \\ z &= z' \end{aligned}$$

(Figure 1.1). The rotation matrix of the platform relative to the base is given by

$$\begin{aligned} {}^{P}R_{B} &= R_z(\psi)R_y(\theta)R_x(\varphi) \\ &= \begin{bmatrix} \cos\psi & -\sin\psi & 0 \\ \sin\psi & \cos\psi & 0 \\ 0 & 0 & 1 \end{bmatrix} \begin{bmatrix} \cos\theta & 0 & \sin\theta \\ 0 & 1 & 0 \\ -\sin\theta & 0 & \cos\theta \end{bmatrix} \begin{bmatrix} 1 & 0 & 0 \\ 0 & \cos\varphi & -\sin\varphi \\ 0 & \sin\varphi & \cos\varphi \end{bmatrix} \\ &= \begin{bmatrix} \cos\theta\cos\psi & -\cos\varphi\sin\psi + \sin\theta\cos\psi\sin\varphi & \sin\psi\sin\varphi + \sin\theta\cos\psi\cos\varphi \\ \cos\theta\sin\psi & \cos\psi\cos\varphi + \sin\theta\sin\psi\sin\varphi & -\cos\psi\sin\varphi + \sin\theta\cos\varphi\sin\psi \\ -\sin\theta & \cos\theta\sin\varphi & \cos\theta\cos\varphi \end{bmatrix} \end{aligned}$$

Email addresses and ORCID numbers: bulentkarakas@gmail.com, 0000-0002-3915-6526 (B. Karakaş), sbaydas@yyu.edu.tr, 0000-0002-1026-9471 (Ş. Baydaş)

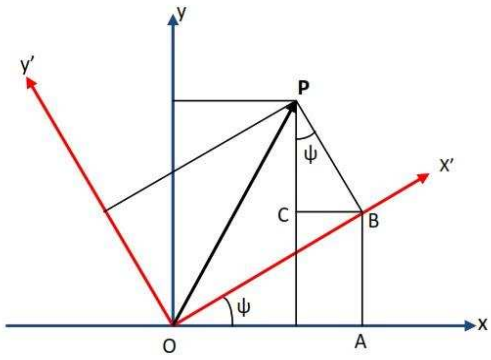

Figure 1.1: Rotation around z-axis

[5, 6]. Now consider a Stewart platform. For the $i-th$ leg (Figure 1.2):

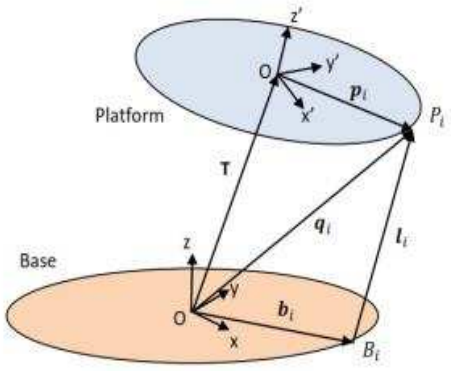

Figure 1.2: Stewart platform

The coordinates q_i of the anchor point with respect to the base reference framework are given by the equation

$$q_i = T + {}^{P}R_B.p_i, i = 1,2,3$$

where T is the translation vector, giving the positional linear displacement of the origin of the platform frame with respect to the base reference framework, and p_i is the vector defining the coordinates of the anchor point p_i with respect to the platform framework.
Similarly the length of the $i-th$ leg is given by

$$l_i = T + {}^{P}R_B.p_i - b_i, i = 1,2,3$$

where b_i is the vector defining the coordinates of the lower anchor point B_i. These 6 equations give the lengths of the 6 legs to achieve the desired position and attitude of the platform.

2. Pronation motion in the concepts of artificial intelligence approach

In kinematics applications, axis, points, orbits are main and important. Especially orbits of points are important and informative. For example, if the orbit of a point under a displacement is on the sphere with radius r and center P, then the displacement is a rotation with pole point P. If the orbits of every points under the displacement is on the perpendicular circular cylinder then the displacement is a rotation with translation. Stewart platform can make rotation, translation or rotation with translation. Let S be a cylinder in Figure 2.1.
Bottom cover is fixed platform, and top cover is moving platform. Every point moves during the movement, and movement is rotation with translation.
Supination and pronation motions can be considered inverse motion each other [7, 8, 9]. So we study only one of them in this study as modelling. Main structure of the model is as follows.
1. The forearm is considered as a cylinder or cone. We consider cylinder.
2. The planes at the elbow and wrist are considered as fixed and moving planes of Stewart platform. The elbow plane is fixed and wrist plane is moving plane.
3. Suppose that the forearm is the cylinder (Figure 2.1).
In (Figure 2.2), L line part is

$$L : (r, 0, z)$$

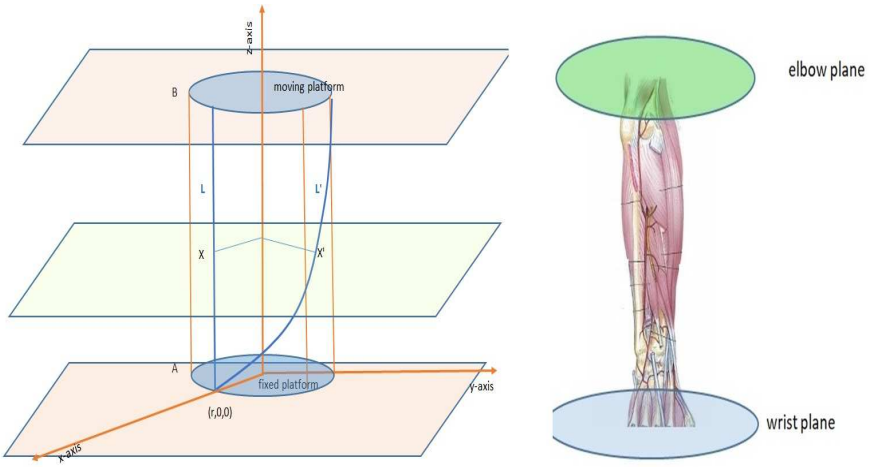

Figure 2.1: Elbow and wrist plane

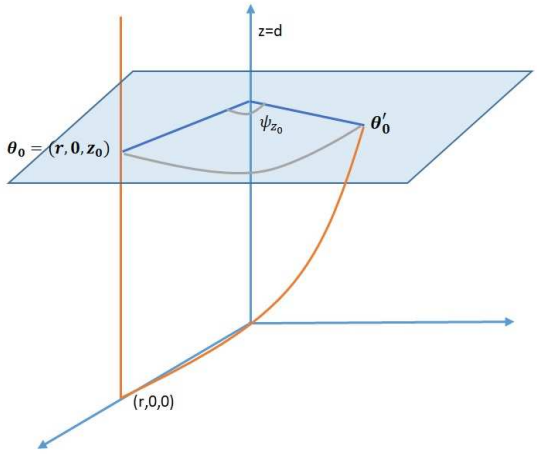

Figure 2.2: $\psi(z_0)$ rotating angle

$a < z < b$, $a, b \in \mathbb{R}$. As a Stewart platform, the matrix of displacement is

$$T + R_z(\psi)R_y(\theta)R_x(\varphi).$$

There are not rotation around $x-$axis and $y-$axis because fixed and moving platforms are parallel to each other. So, displacement matrix in this case is

$$T + R_z(\psi).$$

Translation part of displacement, in case of pronation motion, must be evaluated in pronation. Rotation angle is limited ψ_0 and ψ_e, $\psi_0 \leq \psi_z \leq \psi_e$ where $\psi_0 = 0$ and ψ_e is final value.
At the $z = z_0$ rotation plane, rotation angle is

$$\psi_{z_0} = \frac{z_0}{L}\psi_e.$$

So, P_m pronation rotation matrix is given as follows

$$P_m = \begin{bmatrix} \cos\psi_z & -\sin\psi_z & 0 \\ \sin\psi_z & \cos\psi_z & 0 \\ 0 & 0 & 1 \end{bmatrix}. \tag{2.1}$$

Let X be a representative point of the line d, $d = \{(x_0, y_0, z) \mid 0 \leq z \leq z_e\}$, then we have

$$\alpha(z) = P_m X = \begin{bmatrix} \cos\psi_z & -\sin\psi_z & 0 \\ \sin\psi_z & \cos\psi_z & 0 \\ 0 & 0 & 1 \end{bmatrix} \begin{bmatrix} x_0 \\ y_0 \\ z \end{bmatrix}, \quad X = (x_0, y_0, z), \quad x_0^2 + y_0^2 = r^2$$

and

$$\alpha(z) = (x_0\cos\psi_z - y_0\sin\psi_z, x_0\sin\psi_z + y_0\cos\psi_z, z). \tag{2.2}$$

3. Properties of the motion

We will give some theorems about the motion using the equations (2.1) and (2.2).

Theorem 3.1. *$\alpha(z) = P_m(d)$ is a helix.*

Proof.

$$\begin{aligned}
\alpha(z) &= (x_0\cos\psi_z - y_0\sin\psi_z, x_0\sin\psi_z + y_0\cos\psi_z, z)\\
\alpha'(z) &= (-\lambda x_0\sin\psi_z - \lambda y_0\cos\psi_z, \lambda x_0\cos\psi_z - \lambda y_0\sin\psi_z, 1)\\
\alpha''(z) &= (-\lambda^2 x_0\cos\psi_z + \lambda^2 y_0\sin\psi_z, -\lambda^2 x_0\sin\psi_z - \lambda^2 y_0\cos\psi_z, 0)
\end{aligned}$$

$$\begin{aligned}
\|\alpha'(z)\| &= \lambda^2 x_0^2\sin^2\psi_z + \lambda^2 y_0^2\cos^2\psi_z + 2\lambda^2 x_0 y_0\sin\psi_z\cos\psi_z\\
&\quad +\lambda^2 x_0^2\cos^2\psi_z + \lambda^2 y_0^2\sin^2\psi_z - 2\lambda^2 x_0 y_0\sin\psi_z\cos\psi_z + 1)\\
&= \sqrt{\lambda^2 x_0^2\sin^2\psi_z + \lambda^2 x_0^2\cos^2\psi_z + \lambda^2 y_0^2\cos^2\psi_z + \lambda^2 y_0^2\sin^2\psi_z + 1}\\
&= \sqrt{\lambda^2 x_0^2 + \lambda^2 y_0^2 + 1}\\
&= \sqrt{\lambda^2 r^2 + 1}.
\end{aligned}$$

Let $k = \sqrt{\lambda^2 r^2 + 1}$, $\lambda = \frac{\psi_e}{L}$, so we have Frenet vectors as follows.

$$\begin{aligned}
\overrightarrow{t}(z) &= \frac{1}{k}(-\lambda x_0\sin\psi_z - \lambda y_0\cos\psi_z, \lambda x_0\cos\psi_z - \lambda y_0\sin\psi_z, 1)\\
\overrightarrow{n}(z) &= \frac{1}{\lambda^2 r}(-\lambda^2 x_0\cos\psi_z + \lambda^2 y_0\sin\psi_z, -\lambda^2 x_0\sin\psi_z - \lambda^2 y_0\cos\psi_z, 0)\\
&= \frac{1}{r}(-x_0\cos\psi_z + y_0\sin\psi_z, -x_0\sin\psi_z - y_0\cos\psi_z, 0)\\
\overrightarrow{b}(z) &= (\frac{1}{k}(x_0\sin\psi_z + y_0\cos\psi_z), \frac{1}{k}(-x_0\cos\psi_z + y_0\sin\psi_z), \frac{\lambda r}{k})\\
&= (\frac{x_0}{k}\sin\psi_z + \frac{y_0}{k}\cos\psi_z, \frac{-x_0}{k}\cos\psi_z + \frac{y_0}{k}\sin\psi_z, \frac{\lambda r}{k}).
\end{aligned}$$

The first and second curvature of $\alpha(z)$ are

$$\begin{aligned}
\kappa &= \|\alpha''(z)\| = \lambda^2 r = (\frac{\psi_e}{L})^2 r,\\
\tau &= \|b'(z)\| = \frac{\lambda r}{k} = \frac{\psi_e r}{Lk}.
\end{aligned}$$

Therefore,

$$\frac{\kappa}{\tau} = \frac{\psi_e k}{L}$$

is fixed. Hence, $\alpha(z)$ is a helix. □

Theorem 3.2. *Let X be series of z, and Y be series of the length of the curve $\alpha(z)$. Then correlation between X and Y is equal to 1.*

Proof.

$$\alpha(z) = (x_0\cos\psi_z - y_0\sin\psi_z, x_0\sin\psi_z + y_0\cos\psi_z, z)$$

is the picture of X.

$$\alpha'(z) = (-\lambda x_0\sin\psi_z - \lambda y_0\cos\psi_z, \lambda x_0\cos\psi_z - \lambda y_0\sin\psi_z, 1)$$

and we calculate $\|\alpha'(z)\|$ as

$$\|\alpha'(z)\| = \sqrt{\lambda^2 r^2 + 1}, \quad \lambda = \frac{\psi_e}{L}.$$

Then every point at z_0, we have

$$L_{z_0} = \int_0^{z_0}\sqrt{\lambda^2 r^2 + 1}dz = \sqrt{\lambda^2 r^2 + 1}z_0.$$

In this case, the series X and Y are written.

$$\begin{aligned}
X &= \{0, 0.1, ..., Z_e\},\\
Y &= \{0, ..., \varphi_e\},
\end{aligned}$$

where Z_e is the last value of z and φ_e is the last rotation angle. For every x_i, we have $y_i = \sqrt{\lambda^2 r^2 + 1}x_i$, $\sqrt{\lambda^2 r^2 + 1} = c, c > 0$.
We know that correlation of the series X and Y is given by

$$cor(X,Y) = \frac{n\sum x_i y_i - (\sum x_i)(\sum y_i)}{\sqrt{n\sum x_i^2 - (\sum x_i)^2}\sqrt{n\sum y_i^2 - (\sum y_i)^2}}.$$

For our series, we have

$$\begin{aligned} cor(X,Y) &= = \frac{n\sum x_i(cx_i) - (\sum x_i)(\sum cx_i)}{\sqrt{n\sum x_i^2 - (\sum x_i)^2}\sqrt{n\sum (cx_i)^2 - (\sum cx_i)^2}} \\ &= \frac{c(n\sum x_i^2 - (\sum x_i)^2)}{c\sqrt{n\sum x_i^2 - (\sum x_i)^2}\sqrt{n\sum {x_i}^2 - (\sum x_i)^2}} \\ &= 1. \end{aligned}$$

□

4. Application

Example 4.1. *Let $L = 20cm$, $r = 3cm$, $\psi_e = \frac{\pi}{3}$, step= 0.5. Then we have the series X and Y.*
$X = \{$ 0.5, 1, 1.5, 2, 2.5, 3, 3.5, 4, 4.5, 5, 5.5, 6, 6.5, ..., 19, 19.5, 20 $\}$
$Y = \{$ 0.50615, 1.0123, 1.51845, ..., 18.2214, 18.72755, 19.2337, 19.73985, 20.246 $\}$
Thus, we have $cor(X,Y) = 1$.

Matlab programme m-file and (Figure 4.1) of this example are as follows.

```
cc=5
grid on
axis([-cc cc -cc cc 0 4*cc])
xlabel('x axis'); ylabel('y axis'); zlabel('z axis')
line([2 2],[0 0],[0 20],'LineWidth',4,'color',[.2 .2 .5]);
line([0 0 ],[2 2 ],[0 20],'LineWidth',4,'color',[.2 .3 .5]);
line([-2 -2],[0 0],[0 20],'LineWidth',4,'color',[.2 .4 .5])
L=20
for z=0:0.1:20
d=(pi/3)/20
r=3
c=((r^2*d^2+1))^(1/2)
u=((pi/3)/L)*z
A=[ cos(u) sin(u) 0
-sin(u) cos(u) 0
0 0 1]
P=[2 ; 0; z]
Q=[0 ;2; z]
D=[-2 ; 0; z]
E=A*Q
B=A*P
C=A*D
hold on
plot3(C(1),C(2),C(3),'.r')
plot3(B(1),B(2),B(3),'.r')
plot3(E(1),E(2),E(3),'.r')
pause(0.01)
end
hold on
text(2+0.5,0, 0, 'P')
text(2,0,21,'Q')
for t=0:1:360
r=2
plot3(r*cosd(t), r*sind(t), 0,'.r')
plot3(r*cosd(t), r*sind(t), 20,'.r')
end
```

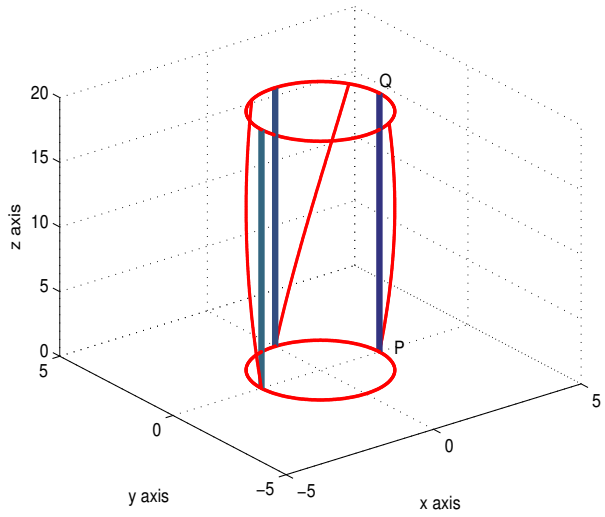

Figure 4.1: Orbits of points

5. Conclusion

We can use the algorithm of Stewart platform motion to create a new motion of supination(or pronation) motion. Supination and pronation motions are inverse motion to each other. So it is sufficient study only one of them. Pronation motion can be taken as Stewart motion which no rotation on x-axis and y-axis. In this case pronation motion has only one parameter. Translation part of pronation motion is uploaded the moving points. We give a relation between rotation angle and third component of moving platform which first and second components are fixed. The Frenet elements of the curve of the motion are calculated. We prove that the image curve is a helix. The correlation between rotation angle and extension of the image curve is exactly equal to 1.

Acknowledgement

This work was supported by YYU BAP (Scientific Research Projects of Van Yuzuncu Yil University) with project number: FBA-2017-5435.

References

[1] D. Stewart, *A platform with six degrees of freedom*, UK Inst. Mech. Eng. Proc., **180**(15) (1965), 371-386.
[2] Y.A. Alyushin, S.A. Elenev, *Mathematical model of Stewart platform motion*, J. Mach. Manuf. Reliab., **39**(4) (2010), 305-312.
[3] G. Zhang, *Classification of direct kinematics to planar generalized Stewart platforms*, Comput. Geom., **45**(8) (2012), 458-473.
[4] S. Zhibin, M. Tianyu, N. Chao, N. Yijun, *A new skeleton model and the motion rhythm analysis for human shoulder complex oriented to rehabilitation robotics*, Appl. Bionics Biomechanics, (2018), Article ID 2719631, 15 pages.
[5] O. Bottema, B. Roth, *Theoretical Kinematics*, Dover Publications, New York, 1990.
[6] J.M. McCarthy, *Geometric Design of Linkages*, Springer Verlag, New York, 2000.
[7] E. Kreighbaum, K.M. Barthels, *Biomechanics*, Allyn and Bacon, Boston, 1996.
[8] E.Y.K. Ng, H.S. Borovetz, E. Soudah, Z. Sun, *Numerical methods and applications in biomechanical modeling*, Comput. Math. Methods Med., (2013), Article ID 727830, 2 pages.
[9] Y.C. Strauch, *Atlas of Hand Anatomy and Clinical Implications*, Mosby an Affiliate of Elsevier, China, 2004.

Journal of Mathematical Sciences and Modelling, 4 (1) (2021) 7-18
Research Article

Journal of Mathematical Sciences and Modelling

Journal Homepage: www.dergipark.gov.tr/jmsm
ISSN 2636-8692
DOI: http://dx.doi.org/10.33187/jmsm.869698

A New Moving Frame for Trajectories with Non-Vanishing Angular Momentum

Kahraman Esen Özen[1*] **and Murat Tosun**[2]

[1]*Sakarya, Turkey*
[2]*Department of Mathematics, Faculty of Science and Arts, Sakarya University, Sakarya, Turkey*
[*]*Corresponding author*

Article Info

Keywords: *Angular momentum, Kinematics of a particle, Moving frame, Plane and space curves, Slant helices.*
2010 AMS: *70B99, 14H50.*
Received: *20 January 2021*
Accepted: *26 March 2021*
Available online: *30 April 2021*

Abstract

The theory of curves has a very long history. Moving frames defined on curves are important parts of this theory. They have never lost their importance. A point particle of constant mass moving along a trajectory in space may be seen as a point of the trajectory. Therefore, there is a very close relationship between the differential geometry of the trajectory and the kinematics of the particle moving on it. One of the most important elements of the particle kinematics is the jerk vector of the moving particle. Recently, a new resolution of the jerk vector, along the tangential direction and two special radial directions, has been presented by Özen et al. (JTAM 57(2)(2019)). By means of these two special radial directions, we introduce a new moving frame for the trajectory of a moving particle with non vanishing angular momentum in this study. Then, according to this frame, some characterizations for the trajectory to be a rectifying curve, an osculating curve, a normal curve, a planar curve and a general helix are given. Also, slant helical trajectories are defined with respect to this frame. Afterwards, the necessary and sufficient conditions for the trajectory to be a slant helical trajectory (according to this frame) are obtained and some special cases of these trajectories are investigated. Moreover, we provide an illustrative numerical example to explain how this frame is constructed. This frame is a new contribution to the field and it may be useful in some specific applications of differential geometry, kinematics and robotics in the future.

1. Introduction and preliminaries

In differential geometry, the local theory of space curves plays an important role. The discovery of the Serret-Frenet formulas in 1847 was a milestone for the researchers who are interested in this theory. Despite its long history, it is still an issue of interest. The moving frames adapted to curves are useful tools for investigating this theory. From the discovery of the Serret-Frenet frame until now, many researchers have presented lots of interesting studies on this theory by using Serret-Frenet frame. Some of these studies can be found in [1]-[6].

From past to present, many researchers have developed new moving frames which have a common base vector with the Serret-Frenet frame. For example R. L. Bishop introduced parallel transport frame (or Bishop frame) in 1975 [7]. The first base vector of Serret-Frenet frame is included by this frame. A similar study was carried out by Yılmaz and Turgut in 2010 by using the third base vector of the Serret-Frenet frame [8]. The authors called this frame as Type-2 Bishop frame. In 2019, a new version of Bishop frame was introduced by inspiring from these studies and by taking into consideration the second base vector of Serret-Frenet frame [9]. This frame is called Type-3 Bishop frame. There can be found many interesting studies such as [7]-[13] on various moving frames in the literature.

In Euclidean 3-space, a moving point particle of constant mass has a position vector according to the moving frame we are working on. By this way, any point on the trajectory can be represented by this particle. So, there is a very close relationship between the kinematics of a moving particle and the differential geometry of the trajectory which is the oriented curve traced out by this particle. As a result of this

***Email addresses and ORCID numbers*: kahraman.ozen1@ogr.sakarya.edu.tr, 0000-0002-3299-6709 (K. E. Özen), tosun@sakarya.edu.tr, 0000-0002-4888-1412 (M. Tosun)**

case, moving frames have been used as very useful tools to investigate the concepts on the kinematics of a moving particle such as position, velocity, acceleration and jerk vectors. Kinematics equations are used to determine the motion and to reach a desired position in robotics. To obtain an equation which includes all the position, velocity, acceleration and jerk, and to give the relationship between them provides various advantages for investigating some concepts in robotics such as minimum jerk trajectory generation. These facts and the importance of the position vector have motivated us in the process of preparing this study. We have constructed a new moving frame for the trajectories having non-vanishing angular momentum by using the own position vector of the moving particle. We expect that for the researchers studying on modern robotics, this moving frame will enable more convenient observation environment to understand the relationships between the basic concepts of kinematics and the basic concepts of inverse kinematics in the future.
Let us take into consideration the $3-$dimensional Euclidean space E^3 with the standard inner product:

$$\langle \mathbf{K}, \mathbf{L} \rangle = k_1 l_1 + k_2 l_2 + k_3 l_3 \tag{1.1}$$

where $\mathbf{K} = (k_1\,,\, k_2\,,\, k_3)\,,\ \mathbf{L} = (l_1\,,\, l_2\,,\, l_3)$ are arbitrary vectors in this space. The norm of the vector $\mathbf{K}$ is expressed as $\|\mathbf{K}\| = \sqrt{\langle \mathbf{K}, \mathbf{K} \rangle}$. If a differentiable curve $\chi = \chi(s) : I \subset \mathbb{R} \to E^3$ satisfies the equality $\left\| \frac{d\chi}{ds} \right\| = 1$ for all $s \in I$, this curve is said to be a unit speed curve. In that case, s is said to be arc-length parameter of this curve. A differentiable curve is called regular curve if its derivative is nonzero along the curve. Any regular curve can be reparameterized by the arc-length [14]. In the rest of this section, curves will be supposed to be regular and unit speed. Another thing that can be of importance is that the differentiation with respect to the arc-length parameter s will be denoted by a dash throughout the present study.

It is well known that the unit tangent vector $\mathbf{T} = \delta'$ of a given curve δ is determined uniquely. When the tangential components of two moving frames are common, these frames are called as equivalent frames. For example, Serret-Frenet frame and Bishop frame are equivalent frames.

Let $\{\mathbf{T}, \mathbf{N_1}, \mathbf{N_2}\}$ be a moving frame of a space curve which includes the unit tangent vector $\mathbf{T}$ and two normal unit vectors $\mathbf{N_1}$, $\mathbf{N_2}$. These three vectors together form a positively oriented orthonormal basis of the $3-$dimensional Euclidean space E^3 attached to each point of the curve. Because of the orthonormality, the matrix form of derivative formulas are given as in the following:

$$\begin{pmatrix} \mathbf{T}' \\ \mathbf{N_1}' \\ \mathbf{N_2}' \end{pmatrix} = \begin{pmatrix} 0 & k_1 & k_2 \\ -k_1 & 0 & k_3 \\ -k_2 & -k_3 & 0 \end{pmatrix} \begin{pmatrix} \mathbf{T} \\ \mathbf{N_1} \\ \mathbf{N_2} \end{pmatrix} \tag{1.2}$$

where k_1, k_2, and k_3 are continuous coefficient functions. These coefficient functions are sufficient to characterize the geometry of the curve [15].

For the Serret-Frenet frame $k_2 = 0$. Also, $\mathbf{N_1}, \mathbf{N_2}, k_1$ and k_3 are commonly denoted by $\mathbf{N}, \mathbf{B}, \kappa$ and τ, respectively. So, the derivative formulas take the following form:

$$\begin{pmatrix} \mathbf{T}' \\ \mathbf{N}' \\ \mathbf{B}' \end{pmatrix} = \begin{pmatrix} 0 & \kappa & 0 \\ -\kappa & 0 & \tau \\ 0 & -\tau & 0 \end{pmatrix} \begin{pmatrix} \mathbf{T} \\ \mathbf{N} \\ \mathbf{B} \end{pmatrix}. \tag{1.3}$$

Here, the vector $\mathbf{N} = \frac{\delta''}{\|\delta''\|}$ and $\mathbf{B} = \mathbf{T} \wedge \mathbf{N}$ are specially called as principal normal vector and binormal vector of the given curve δ, respectively. Also, the function $\kappa = \langle \mathbf{T}', \mathbf{N} \rangle$ is called as the curvature function, while the function $\tau = -\langle \mathbf{B}', \mathbf{N} \rangle$ is called as the torsion function [14]. In the rest of the study, we assume everywhere $\kappa \neq 0$.

This article is organized as follows. In Section 2, we explain how our frame is constructed and give the relation matrix between this frame and Serret-Frenet frame. Then, we obtain derivative formulas and complete the set of apparatus of this frame. Also, an illustrative example is given and the angular velocity vector is obtained for this frame. In Section 3, we obtain some necessary and sufficient conditions for the trajectory to be a rectifying curve, an osculating curve, a normal curve, a planar curve and a general helix. In Section 4, we define slant helical trajectories according to this frame. Then we give a characterization for these trajectories and investigate some special cases of these trajectories.

2. Positional adapted frame

Let us take into consideration a moving point particle of constant mass m in space E^3. Choose an arbitrary fixed origin O in space and denote by $\mathbf{x}$ the position vector of this particle at time t. Let the curve $\alpha = \alpha(s)$ be the unit speed parametrization of the trajectory of the particle where the arc-length s of α corresponds to time t. Then, the unit tangent vector, velocity vector and linear momentum vector at the point $\alpha(s)$ (at time t) are given by

$$\begin{aligned} \mathbf{T}(s) &= \frac{d\mathbf{x}}{ds} \\ \mathbf{v}(t) &= \frac{d\mathbf{x}}{dt} = \left(\frac{ds}{dt}\right)\mathbf{T}(s) \\ \mathbf{p}(t) &= m\mathbf{v}(t) = m\left(\frac{ds}{dt}\right)\mathbf{T}(s), \end{aligned} \tag{2.1}$$

respectively [16]. On the other hand, we can write the following:

$$\mathbf{x} = \langle \alpha(s), \mathbf{T}(s) \rangle \mathbf{T}(s) + \langle \alpha(s), \mathbf{N}(s) \rangle \mathbf{N}(s) + \langle \alpha(s), \mathbf{B}(s) \rangle \mathbf{B}(s) \tag{2.2}$$

at the point $\alpha(s)$ (at time t) with respect to Serret-Frenet frame. By vector product of the position vector and the linear momentum vector at time t, the angular momentum vector of the particle about O is obtained as follows:

$$\mathbf{H}^O = m\,\langle \alpha(s), \mathbf{B}(s)\rangle \left(\frac{ds}{dt}\right)\mathbf{N}(s) - m\,\langle \alpha(s), \mathbf{N}(s)\rangle \left(\frac{ds}{dt}\right)\mathbf{B}(s). \tag{2.3}$$

In the rest of the study, we assume that angular momentum vector of the particle never vanishes. That is, we restrict ourselves to the trajectories having non-vanishing angular momentum. By this assumption, we ensure the coefficient functions $\langle \alpha(s), \mathbf{N}(s)\rangle$ and $\langle \alpha(s), \mathbf{B}(s)\rangle$ of the position vector not to be zero at the same time. In other words, we ensure that the tangent line never passes through the origin along the trajectory. Here we will use the special radial directions discussed in the study [17].

Now we return to the position vector in the equation (2.2). The opposite of this vector is given by

$$-\mathbf{x} = \langle -\alpha(s), \mathbf{T}(s)\rangle \mathbf{T}(s) + \langle -\alpha(s), \mathbf{N}(s)\rangle \mathbf{N}(s) + \langle -\alpha(s), \mathbf{B}(s)\rangle \mathbf{B}(s). \tag{2.4}$$

The projections of this vector on the instantaneous osculating plane $\pi_1(s)$ and instantaneous rectifying plane $\pi_2(s)$ give us two vectors which will play an important role to construct our moving frame. These cases are explained in detail below:

The vector, whose starting point is $\alpha(s)$ and endpoint is the foot of the perpendicular that is from O to $\pi_1(s)$, can be written as

$$\mathbf{r}(s) = \langle -\alpha(s), \mathbf{T}(s)\rangle \mathbf{T}(s) + \langle -\alpha(s), \mathbf{N}(s)\rangle \mathbf{N}(s) \tag{2.5}$$

and corresponds to the aforesaid projection on $\pi_1(s)$. On the other hand, the vector, whose starting point is $\alpha(s)$ and endpoint is the foot of the perpendicular that is from O to $\pi_2(s)$, can be written as

$$\mathbf{r}^*(s) = \langle -\alpha(s), \mathbf{T}(s)\rangle \mathbf{T}(s) + \langle -\alpha(s), \mathbf{B}(s)\rangle \mathbf{B}(s) \tag{2.6}$$

and corresponds to the aforesaid projection on $\pi_2(s)$. Since the coefficient functions of the unit tangent vector are same in both equations (2.5) and (2.6), we can easily obtain the following vector

$$\mathbf{r}(s) - \mathbf{r}^*(s) = \langle -\alpha(s), \mathbf{N}(s)\rangle \mathbf{N}(s) + \langle \alpha(s), \mathbf{B}(s)\rangle \mathbf{B}(s) \tag{2.7}$$

whose starting point is $\alpha(s)$ and which lies on the instantaneous normal plane $\pi_3(s)$. Notice that the vector $\mathbf{r}(s) - \mathbf{r}^*(s)$ is equivalent to the vector whose starting point is the aforementioned foot on $\pi_2(s)$ and endpoint is the other aforementioned foot on $\pi_1(s)$ (see Figure 2.1).

Let us discuss on the determination of the unit vector in direction of the vector $\mathbf{r}(s) - \mathbf{r}^*(s)$. When both the planes $\pi_1(s)$ and $\pi_2(s)$ do not contain the origin, the foots are distinct from each other and from the origin. Thus two distinct points (foots) generate the non-zero vector $\mathbf{r}(s) - \mathbf{r}^*(s)$. So, the desired unit vector can be immediately determined. If only one of the planes $\pi_1(s)$ and $\pi_2(s)$ passes through the origin, the foot of the perpendicular on the plane, containing origin, is taken as the origin. Of course, the other foot on the other plane is distinct from the origin. Then, the desired unit vector is obtained similarly. The case both the planes $\pi_1(s)$ and $\pi_2(s)$ contain the origin simultaneously causes not to be determined of the desired unit vector since the both of the aforementioned foots correspond to the origin in this case. That situation occurs only when the tangent line passes through the origin. Fortunately, our assumption, on the angular momentum vector, averts this case. Let the unit vector in direction of the vector $\mathbf{r}(s) - \mathbf{r}^*(s)$ be shown with $\mathbf{Y}(s)$. That is,

$$\mathbf{Y}(s) = \frac{\mathbf{r}(s) - \mathbf{r}^*(s)}{\|\mathbf{r}(s) - \mathbf{r}^*(s)\|} = \frac{\langle -\alpha(s), \mathbf{N}(s)\rangle}{\sqrt{\langle \alpha(s), \mathbf{N}(s)\rangle^2 + \langle \alpha(s), \mathbf{B}(s)\rangle^2}}\mathbf{N}(s) + \frac{\langle \alpha(s), \mathbf{B}(s)\rangle}{\sqrt{\langle \alpha(s), \mathbf{N}(s)\rangle^2 + \langle \alpha(s), \mathbf{B}(s)\rangle^2}}\mathbf{B}(s). \tag{2.8}$$

By vector product the vectors $\mathbf{Y}(s)$ and $\mathbf{T}(s)$, we can obtain the another basis vector. We denote it by $\mathbf{M}(s)$. Then, we have

$$\mathbf{M}(s) = \mathbf{Y}(s) \wedge \mathbf{T}(s) = \frac{\langle \alpha(s), \mathbf{B}(s)\rangle}{\sqrt{\langle \alpha(s), \mathbf{N}(s)\rangle^2 + \langle \alpha(s), \mathbf{B}(s)\rangle^2}}\mathbf{N}(s) + \frac{\langle \alpha(s), \mathbf{N}(s)\rangle}{\sqrt{\langle \alpha(s), \mathbf{N}(s)\rangle^2 + \langle \alpha(s), \mathbf{B}(s)\rangle^2}}\mathbf{B}(s). \tag{2.9}$$

This completes the positively oriented orthonormal moving frame $\{\mathbf{T}(s), \mathbf{M}(s), \mathbf{Y}(s)\}$.

Since the vectors $\mathbf{N}(s)$, $\mathbf{B}(s)$, $\mathbf{M}(s)$ and $\mathbf{Y}(s)$ lie on the instantaneous normal plane $\pi_3(s)$, there is a relation between the Serret-Frenet frame and this frame as in the following:

$$\begin{pmatrix} \mathbf{T}(s) \\ \mathbf{M}(s) \\ \mathbf{Y}(s) \end{pmatrix} = \begin{pmatrix} 1 & 0 & 0 \\ 0 & \cos\Omega(s) & -\sin\Omega(s) \\ 0 & \sin\Omega(s) & \cos\Omega(s) \end{pmatrix} \begin{pmatrix} \mathbf{T}(s) \\ \mathbf{N}(s) \\ \mathbf{B}(s) \end{pmatrix} \tag{2.10}$$

where $\Omega(s)$ is the angle between the vectors $\mathbf{B}(s)$ and $\mathbf{Y}(s)$ which is positively oriented from $\mathbf{B}(s)$ to $\mathbf{Y}(s)$ (see Figure 2.1).

By using the matrix equations (1.3) and (2.10), we can easily write

$$\begin{aligned} \mathbf{M}'(s) &= (\cos\Omega(s)\mathbf{N}(s) - \sin\Omega(s)\mathbf{B}(s))' \\ &= -\Omega'(s)\sin\Omega(s)\mathbf{N}(s) + \cos\Omega(s)\left(-\kappa(s)\mathbf{T}(s) + \tau(s)\mathbf{B}(s)\right) - \Omega'(s)\cos\Omega(s)\mathbf{B}(s) + \tau(s)\sin\Omega(s)\mathbf{N}(s) \\ &= -\kappa(s)\cos\Omega(s)\mathbf{T}(s) + \left(\tau(s) - \Omega'(s)\right)\left[\sin\Omega(s)\mathbf{N}(s) + \cos\Omega(s)\mathbf{B}(s)\right] \\ &= \left(-\kappa(s)\cos\Omega(s)\right)\mathbf{T}(s) + \left(\tau(s) - \Omega'(s)\right)\mathbf{Y}(s) \end{aligned}$$

and

$$\begin{aligned}\mathbf{Y}'(s) &= (\sin\Omega(s)\mathbf{N}(s)+\cos\Omega(s)\mathbf{B}(s))'\\ &= -\Omega'(s)\cos\Omega(s)\mathbf{N}(s)+\sin\Omega(s)\left(-\kappa(s)\mathbf{T}(s)+\tau(s)\mathbf{B}(s)\right)-\Omega'(s)\sin\Omega(s)\mathbf{B}(s)-\tau(s)\cos\Omega(s)\mathbf{N}(s)\\ &= -\kappa(s)\sin\Omega(s)\mathbf{T}(s)+\left(\Omega'(s)-\tau(s)\right)\left[\cos\Omega(s)\mathbf{N}(s)-\sin\Omega(s)\mathbf{B}(s)\right]\\ &= \left(-\kappa(s)\sin\Omega(s)\right)\mathbf{T}(s)+\left(\Omega'(s)-\tau(s)\right)\mathbf{M}(s).\end{aligned}$$

Then, differentiating the vector $\mathbf{M}(s)\wedge\mathbf{Y}(s)$ yields the following:

$$\begin{aligned}\mathbf{T}'(s) &= (\mathbf{M}(s)\wedge\mathbf{Y}(s))'\\ &= \mathbf{M}'(s)\wedge\mathbf{Y}(s)+\mathbf{M}(s)\wedge\mathbf{Y}'(s)\\ &= \left[\left(-\kappa(s)\cos\Omega(s)\right)\mathbf{T}(s)+\left(\tau(s)-\Omega'(s)\right)\mathbf{Y}(s)\right]\wedge\mathbf{Y}(s)+\mathbf{M}(s)\wedge\left[\left(-\kappa(s)\sin\Omega(s)\right)\mathbf{T}(s)+\left(\Omega'(s)-\tau(s)\right)\mathbf{M}(s)\right]\\ &= \left(-\kappa(s)\cos\Omega(s)\right)\left(\mathbf{T}(s)\wedge\mathbf{Y}(s)\right)+\left(-\kappa(s)\sin\Omega(s)\right)\left(\mathbf{M}(s)\wedge\mathbf{T}(s)\right)\\ &= \left(\kappa(s)\cos\Omega(s)\right)\mathbf{M}(s)+\left(\kappa(s)\sin\Omega(s)\right)\mathbf{Y}(s).\end{aligned}$$

Thus, the matrix form of the derivative formulas is immediately given by

$$\begin{pmatrix}\mathbf{T}'(s)\\ \mathbf{M}'(s)\\ \mathbf{Y}'(s)\end{pmatrix}=\begin{pmatrix}0 & k_1(s) & k_2(s)\\ -k_1(s) & 0 & k_3(s)\\ -k_2(s) & -k_3(s) & 0\end{pmatrix}\begin{pmatrix}\mathbf{T}(s)\\ \mathbf{M}(s)\\ \mathbf{Y}(s)\end{pmatrix} \tag{2.11}$$

where

$$\begin{aligned}k_1(s) &= \kappa(s)\cos\Omega(s)\\ k_2(s) &= \kappa(s)\sin\Omega(s)\\ k_3(s) &= \tau(s)-\Omega'(s)\\ \tan\Omega(s) &= \frac{k_2(s)}{k_1(s)}\\ \kappa(s) &= \sqrt{{k_1}^2(s)+{k_2}^2(s)}.\end{aligned} \tag{2.12}$$

Based on the relationship of the frame $\{\mathbf{T}(s),\mathbf{M}(s),\mathbf{Y}(s)\}$ to the position vector, we call it as "Positional Adapted Frame". For convenience, we will use the abbreviation PAF instead of the "Positional Adapted Frame" in the rest of the study. Also, we call the set $\{\mathbf{T}(s),\mathbf{M}(s),\mathbf{Y}(s),k_1(s),k_2(s),k_3(s)\}$ as PAF apparatus of the curve $\alpha=\alpha(s)$.

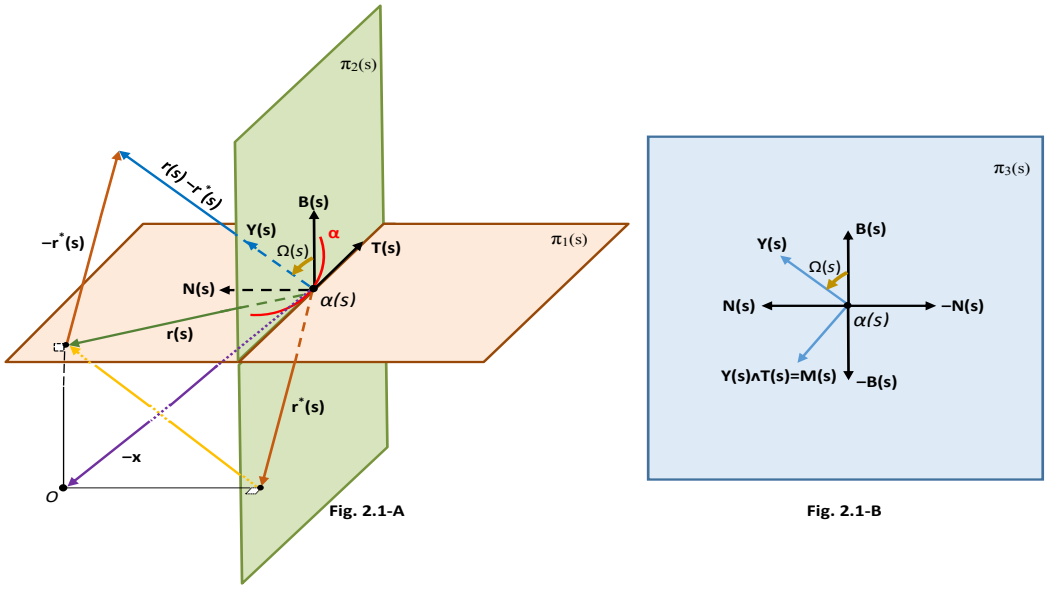

Figure 2.1: An illustration for explaining the construction of PAF

It is well known from linear algebra that a vector can be written uniquely in terms of the basis vectors. This basic knowledge yields the equations

$$\sin\Omega(s) = \frac{-\langle\alpha(s),\mathbf{N}(s)\rangle}{\sqrt{\langle\alpha(s),\mathbf{N}(s)\rangle^2+\langle\alpha(s),\mathbf{B}(s)\rangle^2}} \tag{2.13}$$

$$\cos\Omega(s) = \frac{\langle\alpha(s),\mathbf{B}(s)\rangle}{\sqrt{\langle\alpha(s),\mathbf{N}(s)\rangle^2+\langle\alpha(s),\mathbf{B}(s)\rangle^2}} \tag{2.14}$$

if we compare the equation (2.10) with the equations (2.8) and (2.9). Then, we get

$$\tan\Omega(s) = -\frac{\langle\alpha(s),\mathbf{N}(s)\rangle}{\langle\alpha(s),\mathbf{B}(s)\rangle}. \tag{2.15}$$

Considering the information given in (2.13), (2.14) and (2.15), the rotation angle $\Omega(s)$ is determined as follows:

$$\Omega(s) = \begin{cases} \arctan\left(-\frac{\langle\alpha(s),\mathbf{N}(s)\rangle}{\langle\alpha(s),\mathbf{B}(s)\rangle}\right) \ if\ \ \langle\alpha(s),\mathbf{B}(s)\rangle > 0 \\ \arctan\left(-\frac{\langle\alpha(s),\mathbf{N}(s)\rangle}{\langle\alpha(s),\mathbf{B}(s)\rangle}\right)+\pi \ if\ \ \langle\alpha(s),\mathbf{B}(s)\rangle < 0 \\ -\frac{\pi}{2} \ if\ \ \langle\alpha(s),\mathbf{B}(s)\rangle = 0\,,\ \ \langle\alpha(s),\mathbf{N}(s)\rangle > 0 \\ \frac{\pi}{2} \ if\ \ \langle\alpha(s),\mathbf{B}(s)\rangle = 0\,,\ \ \langle\alpha(s),\mathbf{N}(s)\rangle < 0. \end{cases} \tag{2.16}$$

One can easily complete the calculations by the aid Mathematica program. In the case $\langle\alpha(s),\mathbf{B}(s)\rangle = 0$, $\langle\alpha(s),\mathbf{N}(s)\rangle > 0$, the PAF apparatus $\{\mathbf{T}(s),\mathbf{M}(s),\mathbf{Y}(s),k_1(s),k_2(s),k_3(s)\}$ correspond to $\{\mathbf{T}(s),\mathbf{B}(s),-\mathbf{N}(s),0,-\kappa(s),\tau(s)\}$. Similarly, when $\langle\alpha(s),\mathbf{B}(s)\rangle = 0, \langle\alpha(s),\mathbf{N}(s)\rangle < 0$, the PAF apparatus $\{\mathbf{T}(s),\mathbf{M}(s),\mathbf{Y}(s),k_1(s),k_2(s),k_3(s)\}$ correspond to $\{\mathbf{T}(s),-\mathbf{B}(s),\mathbf{N}(s),0,\kappa(s),\tau(s)\}$.

Now, we will obtain the angular velocity vector for PAF. A better insight into the structure of the derivative formulas, given in (2.11), is presented by means of the angular velocity vector $\omega(s)$. The evolution of PAF $\{\mathbf{T}(s),\mathbf{M}(s),\mathbf{Y}(s)\}$ is specified by its angular velocity via following relations:

$$\begin{aligned} \mathbf{T}'(s) &= \omega(s)\wedge\mathbf{T}(s) \\ \mathbf{M}'(s) &= \omega(s)\wedge\mathbf{M}(s) \\ \mathbf{Y}'(s) &= \omega(s)\wedge\mathbf{Y}(s). \end{aligned} \tag{2.17}$$

Let us determine the vector $\omega(s)$. Suppose that it is written with respect to PAF as in the following:

$$\omega(s) = a(s)\mathbf{T}(s)+b(s)\mathbf{M}(s)+c(s)\mathbf{Y}(s)$$

where $a(s)$, $b(s)$ and $c(s)$ are real-valued functions of the parameter s. Then (2.17) becomes

$$\begin{aligned} \mathbf{T}'(s) &= -b(s)\mathbf{Y}(s)+c(s)\mathbf{M}(s) \\ \mathbf{M}'(s) &= a(s)\mathbf{Y}(s)-c(s)\mathbf{T}(s) \\ \mathbf{Y}'(s) &= -a(s)\mathbf{M}(s)+b(s)\mathbf{T}(s). \end{aligned} \tag{2.18}$$

By comparing (2.11) with (2.18) we get

$$\begin{aligned} a &= k_3 \\ b &= -k_2 \\ c &= k_1. \end{aligned}$$

Therefore, the angular velocity vector is given by

$$\omega(s) = k_3(s)\mathbf{T}(s)-k_2(s)\mathbf{M}(s)+k_1(s)\mathbf{Y}(s) \tag{2.19}$$

for PAF.

Example 2.1. *In E^3, assume that a point particle P of constant mass moves on the trajectory $\delta:(0,k)\to E^3, \delta(s)=\left(8\cos\frac{s}{17},8\sin\frac{s}{17},15\frac{s}{17}\right)$, which is a unit speed curve, where k is a positive real constant. See the trajectory $\delta=\delta(s)$ in Figure 2.2. The Serret-Frenet apparatus of this trajectory are expressed as in [18]:*

$$\begin{aligned} \mathbf{T}(s) &= \left(-\frac{8}{17}\sin\frac{s}{17},\frac{8}{17}\cos\frac{s}{17},\frac{15}{17}\right) \\ \mathbf{N}(s) &= \left(-\cos\frac{s}{17},-\sin\frac{s}{17},0\right) \\ \mathbf{B}(s) &= \left(\frac{15}{17}\sin\frac{s}{17},-\frac{15}{17}\cos\frac{s}{17},\frac{8}{17}\right) \\ \kappa(s) &= \frac{8}{289} \\ \tau(s) &= \frac{15}{289}. \end{aligned}$$

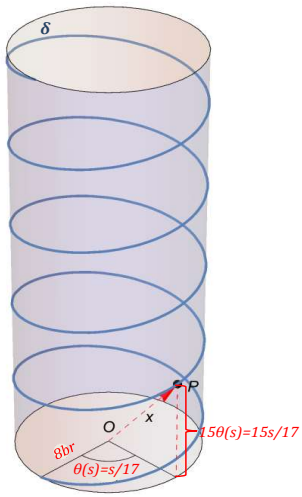

Figure 2.2: An illustration for the trajectory given in Example 2.1

Then, $\langle \delta(s), \mathbf{N}(s)\rangle = -8$ *and* $\langle \delta(s), \mathbf{B}(s)\rangle = \frac{120}{289}s$ *are easily obtained. Since* $\langle \delta(s), \mathbf{B}(s)\rangle > 0$ *for all* $s \in (0,\ k)$, *we get* $\Omega(s) = \arctan\left(\frac{289}{15s}\right)$. *The above information gives us the PAF apparatus as follows:*

$$
\begin{aligned}
\mathbf{T}(s) &= \left(\frac{-8}{17}\sin\frac{s}{17}, \frac{8}{17}\cos\frac{s}{17}, \frac{15}{17}\right)\\
\mathbf{M}(s) &= \left(-\cos\left(\arctan\left(\frac{289}{15s}\right)\right)\cos\frac{s}{17} - \frac{15}{17}\sin\left(\arctan\left(\frac{289}{15s}\right)\right)\sin\frac{s}{17}, -\cos\left(\arctan\left(\frac{289}{15s}\right)\right)\sin\frac{s}{17} + \frac{15}{17}\sin\left(\arctan\left(\frac{289}{15s}\right)\right)\cos\frac{s}{17}, \frac{-8}{17}\sin\left(\arctan\left(\frac{289}{15s}\right)\right)\right)\\
\mathbf{Y}(s) &= \left(-\sin\left(\arctan\left(\frac{289}{15s}\right)\right)\cos\frac{s}{17} + \frac{15}{17}\cos\left(\arctan\left(\frac{289}{15s}\right)\right)\sin\frac{s}{17}, -\sin\left(\arctan\left(\frac{289}{15s}\right)\right)\sin\frac{s}{17} - \frac{15}{17}\cos\left(\arctan\left(\frac{289}{15s}\right)\right)\cos\frac{s}{17}, \frac{8}{17}\cos\left(\arctan\left(\frac{289}{15s}\right)\right)\right)\\
k_1(s) &= \frac{8}{289}\cos\left(\arctan\left(\frac{289}{15s}\right)\right)\\
k_2(s) &= \frac{8}{289}\sin\left(\arctan\left(\frac{289}{15s}\right)\right)\\
k_3(s) &= \frac{15}{289} + \frac{4335}{83521+225s^2}
\end{aligned}
$$

in the light of the equations (2.10) *and* (2.12).

3. Some characterizations for the special cases of the trajectory

In this section, we obtain some conditions including the PAF apparatus for the trajectory to be a rectifying curve, an osculating curve, a normal curve, a planar curve and a general helix in E^3.
It is not difficult to see

$$
\begin{aligned}
k_1(s) &= \kappa(s)\left(\frac{\langle \alpha(s), \mathbf{B}(s)\rangle}{\sqrt{\langle \alpha(s), \mathbf{N}(s)\rangle^2 + \langle \alpha(s), \mathbf{B}(s)\rangle^2}}\right)\\
k_2(s) &= \kappa(s)\left(\frac{-\langle \alpha(s), \mathbf{N}(s)\rangle}{\sqrt{\langle \alpha(s), \mathbf{N}(s)\rangle^2 + \langle \alpha(s), \mathbf{B}(s)\rangle^2}}\right)
\end{aligned}
$$

considering the above derivation. Then, by keeping $\kappa \neq 0$ and the assumption related to angular momentum in mind, it can be said that $k_1(s)$ and $k_2(s)$ can not be equal to zero at the same time and they verify the propositions

$$
\begin{aligned}
k_1(s) = 0 \quad &\Leftrightarrow \quad \langle \alpha(s), \mathbf{B}(s)\rangle = 0\\
k_2(s) = 0 \quad &\Leftrightarrow \quad \langle \alpha(s), \mathbf{N}(s)\rangle = 0.
\end{aligned}
$$

So, the equation $k_1(s)\langle \alpha(s), \mathbf{N}(s)\rangle + k_2(s)\langle \alpha(s), \mathbf{B}(s)\rangle = 0$ is satisfied if $k_1(s) = 0$. Also, from the above propositions and the equations $(2.12)_4$ and (2.15) we have the following:

$$
\frac{k_2(s)}{k_1(s)} = -\frac{\langle \alpha(s), \mathbf{N}(s)\rangle}{\langle \alpha(s), \mathbf{B}(s)\rangle} \tag{3.1}
$$

where $k_1(s) \neq 0$. Thus, the aforementioned equation

$$
k_1(s)\langle \alpha(s), \mathbf{N}(s)\rangle + k_2(s)\langle \alpha(s), \mathbf{B}(s)\rangle = 0 \tag{3.2}
$$

is satisfied for all the s values of parameter.

A curve $\alpha = \alpha(s)$ is called as osculating curve (rectifying curve or normal curve) if its position vector always lies in its osculating plane (rectifying plane or normal plane) (see [4]-[6] for more details). Considering these definitions, the following theorems can be given.

Theorem 3.1. *In E^3, suppose that a point particle of constant mass moves on its trajectory having non-vanishing angular momentum. Let $\alpha = \alpha(s)$ be the unit speed parametrization of the trajectory with $\kappa \neq 0$. Then, α is a rectifying curve if and only if $k_2 = 0$.*

Proof. Let $\alpha = \alpha(s)$ be the unit speed parametrization of the trajectory with $\kappa \neq 0$. Assume that α is a rectifying curve. Then its position vector always lies on its rectifying plane. So, $\langle \alpha(s), \mathbf{N}(s) \rangle = 0$ for all the values s of the arc-length parameter. Taking into consideration the equation (3.2), we get

$$k_2(s) \langle \alpha(s), \mathbf{B}(s) \rangle = 0 \tag{3.3}$$

for all s. Due to the non-vanishing angular momentum, the tangent line never passes through the origin O. Thus, $\langle \alpha(s), \mathbf{B}(s) \rangle$ never vanishes along the rectifying trajectory α. Using this information in the equation (3.3) completes the first part of the proof.

On the contrary, assume that $k_2 = 0$. From (3.2), we get

$$\forall s, \quad k_1(s) \langle \alpha(s), \mathbf{N}(s) \rangle = 0.$$

We know that $k_1(s)$ and $k_2(s)$ can not be equal to zero at the same time. So, we can ensure that $k_1(s)$ never vanishes. This yields the following

$$\forall s, \quad \langle \alpha(s), \mathbf{N}(s) \rangle = 0$$

which means that $\alpha = \alpha(s)$ is a rectifying curve. □

Theorem 3.2. *In E^3, assume that a point particle of constant mass moves on its trajectory having non-vanishing angular momentum. Let $\alpha = \alpha(s)$ be the unit speed parametrization of the trajectory with $\kappa \neq 0$. In this case, α is an osculating curve if and only if $k_1 = 0$.*

Proof. Let $\alpha = \alpha(s)$ be the unit speed parametrization of the trajectory with $\kappa \neq 0$. Suppose that α is an osculating curve. In that case, its position vector always lies on its osculating plane. Thus, $\langle \alpha(s), \mathbf{B}(s) \rangle = 0$ for all the values s of the arc-length parameter. Considering the equation (3.2), we get

$$k_1(s) \langle \alpha(s), \mathbf{N}(s) \rangle = 0$$

for all s. Similarly previous proof, in the light of non-vanishing angular momentum we can ensure that the tangent line never passes through the origin O. So, $\langle \alpha(s), \mathbf{N}(s) \rangle$ never vanishes along the osculating trajectory α. Then we conclude

$$\forall s, \quad k_1(s) = 0$$

and finish the first part of the proof.

On the contrary, suppose that $k_1 = 0$. Then from the equation (3.2)

$$\forall s, \quad k_2(s) \langle \alpha(s), \mathbf{B}(s) \rangle = 0$$

can be written. Since $k_1(s)$ and $k_2(s)$ are not equal to zero at the same time, we can say

$$\forall s, \quad k_2(s) \neq 0.$$

This gives us the following

$$\forall s, \quad \langle \alpha(s), \mathbf{B}(s) \rangle = 0$$

which means that $\alpha = \alpha(s)$ is an osculating curve. □

Theorem 3.3. *In E^3, assume that a point particle of constant mass moves on its trajectory having non-vanishing angular momentum. Let $\alpha = \alpha(s)$ be the unit speed parametrization of the trajectory with $\kappa \neq 0$. Then the following properties hold:*

1. *If α is a normal curve, then the differential equation $k_2 {k_1}' - k_1 {k_2}' - k_3({k_1}^2 + {k_2}^2) - \Omega'({k_1}^2 + {k_2}^2) = 0$ is satisfied along α.*
2. *If the differential equation $k_2 {k_1}' - k_1 {k_2}' - k_3({k_1}^2 + {k_2}^2) - \Omega'({k_1}^2 + {k_2}^2) = 0$ is satisfied along α with $k_1, k_2 \neq 0$, then α is a normal curve.*

Proof. Before starting the proofs of items, we need some preparation. Let $\alpha = \alpha(s)$ be the unit speed parametrization of the trajectory with $\kappa \neq 0$. One can easily find the equation

$$\left(k_1(s)\sqrt{{k_1}^2(s) + {k_2}^2(s)}\right) \langle \alpha(s), \mathbf{T}(s) \rangle + \left(k_2(s)(k_3(s) + \Omega'(s)) - {k_1}'(s)\right) \langle \alpha(s), \mathbf{N}(s) \rangle + \left(-k_1(s)(k_3(s) + \Omega'(s)) - {k_2}'(s)\right) \langle \alpha(s), \mathbf{B}(s) \rangle = 0 \tag{3.4}$$

by differentiating the equation (3.2) and using the relations between the PAF apparatus and Serret-Frenet apparatus. We can obtain the equation

$$\left(-k_1(s)k_2(s)\sqrt{{k_1}^2(s) + {k_2}^2(s)}\right) \langle \alpha(s), \mathbf{T}(s) \rangle + \left(k_2(s){k_1}'(s) - k_1(s){k_2}'(s) - k_3({k_1}^2(s) + {k_2}^2(s)) - \Omega'(s)({k_1}^2(s) + {k_2}^2(s))\right) \langle \alpha(s), \mathbf{N}(s) \rangle = 0 \tag{3.5}$$

if we apply necessary operations to the equations (3.2) and (3.4) side by side. Note that the equation (3.5) plays an important role in the rest of the proof. Now we can discuss the items:

1. Assume that α is a normal curve. Then its position vector always lies on its normal plane. So,

$$\langle \alpha(s), \mathbf{T}(s) \rangle = 0 \tag{3.6}$$

for all the values s of the arc-length parameter. Taking into account of the equation (3.5), we obtain

$$\Big(k_2(s)k_1'(s) - k_1(s)k_2'(s) - k_3(k_1^2(s) + k_2^2(s)) - \Omega'(s)(k_1^2(s) + k_2^2(s)) \Big) \langle \alpha(s), \mathbf{N}(s) \rangle = 0 \tag{3.7}$$

for all s. On the other hand, differentiating the equation (3.6) yields the following:

$$\forall s, \quad \langle \alpha(s), \mathbf{N}(s) \rangle = -\frac{1}{\kappa(s)} \neq 0. \tag{3.8}$$

From the equations (3.7) and (3.8), we conclude

$$k_2 k_1' - k_1 k_2' - k_3(k_1^2 + k_2^2) - \Omega'(k_1^2 + k_2^2) = 0$$

and finish the proof of this item.

2. Assume that the differential equation $k_2 k_1' - k_1 k_2' - k_3(k_1^2 + k_2^2) - \Omega'(k_1^2 + k_2^2) = 0$ is satisfied along α with $k_1, k_2 \neq 0$. From the equation (3.5), we can write

$$\forall s, \quad \left(-k_1(s)k_2(s)\sqrt{k_1^2(s) + k_2^2(s)} \right) \langle \alpha(s), \mathbf{T}(s) \rangle = 0.$$

Since $k_1, k_2 \neq 0$, we obtain

$$\forall s, \quad \langle \alpha(s), \mathbf{T}(s) \rangle = 0$$

which means that $\alpha = \alpha(s)$ is a normal curve.

□

It is well known that a unit speed curve in E^3 is a planar curve if and only if the torsion vanishes along this curve (see [14]). Considering this information and the equation $(2.12)_3$, the following corollary can be given according to PAF without proof.

Corollary 3.4. *In E^3, assume that a point particle of constant mass moves on its trajectory having non-vanishing angular momentum. Let $\alpha = \alpha(s)$ be the unit speed parametrization of the trajectory with $\kappa \neq 0$. In this case, α is a planar curve if and only if $k_3 = -\Omega'$.*

Another well-known class of curves is the class of general helices. In E^3, a unit speed curve $\alpha = \alpha(s)$ is a general helix if the unit tangent vector of this curve makes a constant angle θ with a fixed unit vector $\mathbf{u}$; namely,

$$\langle \mathbf{T}(s), \mathbf{u} \rangle = \cos\theta$$

for all the s values of parameter. Also, in E^3, the necessary and sufficient condition for the curve with $\kappa \neq 0$ to be general helix is that ratio of torsion to curvature is constant (see [19]). In the light of this information, we can give the following corollary according to PAF.

Corollary 3.5. *In E^3, assume that a point particle of constant mass moves on its trajectory having non-vanishing angular momentum. Let $\alpha = \alpha(s)$ be the unit speed parametrization of the trajectory with $\kappa \neq 0$. In this case, α is a general helix if and only if*

$$\frac{k_3 + \Omega'}{\sqrt{k_1^2 + k_2^2}} = constant.$$

Proof. Let the trajectory $\alpha = \alpha(s)$ be general helix in 3-dimensional Euclidean space E^3. Then, we have a fixed unit vector $\mathbf{u}$ and a constant angle θ satisfying

$$\langle \mathbf{T}, \mathbf{u} \rangle = \cos\theta$$

from the definition. By differentiating this equation we obtain

$$\langle \mathbf{T}', \mathbf{u} \rangle = \langle k_1\mathbf{M} + k_2\mathbf{Y}, \mathbf{u} \rangle = \left\langle \sqrt{k_1^2 + k_2^2}\cos\Omega\mathbf{M} + \sqrt{k_1^2 + k_2^2}\sin\Omega\mathbf{Y}, \mathbf{u} \right\rangle = \sqrt{k_1^2 + k_2^2}\,\langle \cos\Omega\mathbf{M} + \sin\Omega\mathbf{Y}, \mathbf{u} \rangle = 0$$

and so

$$\langle \cos\Omega\mathbf{M} + \sin\Omega\mathbf{Y}, \mathbf{u} \rangle = 0.$$

Since $\mathbf{T} \wedge (\cos\Omega\mathbf{M} + \sin\Omega\mathbf{Y}) = -\sin\Omega\mathbf{M} + \cos\Omega\mathbf{Y}$, the unit vectors $\mathbf{T}, \cos\Omega\mathbf{M} + \sin\Omega\mathbf{Y}, -\sin\Omega\mathbf{M} + \cos\Omega\mathbf{Y}$ compose a right-handed orthonormal system. Then, we can conclude $\mathbf{u} \in Sp\{\mathbf{T}, -\sin\Omega\mathbf{M} + \cos\Omega\mathbf{Y}\}$. Hence

$$\mathbf{u} = \cos\theta\,\mathbf{T} + \sin\theta(-\sin\Omega\mathbf{M} + \cos\Omega\mathbf{Y}).$$

By differentiation we get

$$\begin{aligned} 0 &= \cos\theta\,\mathbf{T}' + \sin\theta(-\sin\Omega\mathbf{M} + \cos\Omega\mathbf{Y})' \\ &= (k_1\sin\Omega - k_2\cos\Omega)\,\mathbf{T} + \left(k_1\cos\theta - \Omega'\sin\theta\cos\Omega - k_3\sin\theta\cos\Omega\right)\mathbf{M} + \left(k_2\cos\theta - \Omega'\sin\Omega\sin\theta - k_3\sin\Omega\sin\theta\right)\mathbf{Y}. \end{aligned}$$

This last equation yields the equation system

$$\begin{aligned} k_1\sin\Omega - k_2\cos\Omega &= 0 \\ k_1\cos\theta - \Omega'\sin\theta\cos\Omega - k_3\sin\theta\cos\Omega &= 0 \\ k_2\cos\theta - \Omega'\sin\Omega\sin\theta - k_3\sin\Omega\sin\theta &= 0. \end{aligned}$$

Due to the equation $(2.12)_4$, the first equation of this system is satisfied always. Let us consider the second and third equations together. Then, we can write

$$\begin{aligned} k_1\cos\theta &= \sin\theta\cos\Omega(k_3+\Omega') \\ k_2\cos\theta &= \sin\theta\sin\Omega(k_3+\Omega'). \end{aligned}$$

Applying necessary operations these two equations, we obtain

$$\cos^2\theta({k_1}^2+{k_2}^2) = \sin^2\theta(k_3+\Omega')^2$$

and so

$$\frac{k_3+\Omega'}{\sqrt{{k_1}^2+{k_2}^2}} = \cot\theta = \texttt{constant}.$$

On the contrary, suppose that $\cot\theta = \frac{k_3+\Omega'}{\sqrt{{k_1}^2+{k_2}^2}}$. In this case, we can write

$$\sqrt{{k_1}^2+{k_2}^2}\cos\theta - (k_3+\Omega')\sin\theta = 0. \tag{3.9}$$

Differentiating the vector $\mathbf{u} = \cos\theta\,\mathbf{T} + \sin\theta(-\sin\Omega\mathbf{M} + \cos\Omega\mathbf{Y})$ and using the equalities $k_1 = \sqrt{{k_1}^2+{k_2}^2}\cos\Omega$ and $k_2 = \sqrt{{k_1}^2+{k_2}^2}\sin\Omega$, we can easily obtain

$$\mathbf{u}' = (k_1\sin\Omega - k_2\cos\Omega)\,\mathbf{T} + \left(\sqrt{{k_1}^2+{k_2}^2}\cos\Omega\cos\theta - \sin\theta\cos\Omega(k_3+\Omega')\right)\mathbf{M} + \left(\sqrt{{k_1}^2+{k_2}^2}\sin\Omega\cos\theta - \sin\theta\sin\Omega(k_3+\Omega')\right)\mathbf{Y}.$$

This gives us the following

$$\mathbf{u}' = \left(\sqrt{{k_1}^2+{k_2}^2}\cos\theta - (k_3+\Omega')\sin\theta\right)(\cos\Omega\mathbf{M} + \sin\Omega\mathbf{Y}).$$

Substituting the equation (3.9) in the last equation yields

$$\mathbf{u}' = 0.$$

This means that $\mathbf{u}$ is a constant vector. Thus the proof is completed. □

4. Slant helical trajectories according to PAF

Similar to general helix, the slant helix was defined in [20] as a curve whose principal normal vector makes a constant angle with a fixed direction in E^3. That is, if a unit speed curve $\alpha = \alpha(s)$ is a slant helix, then there exist a constant angle γ and a fixed unit vector $\mathbf{w}$ satisfying

$$\langle \mathbf{N}(s), \mathbf{w}\rangle = \cos\gamma$$

for all the s values of parameter. Throughout the study, we refer it classic slant helix by following the known terminology. The characterization for classic slant helices is given by the equation

$$\frac{\kappa^2}{(\kappa^2+\tau^2)^{3/2}}\left(\frac{\tau}{\kappa}\right)' = \texttt{constant}$$

in [20]. After this study, several kind of slant helices have been defined and studied (see [21]-[24] for details). In this section, we define and consider the slant helical trajectories according to PAF and investigate some special cases of them. Note that similar methods and approaches, given in [25], will be followed in this section.

Firstly, we define $\mathbf{M}-$PAF spherical image of the trajectory. We give this spherical image since it is an important part of the characterization of our slant helical trajectories. The remaining PAF spherical images can be topic of a different study of researchers interested.

Definition 4.1. *In E^3, assume that a point particle of constant mass moves on its trajectory having non-vanishing angular momentum. Let $\alpha = \alpha(s)$ be the unit speed parametrization of the trajectory with $\kappa \neq 0$. If we move the second vector field $\mathbf{M}$ of PAF to the center O of the unit sphere S^2, we get a curve which $\mathbf{M}(s)$ draws on S^2. We call this curve as $\mathbf{M}-$PAF spherical image of the trajectory $\alpha = \alpha(s)$ and show it with ξ_M.*

For $\mathbf{M}-$PAF spherical image of the trajectory $\alpha=\alpha(s)$

$$\xi_M(s)=\mathbf{M}(s)$$

can be written. If we differentiate this equation with respect to s, we obtain

$$\begin{aligned}
\xi'_M(s) &= -k_1(s)\mathbf{T}(s)+k_3(s)\mathbf{Y}(s)\\
\xi''_M(s) &= \left[-k_1'(s)-k_2(s)k_3(s)\right]\mathbf{T}(s)-\left[k_1^2(s)+k_3^2(s)\right]\mathbf{M}(s)+\left[-k_1(s)k_2(s)+k_3'(s)\right]\mathbf{Y}(s)\\
\xi'''_M(s) &= \left[-k_1''(s)-k_2'(s)k_3(s)-2k_3'(s)k_2(s)+k_1(s)\left(k_1^2(s)+k_2^2(s)+k_3^2(s)\right)\right]\mathbf{T}(s)-3\left[k_1(s)k_1'(s)+k_3(s)k_3'(s)\right]\mathbf{M}(s)\\
&\quad+\left[k_3''(s)-k_2'(s)k_1(s)-2k_1'(s)k_2(s)-k_3(s)\left(k_1^2(s)+k_2^2(s)+k_3^2(s)\right)\right]\mathbf{Y}(s).
\end{aligned}$$

These equations give us the curvature κ_M and the torsion τ_M of ξ_M as follows:

$$\kappa_M(s) = \frac{\|\xi'_M(s)\wedge\xi''_M(s)\|}{\|\xi'_M(s)\|^3}=\sqrt{1+(\zeta_M(s))^2} \tag{4.1}$$

$$\tau_M(s) = \frac{\langle\xi'_M(s)\wedge\xi''_M(s),\ \xi'''_M(s)\rangle}{\|\xi'_M(s)\wedge\xi''_M(s)\|^2}=\frac{\zeta'_M(s)}{\left(1+(\zeta_M(s))^2\right)\left(k_1^2(s)+k_3^2(s)\right)^{11/2}} \tag{4.2}$$

where

$$\zeta_M(s)=\left(\frac{k_3'k_1-k_1'k_3-k_2(k_1^2+k_3^2)}{(k_1^2+k_3^2)^{3/2}}\right)(s). \tag{4.3}$$

Now, we return to slant helices and define the slant helical trajectories having non-vanishing angular momentum according to PAF as in the next definition.

Definition 4.2. *In E^3, assume that a point particle of constant mass moves on its trajectory having non-vanishing angular momentum. Let $\alpha=\alpha(s)$ be the unit speed parametrization of the trajectory with $\kappa\neq 0$. The trajectory $\alpha=\alpha(s)$ is called a slant helical trajectory (according to PAF) if the second vector field $\mathbf{M}$ of PAF makes a constant angle with a fixed direction.*

As a result of this definition, if the trajectory $\alpha=\alpha(s)$ is a slant helical trajectory according to PAF, then there exist a constant angle β and a fixed unit vector $\mathbf{g}$ satisfying

$$\langle\mathbf{M}(s),\mathbf{g}\rangle=\cos\beta$$

for all the s values of parameter.

Theorem 4.3. *In E^3, assume that a point particle of constant mass moves on its trajectory having non-vanishing angular momentum. Let $\alpha=\alpha(s)$ be the unit speed parametrization of the trajectory with $\kappa\neq 0$ and $(k_1(s),k_3(s))\neq(0,0)$. In that case, α is a slant helical trajectory according to PAF if and only if the function, given in the equation (4.3), is a constant function.*

Proof. Let the trajectory $\alpha=\alpha(s)$ with $\kappa\neq 0$ and $(k_1(s),k_3(s))\neq(0,0)$ be slant helical trajectory according to PAF in 3-dimensional Euclidean space E^3. In that case, from the Definition 4.2, the second vector field $\mathbf{M}$ of PAF makes a constant angle with a fixed direction. Therefore, $\mathbf{M}-$PAF spherical image ξ_M of the trajectory $\alpha=\alpha(s)$ is part of a circle. In other words, it has constant curvature and zero torsion. As we mentioned earlier, the curvature κ_M and the torsion τ_M of ξ_M are as in the equations (4.1) and (4.2). Using the information of constant curvature and zero torsion, we can immediately conclude $\zeta_M(s)=\texttt{constant}$.

On the contrary, assume that $\zeta_M(s)=\texttt{constant}$. In that case, it is very easy to see that $\kappa_M(s)=\texttt{constant}$ and $\tau_M=0$. Thus, $\mathbf{M}-$PAF spherical image ξ_M of the trajectory $\alpha=\alpha(s)$ is part of a circle. This means that $\mathbf{M}$ makes constant angle with a fixed direction and the proof is completed. □

Corollary 4.4. *Let the trajectory $\alpha=\alpha(s)$ be a rectifying curve with $\kappa,k_1\neq 0$. Then, α is a slant helical trajectory according to PAF if and only if*

$$\left(\frac{k_1^2}{(k_1^2+k_3^2)^{3/2}}\left(\frac{k_3}{k_1}\right)'\right)(s) \tag{4.4}$$

is a constant function.

Proof. Let the trajectory $\alpha=\alpha(s)$, which is a rectifying curve with $\kappa,k_1\neq 0$, be a slant helical trajectory according to PAF. Since $\alpha=\alpha(s)$ is a rectifying curve we obtain $k_2=0$ according to Theorem 3.1. If $k_2=0$ is substituted in the equation (4.3), we get this equation as

$$\zeta_M(s)=\left(\frac{k_1^2}{(k_1^2+k_3^2)^{3/2}}\left(\frac{k_3}{k_1}\right)'\right)(s).$$

Then, Theorem 4.3 finishes the first part of the proof. The other part of the proof can be completed in a similar way. □

Corollary 4.5. *Let the trajectory $\alpha=\alpha(s)$ be a rectifying curve with $\kappa,k_1\neq 0$. Then, α is a slant helical trajectory according to PAF if and only if $\alpha=\alpha(s)$ is a classic slant helix.*

Proof. Let the trajectory $\alpha = \alpha(s)$, which is a rectifying curve with $\kappa, k_1 \neq 0$, be a slant helical trajectory according to PAF. Due to the Theorem 3.1, we obtain $k_2 = 0$ for rectifying curve $\alpha = \alpha(s)$. Considering $k_2 = 0$, we get $\sin\Omega = 0$ and so $k_3 = \tau, k_1 = \pm\kappa$. Let us substitute this information in the equation (4.4) and remember the characterization of slant helices given in the beginning of this section. Then, Corollary 4.4 finishes the first part of the proof. In a similar way, one can easily complete the other part of the proof. □

Corollary 4.6. *Let the trajectory $\alpha = \alpha(s)$ be an osculating curve with $\kappa, k_3 \neq 0$. Then, α is a slant helical trajectory according to PAF if and only if*

$$\left(\frac{k_2}{k_3}\right)(s) \tag{4.5}$$

is a constant function.

Proof. Let the trajectory $\alpha = \alpha(s)$, which is an osculating curve with $\kappa, k_3 \neq 0$, be a slant helical trajectory according to PAF. Since $\alpha = \alpha(s)$ is an osculating curve we obtain $k_1 = 0$ according to Theorem 3.2. If $k_1 = 0$ is substituted in the equation (4.3), we get this equation as

$$\zeta_M(s) = \left(-\frac{k_2}{k_3}\right)(s).$$

In that case, Theorem 4.3 finishes the first part of the proof. The other part of the proof can be completed in a similar way. □

Corollary 4.7. *Let the trajectory $\alpha = \alpha(s)$ be an osculating curve with $\kappa, k_3 \neq 0$. Then, α is a slant helical trajectory according to PAF if and only if $\alpha = \alpha(s)$ is a general helix.*

Proof. Let the trajectory $\alpha = \alpha(s)$, which is an osculating curve with $\kappa, k_3 \neq 0$, be a slant helical trajectory according to PAF. Due to the Theorem 3.2, we obtain $k_1 = 0$ for osculating curve $\alpha = \alpha(s)$. Considering $k_1 = 0$, we get $\cos\Omega = 0$ and so $k_3 = \tau, k_2 = \pm\kappa$. Let us substitute this information in the equation (4.5) and remember the characterization of general helices given in the previous section. Then, Corollary 4.6 finishes the first part of the proof. In a similar way, one can easily complete the other part of the proof. □

Now, we will discuss on the determination of the fixed direction (helix axis) for a slant helical trajectory according to PAF. Assume that a point particle of constant mass moves on a slant helical trajectory (according to PAF) having non-vanishing angular momentum in E^3. Let $\alpha = \alpha(s)$ be the unit speed parametrization of this trajectory with $\kappa \neq 0$. In this case, there exist a constant angle β and a fixed unit vector $\mathbf{g}$ satisfying

$$\langle \mathbf{M}, \mathbf{g} \rangle = \cos\beta = \lambda_2$$

where $\mathbf{g} = \lambda_1\mathbf{T} + \lambda_2\mathbf{M} + \lambda_3\mathbf{Y}$. From the last equation, we get

$$\langle -k_1\mathbf{T} + k_3\mathbf{Y}, \mathbf{g} \rangle = 0 \tag{4.6}$$

by means of differentiation with respect to s. This time, let us differentiate the vector $\mathbf{g}$. Then we get

$$(\lambda_1' - \lambda_2 k_1 - \lambda_3 k_2)\mathbf{T} + (\lambda_1 k_1 - \lambda_3 k_3)\mathbf{M} + (\lambda_3' + \lambda_1 k_2 + \lambda_2 k_3)\mathbf{Y} = 0.$$

This yields the following equation system:

$$\begin{aligned} \lambda_1' - \lambda_2 k_1 - \lambda_3 k_2 &= 0 \\ \lambda_1 k_1 - \lambda_3 k_3 &= 0 \\ \lambda_3' + \lambda_1 k_2 + \lambda_2 k_3 &= 0. \end{aligned} \tag{4.7}$$

Here, we will follow similar steps given in [25] to solve this system. If we write $\lambda_1 = \frac{k_3}{k_1}\lambda_3,\ k_1(s) \neq 0$ in the equations $(4.7)_1$ and $(4.7)_3$ and multiply $(4.7)_1$ with $\frac{k_3}{k_1}$, we get the differential equation

$$\left(1 + \left(\frac{k_3}{k_1}\right)^2\right)\lambda_3' + \frac{k_3}{k_1}\left(\frac{k_3}{k_1}\right)'\lambda_3 = 0.$$

One can find the general solution $\lambda_3 = \mu\frac{k_1}{\sqrt{{k_1}^2+{k_3}^2}}$ of this differential equation where μ is the constant of integration. Then, it is not difficult to obtain $\lambda_1 = \mu\frac{k_3}{\sqrt{{k_1}^2+{k_3}^2}}$ from the relation $\lambda_1 = \frac{k_3}{k_1}\lambda_3$. Since the vector $\mathbf{g} = \mu\frac{k_3}{\sqrt{{k_1}^2+{k_3}^2}}\mathbf{T} + \cos\beta\mathbf{M} + \mu\frac{k_1}{\sqrt{{k_1}^2+{k_3}^2}}\mathbf{Y}$ is taken as a unit vector, we can derive the integration constant as $\mu = \pm\sin\beta$. So,

$$\mathbf{g} = \pm\frac{k_3}{\sqrt{{k_1}^2+{k_3}^2}}\sin\beta\mathbf{T} + \cos\beta\mathbf{M} \pm \frac{k_1}{\sqrt{{k_1}^2+{k_3}^2}}\sin\beta\mathbf{Y}$$

can be written. Finally, we must determine the constant angle β. By differentiating the equation (4.6) with respect to arc-length parameter s of the trajectory,

$$\left\langle (-{k_1}' - k_2 k_3)\mathbf{T} + (-{k_1}^2 - {k_3}^2)\mathbf{M} + ({k_3}' - k_1 k_2)\mathbf{Y},\ \pm\frac{k_3}{\sqrt{{k_1}^2+{k_3}^2}}\sin\beta\mathbf{T} + \cos\beta\mathbf{M} \pm \frac{k_1}{\sqrt{{k_1}^2+{k_3}^2}}\sin\beta\mathbf{Y} \right\rangle = 0$$

is obtained. So, we have

$$\pm\sin\beta\left(\frac{k_1k_3{}'-k_3k_1{}'-k_2{k_1}^2-k_2{k_3}^2}{\sqrt{{k_1}^2+{k_3}^2}}\right)-\cos\beta\left({k_1}^2+{k_3}^2\right)=0.$$

This yields the following:

$$\tan\beta=\pm\frac{\left({k_1}^2+{k_3}^2\right)^{3/2}}{k_1k_3{}'-k_3k_1{}'-k_2{k_1}^2-k_2{k_3}^2}.$$

In the light of the above information, one can easily find β and determine the fixed direction generated by the constant vector $\mathbf{g}$ (see $\mathbf{g}$ is constant) for the slant helical trajectory according to PAF.

5. Conclusion

Since there is a very close relation between a moving point particle of constant mass and the trajectory of it, moving frames adapted to the trajectories are very useful tools for studying the kinematics theory. Considering this relation, a new moving frame, which we call it PAF for short, is introduced for the trajectories with non-vanishing angular momentum in this study. Then, some basic topics are investigated by means of PAF. It may be useful for the researchers studying on modern robotics in their observation environment. Furthermore, we expect that it will be one of the preferred tools for discussing many topics of kinematics and differential geometry.

A natural question is to investigate the special trajectories generated by the **TM**, **TY**, **MY** and **TMY**−Smarandache curves according to PAF in Euclidean 3-space. We leave that as a future project.

References

[1] K. Taşköprü, M. Tosun, *Smarandache curves on S^2*, Bol. da Soc. Parana. de Mat., **32**(1) (2014), 51-59.
[2] K. Eren, H. H. Kösal, *Evolution of space curves and the special ruled surfaces with modified orthogonal frame*, AIMS Math., **5**(3) (2020), 2027-2039.
[3] Ö. G. Yıldız, M. Akyiğit, M. Tosun, *On the trajectory ruled surfaces of framed base curves in the Euclidean space*, Math. Methods Appl. Sci., 1-8, (2020), https://doi.org/10.1002/mma.6267
[4] B. Y. Chen, *When does the position vector of a space curve always lie in its rectifying plane?*, Am. Math. Mon., **110**(2) (2003), 147-152.
[5] K. İlarslan, E. Nešović, *Some characterizations of osculating curves in the Euclidean spaces*, Demonstr. Math., **41**(4) (2008), 931-939.
[6] Z. Bozkurt, İ. Gök, O. Z. Okuyucu, F. N. Ekmekci, *Characterizations of rectifying, normal and osculating curves in three dimensional compact Lie groups*, Life Sci. J., **10**(3) (2013), 819-823.
[7] R. L. Bishop, *There is more than one way to frame a curve*, Am. Math. Mon., **82** (1975), 246-251.
[8] S. Yılmaz, M. Turgut, *A new version of Bishop frame and an application to spherical images*, J. Math. Anal. Appl., **371**(2) (2010), 764-776.
[9] M. A. Soliman, N. H. Abdel-All, R. A. Hussien, T. Youssef, *Evolution of space curves using Type-3 Bishop frame*, Caspian J. Math. Sci. 8(1) (2019), 58-73.
[10] M. Dede, C. Ekici, H. Tozak, *Directional tubular surfaces*, Int. J. Algebra, **9**(12) (2015), 527-535.
[11] G. Y. Şentürk, S. Yüce, *Bertrand offsets of ruled surfaces with Darboux Frame*, Results Math., **72**(3) (2017), 1151-1159.
[12] B. Uzunoğlu, İ. Gök, Y. Yaylı, *A new approach on curves of constant precession*, Appl. Math. Comput., **275** (2016), 317-323.
[13] O. Keskin, Y. Yaylı, *An application of N-Bishop frame to spherical images for direction curves*, Int. J. Geom. Methods Mod. Phys., **14**(11) (2017), 1750162.
[14] T. Shifrin, *Differential Geometry: A First Course in Curves and Surfaces*, University of Georgia, Preliminary Version, 2008.
[15] A. Menninger, *Characterization of the slant helix as successor curve of the general helix*, Int. Electron. J. Geom., **7**(2) (2014), 84-91.
[16] J. Casey, *Siacci's resolution of the acceleration vector for a space curve*, Meccanica, **46** (2011), 471-476.
[17] K. E. Özen, F. S. Dündar, M. Tosun, *An alternative approach to jerk in motion along a space curve with applications*, J. Theor. Appl. Mech., **57**(2) (2019), 435-444.
[18] K. E. Özen, M. Tosun, *On the resolution of the acceleration vector according to Bishop frame*, Univers. J. Math. Appl., **4**(1) (2021), 26-32.
[19] D. J. Struik, *Lectures on Classical Differential Geometry*, Dover, New-York, 1988.
[20] S. Izumiya, N. Takeuchi, *New special curves and developable surfaces*, Turk. J. Math. **28** (2004) 153-163.
[21] B. Bükcü, M. K. Karacan. *The slant helices according to Bishop frame*, Int. J. Comput. Math. Sci., **3** (2009), 67-70.
[22] A. T. Ali, M. Turgut, *Some characterizations of slant helices in the Euclidean space E^n*, Hacet. J. Math. Stat. **39**(3) (2010), 327-336.
[23] O. Z. Okuyucu, İ. Gök, Y. Yaylı, N. Ekmekci, *Slant helices in three dimensional Lie groups*, Appl. Math. Comput., **221** (2013), 672-683.
[24] P. Lucas, J. A. Ortega-Yagües, *Helix surfaces and slant helices in the three-dimensional anti-De Sitter space*, RACSAM **111**(4) (2017), 1201-1222.
[25] N. Macit, M. Düldül, *Relatively normal-slant helices lying on a surface and their characterizations*, Hacet. J. Math. Stat., **46**(3) (2017), 397-408.

Journal of Mathematical Sciences and Modelling, 4 (1) (2021) 19-24
Research Article

Journal of Mathematical Sciences and Modelling

Journal Homepage: www.dergipark.gov.tr/jmsm
ISSN 2636-8692
DOI: http://dx.doi.org/10.33187/jmsm.828002

Upper Bound of Difference Operator on Some Matrix Domains

Lotfollah Karimi[1*] and Maryam Sinaei[2]

[1]*Department of Basic Science, Hamedan University of Technology, Hamedan, Iran*
[2]*Department of mathematics, Azad university of Shiraz, Shiraz branch, Shiraz, Iran*
[*]*Corresponding author*

Article Info

Keywords: *Cesàro matrix, Difference operator, Hilbert matrix, Norm, Sequence space.*
2010 AMS: *26D15, 40C05, 40G05, 47B37.*
Received: *18 November 2020*
Accepted: *6 April 2021*
Available online: *30 April 2021*

Abstract

In this study, we investigate the norm of difference operator on some sequence spaces such as Hilbert and Cesàro matrix domains. Therefore the present study is a complement for those results obtained in [1].

1. Introduction

Let $p > 1$ and ω denote the set of all real-valued sequences. The Banach space ℓ_p is the set of all real sequences $x = (x_k)_{k=0}^{\infty} \in \omega$ such that

$$\|x\|_{\ell_p} = \left(\sum_{k=0}^{\infty} |x_k|^p \right)^{1/p} < \infty.$$

We use the notations Δ^B and Δ^F to indicate the backward and forward difference matrices, respectively. These matrices are defined by

$$\delta^B_{j,k} = \begin{cases} 1 & k = j \\ -1 & k = j-1 \\ 0 & otherwise, \end{cases} \quad and \quad \delta^F_{j,k} = \begin{cases} 1 & k = j \\ -1 & k = j+1 \\ 0 & otherwise. \end{cases} \tag{1.1}$$

Also Roopaei in [2] has introduced the notations $\ell_p(\Delta^B)$ and $\ell_p(\Delta^F)$ for the backward and forward difference sequence spaces defined by,

$$\ell_p(\Delta^B) = \left\{ x = (x_n) \, : \, \sum_{n=1}^{\infty} |x_n - x_{n-1}|^p < \infty \right\},$$

and

$$\ell_p(\Delta^F) = \left\{ x = (x_n) \, : \, \sum_{n=1}^{\infty} |x_n - x_{n+1}|^p < \infty \right\},$$

respectively. The domains $c_0(\Delta^F)$, $c(\Delta^F)$ and $\ell_\infty(\Delta^F)$ of the forward difference matrix Δ^F in the spaces c_0, c and ℓ_∞ are introduced by Kizmaz [3]. Aftermore, the domain bv_p of the backward difference matrix Δ^B in the space ℓ_p have recently been investigated for $0 < p < 1$ by Altay and Başar [4], and for $1 \leq p \leq \infty$ by Başar and Altay [5].

The infinite Cesàro operator is defined by

$$c_{j,k} = \begin{cases} \frac{1}{j+1} & 0 \leq k \leq j \\ 0 & otherwise, \end{cases}$$

***Email address and ORCID number*: lkarimi@hut.ac.ir, 0000-0002-2725-7960 (L. Karimi), marysinaei@yahoo.com, 0000-0002-4414-524X (M. Sinaei)**

for all $j,k \in \mathbb{N}$. That is,

$$C = \begin{pmatrix} 1 & 0 & 0 & \cdots \\ 1/2 & 1/2 & 0 & \cdots \\ 1/3 & 1/3 & 1/3 & \cdots \\ \vdots & \vdots & \vdots & \ddots \end{pmatrix}.$$

This operator has the ℓ_p-norm $\|C\|_{\ell_p} = p^*$, where p^* is the conjugate of p i.e. $\frac{1}{p} + \frac{1}{p^*} = 1$.

Suppose that $N \geq 1$ is a real number. The generalized Cesàro matrix, $C^N = (c^N_{j,k})$,

$$c^N_{j,k} = \begin{cases} \frac{1}{j+N} & 0 \leq k \leq j \\ 0 & otherwise, \end{cases}$$

has the ℓ_p-norm $\|C^N\|_{\ell_p} = p^*$ ([6], Lemma 2.3), and the entries

$$C^N = \begin{pmatrix} \frac{1}{N} & 0 & 0 & \cdots \\ \frac{1}{1+N} & \frac{1}{1+N} & 0 & \cdots \\ \frac{1}{2+N} & \frac{1}{2+N} & \frac{1}{2+N} & \cdots \\ \vdots & \vdots & \vdots & \ddots \end{pmatrix}.$$

Note that, C^1 is the well-known Cesàro matrix C. For more examples

$$C^2 = \begin{pmatrix} 1/2 & 0 & 0 & \cdots \\ 1/3 & 1/3 & 0 & \cdots \\ 1/4 & 1/4 & 1/4 & \cdots \\ \vdots & \vdots & \vdots & \ddots \end{pmatrix} \quad and \quad C^3 = \begin{pmatrix} 1/3 & 0 & 0 & \cdots \\ 1/4 & 1/4 & 0 & \cdots \\ 1/5 & 1/5 & 1/5 & \cdots \\ \vdots & \vdots & \vdots & \ddots \end{pmatrix}.$$

There are several research on the problem of finding the norm of operators on matrix domains while there are very limited papers about the norm of difference operators. Roopaei has recently computed the norm of backward difference operator on some sequence spaces and the present study is a complement for those results obtained in [1].

2. Norm of operators on matrix domains

The operator T is called bounded, if the inequality $\|Tx\|_{\ell_p} \leq K\|x\|_{\ell_p}$ holds for all sequences $x \in \ell_p$, while the constant K is not depending on x. The constant K is called an upper bound for operator T and the smallest possible value of K is called the norm of T.
The domain X_T of an infinite matrix T in a sequence space X is defined as

$$X_T = \{x \in \omega : Tx \in X\}$$

which is also a sequence space. It is easy to see that for an invertible matrix T, the matrix domain T_p is a normed space with $\|x\|_{T_p} := \|Tx\|_{\ell_p}$. By using matrix domains of special triangular matrices in classical spaces, many authors have introduced and studied new Banach spaces. For the relevant literature, we refer to the papers [7, 8, 9, 10, 11, 12, 13] and textbook [14]. Recently, Roopaei has computed the norm of operators on several matrix domains in [2, 15, 16, 17, 18, 19, 20, 21].

Lemma 2.1 ([18], Lemma 3.1)**.** *Let U be a bounded operator on ℓ_p and A_p and B_p are two matrix domains such that $A_p \simeq \ell_p$.*

- *If BT is a bounded operator on ℓ_p, then T is a bounded operator from ℓ_p into B_p and $\|T\|_{\ell_p,B_p} = \|BT\|_{\ell_p}$.*
- *If T has a factorization of the form $T = UA$, then T is a bounded operator from the matrix domain A_p into ℓ_p and $\|T\|_{A_p,\ell_p} = \|U\|_{\ell_p}$.*
- *If $BT = UA$, then T is a bounded operator from the matrix domain A_p into B_p and*

$$\|T\|_{A_p,B_p} = \|U\|_{\ell_p}.$$

In particular, if $AT = UA$, then T is a bounded operator from the matrix domain A_p into A_p and $\|T\|_{A_p} = \|U\|_{\ell_p}$. Also, if T and A commute then $\|T\|_{A_p} = \|T\|_{\ell_p}$.

2.1. Norm of difference operator on the Hilbert sequence space

Recall the definition of Hilbert matrix $H = (h_{j,k})$, which is defined by

$$h_{j,k} = \frac{1}{j+k+1} \qquad (j,k = 0,1,\ldots).$$

That is

$$H = \begin{pmatrix} 1 & 1/2 & 1/3 & \cdots \\ 1/2 & 1/3 & 1/4 & \cdots \\ 1/3 & 1/4 & 1/5 & \cdots \\ \vdots & \vdots & \vdots & \ddots \end{pmatrix}.$$

We know that H is a bounded operator on ℓ_p with $\|H\|_{\ell_p} = \pi \csc(\pi/p)$ ([22], Theorem 323).
The sequence space associated with the Hilbert matrix, H_p, is defined by

$$H_p = \left\{ x = (x_k) \in \omega : \sum_{j=0}^{\infty} \left| \sum_{k=0}^{\infty} \frac{x_k}{j+k+1} \right|^p < \infty \right\},$$

and has the following norm

$$\|x\|_{H_p} = \left(\sum_{j=0}^{\infty} \left| \sum_{k=0}^{\infty} \frac{x_k}{j+k+1} \right|^p \right)^{\frac{1}{p}}.$$

Theorem 2.2 ([22], Theorem 275)**.** *Let $p > 1$ and $T = (t_{j,k})$ be a matrix operator with $t_{j,k} \geq 0$ for all j,k. Suppose that C, R are two strictly positive numbers such that*

$$\sum_{j=0}^{\infty} t_{j,k} \leq C \quad for\ all\ k, \qquad \sum_{k=0}^{\infty} t_{j,k} \leq R \quad for\ all\ j,$$

bounds for column and row sums respectively. Then

$$\|T\|_{\ell_p} \leq R^{1/p^*} C^{1/p}.$$

The above theorem also known as Schur's theorem.

Theorem 2.3. *The ℓ_p norm of the backward difference operator on the Hilbert matrix domain H_p, is the ℓ_p-norm of forward difference operator on H_p and*

$(a) \|\Delta^B\|_{H_p,H_p} = \|\Delta^F\|_{\ell_p}$,
$(b) \|\Delta^B\|_{\ell_p,H_p} \leq 1$.

Proof. (a) Let $A = H\Delta^B$. The matrix $A = (a_{j,k})$ has the entries

$$a_{i,k} = \sum_{j=k,k+1} h_{i,j}\delta^B_{j,k} = \frac{1}{i+k+1} - \frac{1}{i+k+2} = \frac{1}{(i+k+1)(i+k+2)}.$$

Obviously, A is a symmetric matrix which implies that $H\Delta^B = \Delta^F H$. Now,

$$\begin{aligned} \|\Delta^B\|_{H_p,H_p} &= \sup_{x \in H_p} \frac{\|H\Delta^B x\|_{\ell_p}}{\|x\|_{H_p}} = \sup_{x \in H_p} \frac{\|\Delta^F Hx\|_{\ell_p}}{\|Hx\|_{\ell_p}} \\ &= \sup_{y \in \ell_p} \frac{\|\Delta^F y\|_{\ell_p}}{\|y\|_{\ell_p}} = \|\Delta^F\|_{\ell_p}. \end{aligned}$$

(b) Let A be the matrix defined in part (a). According to Lemma 2.1 part (i)

$$\|\Delta^B\|_{\ell_p,H_p} = \|H\Delta^B\|_{\ell_p} = \|A\|_{\ell_p}.$$

By a simple calculation

$$u_k = \sum_{j=0}^{\infty} a_{j,k} = \frac{1}{k+1},$$

where u_k is the k^{th} column sum of A. Since $1 = u_0 > u_1 > \cdots$ and A is symmetric, hence R and C are both 1 in Schur's theorem. Therefore $\|A\|_{\ell_p} \leq 1$. □

2.2. Norm of difference operator on the Cesàro sequence space

In this part of study, we intend to compute the norm of backward difference operator on the Cesàro sequence space. To do this we need the definition of the generalized Cesàro matrix domain.
The matrix domain associated with the generalized Cesàro matrix [15] is the set

$$C_p^N = \left\{ x = (x_k) \in \omega : \sum_{j=0}^{\infty} \left| \sum_{k=0}^{j} \frac{x_k}{j+N} \right|^p < \infty \right\},$$

which has the following norm

$$\|x\|_{C_p^N} = \left(\sum_{j=0}^{\infty} \left| \sum_{k=0}^{j} \frac{x_k}{j+N} \right|^p \right)^{\frac{1}{p}}.$$

Note that, by letting $N = 1$ we obtain the well-known Cesàro sequence space.

Remark 2.4. *In [23], Ng and Lee introduced the Cesàro sequence spaces X_p and X_∞ of non-absolute type as the domains of Cesàro matrix C_1 of order one in the spaces ℓ_p and ℓ_∞, where $1 \leq p < \infty$. Recently, Şengönül and Başar [24] studied the Cesàro sequence spaces $\widetilde{c}_0$ and $\widetilde{c}$ of non-absolute type as the domains of Cesàro matrix C_1 of order one in the spaces c_0 and c, also Roopaei et al [25] and Roopaei and Başar [10] have investigated the Cesáro space C_p^n for $p \geq 1$ and $0 < p < 1$, respectively.*

Theorem 2.5. *The backward difference operator Δ^B is a bounded operator from ℓ_p into the generalized Cesàro matrix domain C_p^N and*

$$\|\Delta^B\|_{\ell_p, C_p^N} = \frac{1}{N}.$$

In particular, the backward difference operator is a bounded operator from ℓ_p into C_p and $\|\Delta^B\|_{\ell_p, C_p} = 1$.

Proof. Let $D = C^N \Delta^B$. By a simple calculation, we deduce that the matrix $D = (d_{j,k})$ is a diagonal matrix with entries

$$D = \begin{pmatrix} \frac{1}{N} & 0 & 0 & \cdots \\ 0 & \frac{1}{1+N} & 0 & \cdots \\ 0 & 0 & \frac{1}{2+N} & \cdots \\ \vdots & \vdots & \vdots & \ddots \end{pmatrix}. \tag{2.1}$$

Now, according to Lemma 2.1

$$\|\Delta^B\|_{\ell_p, C_p^N} = \|C^N \Delta^B\|_{\ell_p} = \|D\|_{\ell_p} = \sup_j d_{j,j} = \frac{1}{N}.$$

In particular, for $N = 1$, C_p^1 is the well-known Cesàro matrix domain C_p. Therefore we have the result. □

Corollary 2.6. *The generalized Copson operator is a bounded operator from ℓ_p into the forward difference matrix domain $\ell_p(\Delta^F)$ and*

$$\|C^{Nt}\|_{\ell_p, \ell_p(\Delta^F)} = \frac{1}{N}.$$

In particular, Copson operator is a bounded operator from ℓ_p into $\ell_p(\Delta^F)$ and $\|C^t\|_{\ell_p, \ell_p(\Delta^F)} = 1$.

Proof. According to Lemma 2.1 and previous theorem

$$\begin{aligned} \|C^{Nt}\|_{\ell_p, \ell_p(\Delta^F)} &= \|\Delta^F C^{Nt}\|_{\ell_p} = \|(C^N \Delta^B)^t\|_{\ell_p} \\ &= \|D^t\|_{\ell_p} = \sup_j d_{j,j} = \frac{1}{N}, \end{aligned}$$

where D is the diagonal matrix defined in the relation (2.1). □

Theorem 2.7. *The backward difference operator is a bounded operator from the generalized Copson space into the generalized Cesàro matrix domain and*

$$\|\Delta^B\|_{C_p^{Nt}, C_p^N} = \|\Delta^F\|_{\ell_p}.$$

In particular, the backward difference operator is a bounded operator from the Copson matrix domain into the Cesàro matrix domain and $\|\Delta^B\|_{C_p^t, C_p} = \|\Delta^F\|_{\ell_p}$.

Proof. Through the proof of Theorem 2.5 we knew that $C^N \Delta^B = \Delta^F C^{Nt}$. Now, according to Lemma 2.1 we have

$$\begin{aligned} \|\Delta^B\|_{C_p^{Nt}, C_p^N} &= \sup_{x \in C_p^{Nt}} \frac{\|\Delta^B x\|_{C_p^N}}{\|x\|_{C_p^{Nt}}} = \sup_{x \in C_p^{Nt}} \frac{\|C^N \Delta^B x\|_{\ell_p}}{\|C^{Nt} x\|_{\ell_p}} \\ &= \sup_{x \in C_p^{Nt}} \frac{\|\Delta^F C^{Nt} x\|_{\ell_p}}{\|C^{Nt} x\|_{\ell_p}} = \sup_{y \in \ell_p} \frac{\|\Delta^F y\|_{\ell_p}}{\|y\|_{\ell_p}} \\ &= \|\Delta^F\|_{\ell_p}, \end{aligned}$$

that completes the proof. □

Corollary 2.8. *The generalized Copson operator is a bounded operator from the backward difference matrix domain $\ell_p(\Delta^B)$ into the forward difference space $\ell_p(\Delta^F)$ and*

$$\|C^{Nt}\|_{\ell_p(\Delta^B), \ell_p(\Delta^F)} = p^*.$$

In particular, Copson operator is a bounded operator from $\ell_p(\Delta^B)$ into $\ell_p(\Delta^F)$ and $\|C^t\|_{\ell_p(\Delta^B), \ell_p(\Delta^F)} = p^*$.

Proof. The proof is similar to the proof of Theorem 2.7. □

In sequel we intend to generalize the result of Theorem 2.7 for the backward difference operator of order n. At first we need some definitions. Let us recall the backward difference matrix of order n, $\Delta^n = (\delta^n_{j,k})$, which is a lower triangular matrix with the entries

$$\delta^n_{j,k} = \begin{cases} (-1)^{(j-k)}\binom{n}{j-k} & k \le j \le n+k, \\ 0 & otherwise. \end{cases}$$

This matrix has the inverse $\Delta^{-n} = (\delta^{-n}_{j,k})$ with the following entries

$$\delta^{-n}_{j,k} = \begin{cases} \binom{n+j-k-1}{j-k} & j \ge k, \\ 0 & otherwise. \end{cases} \tag{2.2}$$

Note that, for $n = 1$, the backward difference of order 1 is Δ^B that was defined by relation (1.1).
The Hausdorff matrix $H^\mu = (h_{j,k})_{j,k=0}^\infty$, is defined by:

$$h_{j,k} = \begin{cases} \int_0^1 \binom{j}{k}\theta^k(1-\theta)^{j-k}d\mu(\theta) & 0 \le k \le j \\ 0 & k > j, \end{cases}$$

where μ is a probability measure on $[0,1]$. The Hausdorff matrix contains some famous classes of matrices. By letting $d\mu(\theta) = n(1-\theta)^{n-1}d\theta$ in the definition of the Hausdorff matrix, the Cesàro matrix of order n, $C^n = (c^n_{j,k})$, is defined as follows

$$c^n_{j,k} = \begin{cases} \frac{\binom{n+j-k-1}{j-k}}{\binom{n+j}{j}} & 0 \le k \le j, \\ 0 & otherwise. \end{cases}$$

Note that, C^1 is the well-known Cesàro matrix C.
The sequence space C^n_p is defined as the set of all sequences whose C^n-transforms are in the space ℓ_p; that is

$$C^n_p = \left\{ x = (x_j) \in \omega : \sum_{j=0}^{\infty} \left| \frac{1}{\binom{n+j}{j}} \sum_{k=0}^{j} \binom{n+j-k-1}{j-k} x_k \right|^p < \infty \right\},$$

which is a Banach space with the norm

$$\|x\|_{C^n_p} = \left(\sum_{j=0}^{\infty} \left| \frac{1}{\binom{n+j}{j}} \sum_{k=0}^{j} \binom{n+j-k-1}{j-k} x_k \right|^p \right)^{1/p}.$$

The Copson matrix domain C^{nt}_p is defined similarly which is isomorphic to the ℓ_p space by Theorem 2.3 of [18]. Roopaei in [17], through the proof of Corollary 3.6, has showed that $C^n\Delta^{n_B}$ is a diagonal matrix. Hence $C^n\Delta^{n_B} = \Delta^{n_F}C^{nt}$, where Δ^{n_F} is the forward difference operator of order n.
Now, as a result of Lemma 2.1 part (iii), we have the following result.

Theorem 2.9. *The backward difference operator of order n, Δ^{n_B}, is a bounded operator from the Copson matrix domain into the Cesàro matrix domain and*

$$\|\Delta^{n_B}\|_{C^{nt}_p, C^n_p} = \|\Delta^{n_F}\|_{\ell_p}.$$

In particular, the backward difference operator is a bounded operator from the Copson matrix domain into the Cesàro matrix domain and $\|\Delta^B\|_{C^t_p, C_p} = \|\Delta^F\|_{\ell_p}$.

We have also the following corollary which has a proof similar to the above theorem.

Corollary 2.10 ([18], Theorem 4.3)**.** *The Copson matrix of order n, C^n, is a bounded operator from $\ell_p(\Delta^{n_B})$ into $\ell_p(\Delta^{n_F})$ and*

$$\|C^n\|_{\ell_p(\Delta^{n_B}), \ell_p(\Delta^{n_F})} = \frac{\Gamma(n+1)\Gamma(1/p^*)}{\Gamma(n+1/p^*)}.$$

In particular, the Copson matrix is a bounded operator from $\ell_p(\Delta^B)$ into $\ell_p(\Delta^F)$ and

$$\|C\|_{\ell_p(\Delta^B), \ell_p(\Delta^F)} = p^*.$$

Theorem 2.11. *Let n, s and m are non-negative integers that $n = s+m$. The backward difference operator of order n, Δ^{n_B}, is a bounded operator from the matrix domain $\ell_p(\Delta^{m_B})$ into the Cesàro matrix domain C^s_p and*

$$\|\Delta^{n_B}\|_{\ell_p(\Delta^{m_B}), C^s_p} = 1.$$

Proof. From the relation (2.2), one can see that the Cesàro matrix of order n and its inverse can be rewritten based on the backward difference operator and of order $-n$ and its inverse. For $j \geq k$, we have

$$c^n_{j,k} = \frac{\binom{n+j-k-1}{j-k}}{\binom{n+j}{j}} = \frac{\delta^{-n}_{j,k}}{\binom{n+j}{j}}, \quad \text{and} \quad c^{-n}_{j,k} = \delta^n_{j,k}\binom{n+k}{k}.$$

Let us first compute the matrix $C^s\Delta^{n_B}$.

$$(C^s\Delta^{n_B})_{j,k} = \sum_i \frac{\Delta^{-s_B}_{j,i}\Delta^{n_B}_{j,k}}{\binom{s+j}{j}} = \frac{1}{\binom{s+j}{j}}\Delta^m_{j,k}.$$

Hence, $C^s\Delta^{n_B} = U\Delta^{m_B}$, where $U = (u_{j,k})$ is the diagonal matrix defined as $u_{j,j} = \frac{1}{\binom{s+j}{j}}$. Now, according to the Lemma 2.1 we have

$$\begin{aligned}
\|\Delta^{n_B}\|_{\ell_p(\Delta^{m_B}),C^s_p} &= \sup_{x\in\ell_p(\Delta^{m_B})} \frac{\|\Delta^{n_B}x\|_{C^s_p}}{\|x\|_{\ell_p(\Delta^{m_B})}} = \sup_{x\in\ell_p(\Delta^{m_B})} \frac{\|C^s\Delta^{n_B}x\|_{\ell_p}}{\|\Delta^{m_B}x\|_{\ell_p}} \\
&= \sup_{x\in\ell_p(\Delta^{m_B})} \frac{\|U\Delta^{m_B}x\|_{\ell_p}}{\|\Delta^{m_B}x\|_{\ell_p}} = \sup_{y\in\ell_p} \frac{\|Uy\|_{\ell_p}}{\|y\|_{\ell_p}} \\
&= \|U\|_{\ell_p} = \sup_j u_{j,j} = 1.
\end{aligned}$$

□

Corollary 2.12. *Let n, s and m are non-negative integers that $n = s+m$. The backward difference operator of order n, Δ^{n_B}, is a bounded operator from the matrix domain $\ell_p(\Delta^{m_B})$ into the matrix domain $\ell_p(\Delta^{s_B})$ and*

$$\|\Delta^{n_B}\|_{\ell_p(\Delta^{m_B}),\ell_p(\Delta^{s_B})} = 1.$$

Proof. The proof is similar to the proof of the above theorem. □

Acknowledgement

The author wish to thank the referee for a careful reading and valuable comments on the original draft.

References

[1] H. Roopaei, D. Foroutannia, *The norm of backward difference operator Δ^n on certain sequence spaces,* Oper. Matrices, **12**(3) (2018), 867-880.
[2] H. Roopaei, *Norm of Hilbert operator on sequence spaces*, J. Inequal. Appl., **2020**(117), (2020).
[3] H. Kizmaz, *On certain sequence spaces I*, Canad. Math. Bull., **25**(2) (1981), 169-176.
[4] B. Altay, F. Başar, *The fine spectrum and the matrix domain of the difference operator Δ on the sequence space ℓ_p, $(0 < p < 1)$*, Commun. Math. Anal., **2**(2) (2007), 1–11.
[5] F. Başar, B. Altay, *On the space of sequences of p-bounded variation and related matrix mappings*, Ukrainian Math. J., **55**(1) (2003), 136–147.
[6] C. P. Chen, D. C. Luor, Z. y. Ou, *Extensions of Hardy inequality*, J. Math. Anal. Appl., **273** (2002), 160–171.
[7] B. Altay, F. Başar, *Certain topological properties and duals of the matrix domain of a triangle matrix in a sequence space*, J. Math. Anal. Appl., **336**(1) (2007), 632–645.
[8] E. E. Kara, M. İlkhan, *Some properties of generalized Fibonacci sequence spaces*, Linear Multilinear Algebra, **64**(11) (2016), 2208-2223.
[9] F. Başar, *Domain of the composition of some triangles in the space of p-summable sequences*, AIP Conference Proceedings, 1611 (2014), 348–356.
[10] H. Roopaei, F Başar, *On the spaces of Cesàro absolutely p-summable, null, and convergent sequences*, Math. Methods Appl. Sci., **44**(5) (2021), 3670-3685.
[11] H. Roopaei, T. Yaying, *Quasi-Cesàro matrix and associated sequence spaces*, Turk. J. Math., **45**(1) (2021), 153-166.
[12] H. Roopaei, M. İlkhan, *Fractional Cesàro matrix and its associated sequence space*, Concr. Oper., **8**(1), (2021), 24-39.
[13] M. İlkhan, E. E. Kara, *A new Banach space defined by Euler totient matrix operator*, Oper. Matrices, **13**(2) (2019), 527-544.
[14] F. Başar, *Summability Theory and Its Applications*, Bentham Science Publishers, İstanbul, 2012.
[15] H. Roopaei, D. Foroutannia, *The norm of matrix operators on Cesàro weighted sequence space*, Linear Multilinear Algebra, **67**(1) (2019), 175-185.
[16] H. Roopaei, D. Foroutannia, *The norms of certain matrix operators from ℓ_p spaces into $\ell_p(\Delta^n)$ spaces*, Linear Multilinear Algebra, **67**(4) (2019), 767-776.
[17] H. Roopaei, *Norms of summability and Hausdorff mean matrices on difference sequence spaces*, Math. Inequal. Appl., **22**(3) (2019), 983-987.
[18] H. Roopaei, *A study on Copson operator and its associated sequence spaces*, J. Inequal. Appl., **2020**(120) (2020).
[19] H. Roopaei, *A study on Copson operator and its associated sequence spaces II*, J. Inequal. Appl., **2020**(239) (2020).
[20] H. Roopaei, *Bounds of operators on the Hilbert sequence space*, Concr. Oper., **7** (2020), 155-165.
[21] H. Roopaei, *Binomial operator as a Hausdorff operator of the Euler type*, Constr. Math. Anal., **3**(4) (2020), 165-177.
[22] G. H. Hardy, J. E. Littlewood, G. Polya, *Inequalities*, 2nd edition, Cambridge University Press, Cambridge, 2001.
[23] Ng P-N, Lee P-Y, *Cesàro sequence spaces of non-absolute type*, Comment. Math. Prace Mat., 20(2) (1978), 429-433.
[24] M. Şengönül, F. Başar, *Cesàro sequence spaces of non-absolute type which include the spaces c_0 and c*, Soochow J. Math., 31(1) (2005), 107-119.
[25] H. Roopaei, D. Foroutannia, M. İlkhan, E. E. Kara, *Cesàro Spaces and Norm of Operators on These Matrix Domains*, Mediterr. J. Math., 17, 121 (2020).
[26] G. Bennett, *Factorizing the classical inequalities*, Mem. Amer. Math. Soc., **576** (1996).

Journal of Mathematical Sciences and Modelling, 4 (1) (2021) 25-37
Research Article

Journal of Mathematical Sciences and Modelling

Journal Homepage: www.dergipark.gov.tr/jmsm
ISSN 2636-8692
DOI: http://dx.doi.org/10.33187/jmsm.843626

Dynamics and Bifurcation of $x_{n+1} = \frac{\alpha+\beta x_{n-2}}{A+Bx_n+Cx_{n-2}}$

Batool Raddad[1] **and Mohammad Saleh**[1*]

[1]*Department of Mathematics, Birzeit University, P.O.Box 14, West Bank, Palestine*
[*]*Corresponding author*

Article Info

Keywords: *Fixed point, Neimark-Sacker bifurcation, Stability.*
2010 AMS: *3A50, 39A23, 39A28, 39A30.*
Received: *20 December 2020*
Accepted: *19 April 2021*
Available online: *30 April 2021*

Abstract

In this paper, we study dynamics and bifurcation of the third order rational difference equation

$$x_{n+1} = \frac{\alpha+\beta x_{n-2}}{A+Bx_n+Cx_{n-2}}, \quad n = 0,1,2,\ldots$$

with positive parameters α,β,A,B,C and non-negative initial conditions $\{x_{-k},x_{-k+1},\ldots,x_0\}$. We study the dynamic behavior, the sufficient conditions for the existence of the Neimark-Sacker bifurcation, and the direction of the Neimark-Sacker bifurcation. Then, we give numerical examples with figures to support our results.

1. Introduction

The study of dynamical system is the focus of dynamical systems theory, which has application to a wide variety of fields such as mathematics, physics, chemistry, biology, medicine, engineering and economics. Dynamical systems are a fundamental part of bifurcation theory which studies the changes in the qualitative or topological structure of systems. A bifurcation occurs when a small change made to the bifurcation parameter of a system causes a qualitative or topological change in its behavior.
In this paper, we will study the third order rational difference equation

$$x_{n+1} = \frac{\alpha+\beta x_{n-2}}{A+Bx_n+Cx_{n-2}}, \quad n = 0,1,2,\ldots. \tag{1.1}$$

We focus on the dynamic behavior of the positive fixed points and the type of bifurcation exists where the change of stability occurs. Then, numerical examples are treated to support our results.
Local and global stability, period two solutions, boundedness, invariant intervals and semicycles of

$$x_{n+1} = \frac{\alpha+\beta x_{n-k}}{A+Bx_n+Cx_{n-k}}, \quad n = 0,1,2,\ldots \tag{1.2}$$

were studied by Guo-Mei Tang, Lin-Xia Hu, and Gang Ma in [1]. Also, it was shown that (1.2) has no nonnegative prime period-two solutions for even integer k. Equation (1.1) was studied by Ladas in [2].
The aim of this paper is to study the bifurcation of the third order rational difference equation (1.1). The change of variables $x_n = \frac{A}{B}y_n$ convert the rational difference equation (1.1) with five positive parameters into $y_{n+1} = \frac{p+qy_{n-2}}{1+y_n+ry_{n-2}}$, $n = 0,1,2,\ldots$ with three positive parameters p, q, and r, where $p = \frac{B}{A^2}\alpha$, $q = \frac{B}{A}$ and $r = \frac{C}{B}$. Recent studies on dynamics and bifurcation can be found in [3], [4], [5], [6], [7].

***Email address and ORCID number*:** **brdad@birzeit.edu, 0000-0002-2716-5740 (B. Raddad), msaleh@birzeit.edu, 0000-0002-4254-2540 (M. Saleh)**

2. Dynamics of $y_{n+1} = \frac{p+qy_{n-2}}{1+y_n+ry_{n-2}}$

In this section we will study the dynamics of the third order rational difference equation

$$y_{n+1} = \frac{p+qy_{n-2}}{1+y_n+ry_{n-2}} \tag{2.1}$$

with positive parameters p,q, and r, and non-negative initial conditions y_{-2},y_{-1} and y_0. Note that equation (2.1) has the unique positive fixed point $\bar{y} = \frac{q-1+\sqrt{(q-1)^2+4p(1+r)}}{2(1+r)}$.
In order to convert equation (2.1) to a third dimensional system, let $z_n = y_n, x_n = y_{n-1}$ and $t_n = y_{n-2}$. We have the following system

$$\begin{aligned} z_{n+1} &= \frac{p+qt_n}{1+z_n+rt_n} \\ x_{n+1} &= z_n \\ t_{n+1} &= x_n \end{aligned} \tag{2.2}$$

which has the positive fixed point $(\bar{y},\bar{y},\bar{y})$. In order to shift this fixed point to the origin, let $w_n = z_n - \bar{y}$, $v_n = x_n - \bar{y}$ and $u_n = t_n - \bar{y}$. System (2.2) corresponds

$$\begin{aligned} w_{n+1} &= \frac{p+q(u_n+\bar{y})}{1+(w_n+\bar{y})+r(u_n+\bar{y})} - \bar{y} \\ v_{n+1} &= w_n \\ u_{n+1} &= v_n \end{aligned} \tag{2.3}$$

System (2.3) has $(0,0,0)$ as a fixed point.
The Jacobian matrix of system (2.3) is

$$J(w,v,u) = \begin{pmatrix} -\frac{p+q(w_n+\bar{y})}{(1+w_n+\bar{y}+r(u_n+\bar{y}))^2} & 0 & \frac{q(1+w_n+\bar{y})-rp}{(1+w_n+\bar{y}+r(u_n+\bar{y}))^2} \\ 1 & 0 & 0 \\ 0 & 1 & 0 \end{pmatrix}$$

$$J(0,0,0) = \begin{pmatrix} -\frac{p+q\bar{y}}{(1+\bar{y}+r\bar{y})^2} & 0 & \frac{q+q\bar{y}-rp}{(1+\bar{y}+r\bar{y})^2} \\ 1 & 0 & 0 \\ 0 & 1 & 0 \end{pmatrix} = \begin{pmatrix} -\frac{\bar{y}}{1+\bar{y}+r\bar{y}} & 0 & \frac{q-r\bar{y}}{1+\bar{y}+r\bar{y}} \\ 1 & 0 & 0 \\ 0 & 1 & 0 \end{pmatrix}.$$

The characteristic polynomial of the Jacobian matrix J is

$$p(\lambda) = -\lambda^3 - \frac{\bar{y}}{1+\bar{y}+r\bar{y}}\lambda^2 + \frac{q-r\bar{y}}{1+\bar{y}+r\bar{y}}. \tag{2.4}$$

Let $p_1 = \frac{\bar{y}}{1+\bar{y}+r\bar{y}}$, $p_2 = 0$ and $p_3 = -\frac{q-r\bar{y}}{1+\bar{y}+r\bar{y}}$.
We will use the following theorem to determine the stability of the zero solution.

Theorem 2.1. *[8] For the third-order difference equation*

$$x(n+3) + p_1x(n+2) + p_2x(n+1) + p_3x(n) = 0, \tag{2.5}$$

the characteristic polynomial is

$$p(\lambda) = \lambda^3 + p_1\lambda^2 + p_2\lambda + p_3.$$

A necessary and sufficient condition for the zero solution to be asymptotically stable is

$$|\, p_1 + p_3 \,| < 1 + p_2 \quad \textit{and} \quad |\, p_2 - p_1p_3 \,| < 1 - p_3^2. \tag{2.6}$$

Theorem (2.1) implies that the zero solution is asymptotically stable if condition (2.6) holds which is equivalent to

$$|\, \frac{\bar{y}}{1+\bar{y}+r\bar{y}} - \frac{q-r\bar{y}}{1+\bar{y}+r\bar{y}} \,| < 1 \tag{2.7}$$

and

$$|\, \frac{\bar{y}}{1+\bar{y}+r\bar{y}} \times \frac{q-r\bar{y}}{1+\bar{y}+r\bar{y}} \,| < 1 - (\frac{q-r\bar{y}}{1+\bar{y}+r\bar{y}})^2. \tag{2.8}$$

Inequality (2.7) is equivalent to

$$1 + \frac{\bar{y}}{1+\bar{y}+r\bar{y}} - \frac{q-r\bar{y}}{1+\bar{y}+r\bar{y}} > 0, \tag{2.9}$$

and

$$1-\frac{\bar{y}}{1+\bar{y}+r\bar{y}}+\frac{q-r\bar{y}}{1+\bar{y}+r\bar{y}}>0, \tag{2.10}$$

and inequality (2.8) is equivalent to

$$1+\frac{\bar{y}}{1+\bar{y}+r\bar{y}}\times\frac{q-r\bar{y}}{1+\bar{y}+r\bar{y}}-(\frac{q-r\bar{y}}{1+\bar{y}+r\bar{y}})^2>0, \tag{2.11}$$

and

$$1-\frac{\bar{y}}{1+\bar{y}+r\bar{y}}\times\frac{q-r\bar{y}}{1+\bar{y}+r\bar{y}}-(\frac{q-r\bar{y}}{1+\bar{y}+r\bar{y}})^2>0. \tag{2.12}$$

Inequality (2.9) always holds since

$$1+\frac{\bar{y}}{1+\bar{y}+r\bar{y}}-\frac{q-r\bar{y}}{1+\bar{y}+r\bar{y}}=\frac{1-q+2(1+r)\bar{y}}{1+(1+r)\bar{y}}>0.$$

Also, inequality (2.10) holds for all values of the parameters p,q and r since,

$$1-\frac{\bar{y}}{1+\bar{y}+r\bar{y}}+\frac{q-r\bar{y}}{1+\bar{y}+r\bar{y}}=\frac{1+q}{1+(1+r)\bar{y}}>0.$$

Inequality (2.11) is equivalent to

$$1+\frac{q-r\bar{y}}{1+\bar{y}+r\bar{y}}[\frac{\bar{y}}{1+\bar{y}+r\bar{y}}-\frac{q-r\bar{y}}{1+\bar{y}+r\bar{y}}]>0. \tag{2.13}$$

Note that we take $\frac{q-r\bar{y}}{1+\bar{y}+r\bar{y}}$ as a common factor. Now, add -1 to both sides of inequality (2.13), we have

$$\frac{q-r\bar{y}}{1+\bar{y}+r\bar{y}}[\frac{(1+r)\bar{y}-q}{1+\bar{y}+r\bar{y}}]>-1 \tag{2.14}$$

Multiply both sides of (2.14) by $\frac{1+\bar{y}+r\bar{y}}{(1+r)\bar{y}-q}$, for $(1+r)\bar{y}-q<0$, we have

$$\frac{q-r\bar{y}}{1+\bar{y}+r\bar{y}}<\frac{1+\bar{y}+r\bar{y}}{q-(1+r)\bar{y}}.$$

Inequality (2.12) is equivalent to

$$\frac{q-r\bar{y}}{1+\bar{y}+r\bar{y}}[\frac{-\bar{y}}{1+\bar{y}+r\bar{y}}-\frac{q-r\bar{y}}{1+\bar{y}+r\bar{y}}]>-1$$

or,

$$\frac{q-r\bar{y}}{1+\bar{y}+r\bar{y}}[\frac{-\bar{y}-q+r\bar{y}}{1+\bar{y}+r\bar{y}}]>-1. \tag{2.15}$$

Note that for $(1+r)\bar{y}-q<0$, $r\bar{y}-\bar{y}-q<0$. So, if we multiply both sides of (2.15) by $\frac{1+\bar{y}+r\bar{y}}{r\bar{y}-\bar{y}-q}$, we have

$$\frac{q-r\bar{y}}{1+\bar{y}+r\bar{y}}<\frac{1+\bar{y}+r\bar{y}}{q-r\bar{y}+\bar{y}}.$$

Note that for $r\bar{y}-\bar{y}-q<r\bar{y}+\bar{y}-q<0$,

$$0<q-r\bar{y}-\bar{y}<q-r\bar{y}+\bar{y},$$

and hence,

$$\frac{1+\bar{y}+r\bar{y}}{q-r\bar{y}+\bar{y}}<\frac{1+\bar{y}+r\bar{y}}{q-r\bar{y}-\bar{y}}.$$

So for $q-(1+r)\bar{y}>0$, if $\frac{q-r\bar{y}}{1+\bar{y}+r\bar{y}}<\frac{1+\bar{y}+r\bar{y}}{q-r\bar{y}+\bar{y}}$, then $\frac{q-r\bar{y}}{1+\bar{y}+r\bar{y}}<\frac{1+\bar{y}+r\bar{y}}{q-r\bar{y}-\bar{y}}$, and hence, for $q-(1+r)\bar{y}>0$ if inequality (2.12) holds, then inequality (2.11) holds.
Note that if $q-(1+r)\bar{y}>0$, we have

$$q-(1+r)(\frac{q-1+\sqrt{(q-1)^2+4p(1+r)}}{2(1+r)}>0$$

or

$$q-\frac{q-1+\sqrt{(q-1)^2+4p(1+r)}}{2}>0$$

$$q+1-\sqrt{(q-1)^2+4p(1+r)}>0$$

$$q+1>\sqrt{(q-1)^2+4p(1+r)}$$

take the square of both sides, we get

$$q^2+2q+1>q^2-2q+1+4p(1+r)$$

or,

$$4q>4p(1+r)$$

$$p < \frac{q}{1+r}.$$

So for $p < \frac{q}{1+r}$, the zero solution is asymptotically stable if

$$\frac{q-r\bar{y}}{1+\bar{y}+r\bar{y}} < \frac{1+\bar{y}+r\bar{y}}{q-r\bar{y}+\bar{y}}. \tag{2.16}$$

Note that if we fix q and r and choose p as a parameter where $p < \frac{q}{1+r}$, then the stability exchanges at the value of p that satisfies equation $\frac{q-r\bar{y}}{1+\bar{y}+r\bar{y}} = \frac{1+\bar{y}+r\bar{y}}{q-r\bar{y}+\bar{y}}$. Name this value as p^*.

3. Existence of Neimark-Sacker bifurcation of $y_{n+1} = \frac{p+qy_{n-2}}{1+y_n+ry_{n-2}}$

In this section we study Neimark-Sacker bifurcation of (2.1) which occurs at $p = p^*$ as p is the bifurcation parameter. Note that equation (2.1) has no positive distinct periodic solutions of prime period two. Hence, we focus our attention on Neimark-Sacker bifurcation.

Theorem 3.1. *The characteristic polynomial (2.4) $p(\lambda)$ has two complex conjugate roots if one of the following cases holds*

1. $q - r\bar{y} < 0$
2. $\frac{q-r\bar{y}}{1+\bar{y}+r\bar{y}} > \frac{4}{27}(\frac{\bar{y}}{1+\bar{y}+r\bar{y}})^3$

Proof.

$$p(\lambda) = -\lambda^3 - \frac{\bar{y}}{1+\bar{y}+r\bar{y}}\lambda^2 + \frac{q-r\bar{y}}{1+\bar{y}+r\bar{y}}$$
$$\acute{p}(\lambda) = -3\lambda^2 - 2\frac{\bar{y}}{1+\bar{y}+r\bar{y}}\lambda$$

$\acute{p}(\lambda) = 0$ at $\lambda_1^* = -\frac{2}{3}(\frac{\bar{y}}{1+\bar{y}+r\bar{y}})$ or $\lambda_2^* = 0$.
Since, $\bar{y} > 0$, $\lambda_1^* < \lambda_2^*$. $p(\lambda)$ has local minimum value at $\lambda = \lambda_1^*$ and local maximum value at $\lambda = \lambda_2^*$. Note that $\lim_{\lambda\to-\infty} p(\lambda) = \infty$ and $\lim_{\lambda\to\infty} p(\lambda) = -\infty$.
So, $p(\lambda)$ has only one real root if one of the following cases holds

1. $p(\lambda_1^*) > 0$ and hence $p(\lambda_2^*) > p(\lambda_1^*) > 0$.
2. $p(\lambda_2^*) < 0$ and hence $p(\lambda_1^*) < p(\lambda_2^*) < 0$.

So, $p(\lambda)$ has two conjugate complex roots if one of the following holds

1. $p(\lambda_1^*) = -\frac{4}{27}(\frac{\bar{y}}{1+\bar{y}+r\bar{y}})^3 + \frac{q-r\bar{y}}{1+\bar{y}+r\bar{y}} > 0$.
2. $p(\lambda_2^*) = \frac{q-r\bar{y}}{1+\bar{y}+r\bar{y}} < 0$.

Consider case one. Note that $p(0) = \frac{q-r\bar{y}}{1+\bar{y}+r\bar{y}} > 0$ and $p(1) = -1 - \frac{\bar{y}}{1+\bar{y}+r\bar{y}} + \frac{q-r\bar{y}}{1+\bar{y}+r\bar{y}}$. Substitute the value of $\bar{y}$, we have $p(1) = -2\frac{\sqrt{(q-1)^2+4p(1+r)}}{q+1+\sqrt{(q-1)^2+4p(1+r)}} < 0$. So $p(\lambda)$ has a real root ξ such that $\xi \in (0,1)$.
In the second case, by similar argument we can show that $p(\lambda)$ has a real root of modulus less than one. Note that $p(0) < 0$ and $p(-1) > 0$ in this case.
Consider the case where $\frac{q-r\bar{y}}{1+\bar{y}+r\bar{y}} > \frac{4}{27}(\frac{\bar{y}}{1+\bar{y}+r\bar{y}})^3$. We will find where the conditions of Neimark-Sacker conditions hold. □

Theorem 3.2. *For $p < \frac{q}{1+r}$, the characteristic polynomial $p(\lambda)$ has two complex conjugate roots of modulus one and a real root of modulus less than one at $p = p^*$ if $q > 3$.*
Moreover, if $p^* > \frac{\left(2(1+r)\left(\frac{-(13r^2+16r-7)+\sqrt{(13r^2+16r-7)^2+4(6r-9)(9r^3+16r^2+7r)}}{2(9r^3+16r^2+7r)}\right)-(q-1)\right)^2-(q-1)^2}{4(1+r)}$, then Neimark-Sacker conditions hold.

To prove this theorem we need *Viète formula*.

Theorem 3.3. *[9](Viète formula) Given any polynomial of degree n, say*

$$P(x) = a_n x^n + a_{n-1}x^{n-1} + \ldots + a_1 x + a_0$$

with roots $r_1, r_2, \ldots, r_n$. Viète formula say that
$r_1 + r_2 + \ldots + r_n = -\frac{a_{n-1}}{a_n}$,
$(r_1r_2 + r_1r_3 + \ldots + r_1r_n) + (r_2r_3 + r_2r_4 + \ldots + r_2r_n) + \ldots + r_{n-1}r_n = \frac{a_{n-2}}{a_n}$,
$(r_1r_2r_3 + r_1r_2r_4 + \ldots + r_1r_2r_n) + (r_1r_3r_4 + r_1r_3r_5 + \ldots + r_1r_3r_n) + \ldots + r_{n-2}r_{n-1}r_n = -\frac{a_{n-3}}{a_n}$,
$\vdots$
$r_1r_2r_3\ldots r_n = (-1)^n\frac{a_0}{a_n}$.

Proof of theorem (3.2): Consider that $q > 3$ and $p < \frac{q}{1+r}$. Note that for $p < \frac{q}{1+r}$, we have $q-(1+r)\bar{y} > 0$ and hence $q - r\bar{y} > \bar{y}$. Recall that $1 > (\frac{\bar{y}}{1+\bar{y}+r\bar{y}})^2$ so $1 > \frac{4}{27}(\frac{\bar{y}}{1+\bar{y}+r\bar{y}})^2$ and hence, $\bar{y} > \frac{4}{27}(\frac{\bar{y}}{1+\bar{y}+r\bar{y}})^2\bar{y}$. So, $q - r\bar{y} > \bar{y} > \frac{4}{27}(\frac{\bar{y}}{1+\bar{y}+r\bar{y}})^2\bar{y}$. Multiply by $\frac{1}{1+\bar{y}+r\bar{y}}$, we get $\frac{q-r\bar{y}}{1+\bar{y}+r\bar{y}} > \frac{4}{27}(\frac{\bar{y}}{1+\bar{y}+r\bar{y}})^3$.
So, in this case the characteristic polynomial has two complex conjugate roots and another real root of modulus less than one as we have shown in the proof of theorem (3.1).
Now we will show that the modulus of the conjugate roots equals one at $p = p^*$. Let λ_1, λ_2 and λ_3 be the roots of $p(\lambda)$ where, λ_1 and λ_2 are the conjugate roots and λ_3 is the real root. Recall that $\lambda_3 = \xi$ has modulus less than one. By *Viète theorem*, we have

$$\lambda_1 + \lambda_2 + \lambda_3 = -\frac{\bar{y}}{1+\bar{y}+r\bar{y}} \tag{3.1}$$

$$\lambda_1\lambda_2\lambda_3 = \frac{q-r\bar{y}}{1+\bar{y}+r\bar{y}} \tag{3.2}$$

$$\lambda_1\lambda_2 + \lambda_1\lambda_3 + \lambda_2\lambda_3 = 0. \tag{3.3}$$

If λ_1 and λ_2 has modulus equal one, then $\lambda_1\lambda_2 = 1$. From (3.2), we get $\lambda_3 = \frac{q-r\bar{y}}{1+\bar{y}+r\bar{y}}$.
Substitute λ_3 in equation (3.1), we get $\lambda_1 + \lambda_2 + \frac{q-r\bar{y}}{1+\bar{y}+r\bar{y}} = -\frac{\bar{y}}{1+\bar{y}+r\bar{y}}$

$$\lambda_1 + \lambda_2 = -\frac{q-r\bar{y}+\bar{y}}{1+\bar{y}+r\bar{y}}. \tag{3.4}$$

Also, substitute λ_3 in equation (3.3), we get $\lambda_1 + \lambda_2 = -\frac{1}{\lambda_3} = -\frac{1+\bar{y}+r\bar{y}}{q-r\bar{y}}$.
That implies $\frac{q-r\bar{y}}{1+\bar{y}+r\bar{y}} = \frac{1+\bar{y}+r\bar{y}}{q-r\bar{y}+\bar{y}}$. This shows that at $p = p^*$ where p^* satisfies $\frac{q-r\bar{y}}{1+\bar{y}+r\bar{y}} = \frac{1+\bar{y}+r\bar{y}}{q-r\bar{y}+\bar{y}}$, $p(\lambda)$ has two complex conjugate roots of modulus one and a real root of modulus less than one for $p < \frac{q}{1+r}$.
As p is the bifurcation parameter and q and r are fixed, the bifurcation point is p^* which satisfies

$$\frac{q-r\bar{y}}{1+\bar{y}+r\bar{y}} = \frac{1+\bar{y}+r\bar{y}}{q-r\bar{y}+\bar{y}}$$

$$(1+\bar{y}+r\bar{y})^2 = (q-r\bar{y}+\bar{y})(q-r\bar{y})$$

$$(1+r)^2\bar{y}^2 + 2(1+r)\bar{y} + 1 = q^2 - qr\bar{y} + q\bar{y} - qr\bar{y} + r^2\bar{y}^2 - r\bar{y}^2$$

$$(1+3r)\bar{y}^2 + (2(1+r) + q(2r-1))\bar{y} - (q^2-1) = 0. \tag{3.5}$$

Equation (3.5) is a quadratic equation with the following roots

$$\bar{y} = \frac{-(2(1+r)+q(2r-1)) \pm \sqrt{(2(1+r)+q(2r-1))^2 + 4(q^2-1)(1+3r)}}{2(1+3r)}.$$

Since, $\bar{y} > 0$, for $q^2 > 1$

$$\bar{y} = \frac{-(2(1+r)+q(2r-1)) + \sqrt{(2(1+r)+q(2r-1))^2 + 4(q^2-1)(1+3r)}}{2(1+3r)}.$$

Substitute the value of $\bar{y}$, we have
$\frac{q-1+\sqrt{(q-1)^2+4p^*(1+r)}}{2(1+r)} = \frac{-(2(1+r)+q(2r-1))+\sqrt{(2(1+r)+q(2r-1))^2+4(q^2-1)(1+3r)}}{2(1+3r)}$
$\sqrt{(q-1)^2+4p^*(1+r)} = 1-q+2(1+r)\Big(\frac{-(2(1+r)+q(2r-1))+\sqrt{(2(1+r)+q(2r-1))^2+4(q^2-1)(1+3r)}}{2(1+3r)}\Big)$

$$p^* = \frac{\Big(1-q+2[1+r][\frac{-(2(1+r)+q(2r-1))+\sqrt{(2(1+r)+q(2r-1))^2+4(q^2-1)(1+3r)}}{2(1+3r)}]\Big)^2 - (q-1)^2}{4(1+r)}.$$

To check if Neimark-Saker bifurcation exists at p^*, we must show that $e^{ik\theta^*} \neq 1$ for $k = 1,2,3,4$ and $\acute{r}(p^*) \neq 0$ where $\lambda_{1,2} = \cos\theta^* \pm i\sin\theta^*$.
To show that $e^{i\theta^*} \neq 1$, let $\lambda = \cos\theta + i\sin\theta$ and $\bar{\lambda} = \cos\theta - i\sin\theta$ be the complex roots of $p(\lambda)$ at p^*. Substitute λ in $p(\lambda)$, we have $-\lambda^3 - \frac{\bar{y}}{1+\bar{y}+r\bar{y}}\lambda^2 + \frac{q-r\bar{y}}{1+\bar{y}+r\bar{y}} = 0$ or

$$\lambda^3 + \frac{\bar{y}}{1+\bar{y}+r\bar{y}}\lambda^2 - \frac{q-r\bar{y}}{1+\bar{y}+r\bar{y}} = 0. \tag{3.6}$$

Recall that at p^*, $\frac{q-r\bar{y}}{1+\bar{y}+r\bar{y}} = \frac{1+\bar{y}+r\bar{y}}{q-r\bar{y}+\bar{y}}$. So equation (3.6) becomes

$$\lambda^3 + \frac{\bar{y}}{1+\bar{y}+r\bar{y}}\lambda^2 - \frac{1+\bar{y}+r\bar{y}}{q-r\bar{y}+\bar{y}} = 0. \tag{3.7}$$

By similar argument, substitute $\bar{\lambda}$ in $p(\lambda)$ we get

$$\bar{\lambda}^3 + \frac{\bar{y}}{1+\bar{y}+r\bar{y}}\bar{\lambda}^2 - \frac{1+\bar{y}+r\bar{y}}{q-r\bar{y}+\bar{y}} = 0. \tag{3.8}$$

Multiply equation (3.7) by $\bar{\lambda}^2$, we have

$$\lambda + \frac{\bar{y}}{1+\bar{y}+r\bar{y}} - \frac{1+\bar{y}+r\bar{y}}{q-r\bar{y}+\bar{y}}\bar{\lambda}^2 = 0. \tag{3.9}$$

Also, multiply equation (3.8) by λ^2, we have

$$\bar{\lambda} + \frac{\bar{y}}{1+\bar{y}+r\bar{y}} - \frac{1+\bar{y}+r\bar{y}}{q-r\bar{y}+\bar{y}}\lambda^2 = 0. \tag{3.10}$$

Add (3.9) to (3.10), we get

$$\lambda + \bar{\lambda} + 2\left(\frac{\bar{y}}{1+\bar{y}+r\bar{y}}\right) - \frac{1+\bar{y}+r\bar{y}}{q-r\bar{y}+\bar{y}}(\lambda^2 + \bar{\lambda}^2) = 0 \tag{3.11}$$

Note that $\lambda + \bar{\lambda} = 2\cos\theta$ and $\lambda^2 + \bar{\lambda}^2 = 4\cos^2\theta - 2$.
Equation (3.11) becomes $2\cos\theta + 2\frac{\bar{y}}{1+\bar{y}+r\bar{y}} - \frac{1+\bar{y}+r\bar{y}}{q-r\bar{y}+\bar{y}}(4\cos^2\theta - 2) = 0$ or

$$-4\left(\frac{1+\bar{y}+r\bar{y}}{q-r\bar{y}+\bar{y}}\right)\cos^2\theta + 2\cos\theta + 2\left(\frac{\bar{y}}{1+\bar{y}+r\bar{y}}\right) + 2\left(\frac{1+\bar{y}+r\bar{y}}{q-r\bar{y}+\bar{y}}\right) = 0. \tag{3.12}$$

From equation (3.4), we have $\lambda + \bar{\lambda} = -\frac{q-r\bar{y}+\bar{y}}{1+\bar{y}+r\bar{y}}$ and hence, $2\cos\theta = -\frac{q-r\bar{y}+\bar{y}}{1+\bar{y}+r\bar{y}}$. That implies $\cos\theta = -\frac{1}{2}\left(\frac{q-r\bar{y}+\bar{y}}{1+\bar{y}+r\bar{y}}\right)$. Note that this is a root of equation (3.12) since, $-4\left(\frac{1+\bar{y}+r\bar{y}}{q-r\bar{y}+\bar{y}}\right)\left(-\frac{1}{2}\times\frac{q-r\bar{y}+\bar{y}}{1+\bar{y}+r\bar{y}}\right)^2 + 2\left(-\frac{1}{2}\times\frac{q-r\bar{y}+\bar{y}}{1+\bar{y}+r\bar{y}}\right) + 2\left(\frac{\bar{y}}{1+\bar{y}+r\bar{y}}\right) + 2\left(\frac{1+\bar{y}+r\bar{y}}{q-r\bar{y}+\bar{y}}\right) = -2\frac{q-r\bar{y}+\bar{y}}{1+\bar{y}+r\bar{y}} + 2\frac{\bar{y}}{1+\bar{y}+r\bar{y}} + 2\frac{1+\bar{y}+r\bar{y}}{q-r\bar{y}+\bar{y}} = 2\left(-\frac{q-r\bar{y}}{1+\bar{y}+r\bar{y}} + \frac{1+\bar{y}+r\bar{y}}{q-r\bar{y}+\bar{y}}\right) = 2(0) = 0$.
Note that $\frac{q-r\bar{y}}{1+\bar{y}+r\bar{y}} < 1$ or $q - r\bar{y} < 1 + \bar{y} + r\bar{y}$. To show this, note that $0 < 4p(1+r)$, add $(q-1)^2$ to the both sides, we get $(q-1)^2 < (q-1)^2 + 4p(1+r)$. Now, take the square root of the both sides, since we assume $q > 3$, we get $q - 1 < \sqrt{(q-1)^2 + 4p(1+r)}$ or, $q - 1 < \frac{q-1+\sqrt{(q-1)^2+4p(1+r)}}{2}$. That is equivalent to $q - 1 < (1+r)\bar{y}$. So $q - r\bar{y} < 1 + \bar{y} + r\bar{y}$ and hence, $\frac{q-r\bar{y}}{1+\bar{y}+r\bar{y}} < 1$.
Since, $\frac{1+\bar{y}+r\bar{y}}{q-r\bar{y}+\bar{y}} = \frac{q-r\bar{y}}{1+\bar{y}+r\bar{y}} < 1$, $\cos\theta < -\frac{1}{2}$.

Also, note that $\frac{1}{2} < \frac{1+\bar{y}+r\bar{y}}{q-r\bar{y}+\bar{y}}$. To show that we will use that for $q > 3$, we have $2 - q < 0$ and then $\frac{2-q}{1+r} < p$, multiply both sides with 4, we have $8 - 4q < 4p(1+r)$. Add $(q-1)^2$ to the both sides, we get $q^2 - 6q + 9 < (q-1)^2 + 4p(1+r)$ or $(q-3)^2 < (q-1)^2 + 4p(1+r)$. Take the square root of both sides. Since we take $q > 3$, we get $q - 3 < \sqrt{(q-1)^2 + 4p(1+r)}$. Add $q - 1$ to the both sides, we have $2q - 4 < q - 1 + \sqrt{(q-1)^2 + 4p(1+r)}$ or, $q - 2 < (1+r)\bar{y}$ and hence, $q - 2 < (1+3r)\bar{y}$ or, $q - r\bar{y} + \bar{y} < 2 + 2\bar{y} + 2r\bar{y}$ or $\frac{1}{2} < \frac{1+\bar{y}+r\bar{y}}{q-r\bar{y}+\bar{y}}$.
Since, $\frac{1}{2} < \frac{1+\bar{y}+r\bar{y}}{q-r\bar{y}+\bar{y}}$, $\cos\theta > -1$.
So, at p^* where $\frac{1}{2} < \frac{1+\bar{y}+r\bar{y}}{q-r\bar{y}+\bar{y}} = \frac{q-r\bar{y}}{1+\bar{y}+r\bar{y}} < 1$, there exists $\theta^* \in (\frac{\pi}{2}, \pi)$ such that $-1 < \cos\theta^* = -\frac{1}{2}\left(\frac{q-r\bar{y}+\bar{y}}{1+\bar{y}+r\bar{y}}\right) < -\frac{1}{2}$. Note that $e^{ik\theta^*} \neq 1$ for $k = 1, 2, 3, 4$.

To check if $\acute{r}(p^*) \neq 0$, it is enough to show that $\frac{d|\lambda|^2}{dp}\,|_{p=p^*} \neq 0$.

$$p(\lambda) = -\lambda^3 - \frac{\bar{y}}{1+\bar{y}+r\bar{y}}\lambda^2 + \frac{q-r\bar{y}}{1+\bar{y}+r\bar{y}}.$$

$$\frac{d|\lambda|^2}{dp}\,|_{p=p^*} = \frac{d(\lambda\bar{\lambda})}{dp}\,|_{p=p^*} = \left[\lambda\frac{d\bar{\lambda}}{dp} + \bar{\lambda}\frac{d\lambda}{dp}\right]|_{p=p^*} = \lambda\left(\frac{dp(\bar{\lambda})}{dp}\cdot\frac{d\bar{\lambda}}{dp(\bar{\lambda})}\right) + \bar{\lambda}\left(\frac{dp(\lambda)}{dp}\cdot\frac{d\lambda}{dp(\lambda)}\right).$$

$$\frac{d\,|\,\lambda\,|^2}{dp}\,|_{p=p^*} = \bar{\lambda}\left(\frac{-\frac{1}{(1+\bar{y}+r\bar{y})^2\sqrt{(q-1)^2+4p(1+r)}}\lambda^2 - \frac{r}{(1+\bar{y}+r\bar{y})\sqrt{(q-1)^2+4p(1+r)}} - \frac{(1+r)(q-r\bar{y})}{(1+\bar{y}+r\bar{y})^2\sqrt{(q-1)^2+4p(1+r)}}}{-3\lambda^2 - 2\frac{\bar{y}}{1+\bar{y}+r\bar{y}}\lambda}\right)$$

$$+\lambda\left(\frac{-\frac{1}{(1+\bar{y}+r\bar{y})^2\sqrt{(q-1)^2+4p(1+r)}}\bar{\lambda}^2 - \frac{r}{(1+\bar{y}+r\bar{y})\sqrt{(q-1)^2+4p(1+r)}} - \frac{(1+r)(q-r\bar{y})}{(1+\bar{y}+r\bar{y})^2\sqrt{(q-1)^2+4p(1+r)}}}{-3\bar{\lambda}^2 - 2\frac{\bar{y}}{1+\bar{y}+r\bar{y}}\bar{\lambda}}\right)$$

At p^* $\lambda\bar{\lambda} = 1$, so we have

$$\frac{d\,|\,\lambda\,|^2}{dp}\,|_{p=p^*} = \left(\frac{-\frac{1}{(1+\bar{y}+r\bar{y})^2\sqrt{(q-1)^2+4p(1+r)}}\lambda^2 - \frac{r}{(1+\bar{y}+r\bar{y})\sqrt{(q-1)^2+4p(1+r)}} - \frac{(1+r)(q-r\bar{y})}{(1+\bar{y}+r\bar{y})^2\sqrt{(q-1)^2+4p(1+r)}}}{-3\lambda^3 - 2\frac{\bar{y}}{1+\bar{y}+r\bar{y}}\lambda^2}\right)$$

$$+\left(\frac{-\frac{1}{(1+\bar{y}+r\bar{y})^2\sqrt{(q-1)^2+4p(1+r)}}\bar{\lambda}^2 - \frac{r}{(1+\bar{y}+r\bar{y})\sqrt{(q-1)^2+4p(1+r)}} - \frac{(1+r)(q-r\bar{y})}{(1+\bar{y}+r\bar{y})^2\sqrt{(q-1)^2+4p(1+r)}}}{-3\bar{\lambda}^3 - 2\frac{\bar{y}}{1+\bar{y}+r\bar{y}}\bar{\lambda}^2}\right)$$

$$= \left(\frac{\left(-\frac{1}{(1+\bar{y}+r\bar{y})^2\sqrt{(q-1)^2+4p(1+r)}}\lambda^2 - \frac{r}{(1+\bar{y}+r\bar{y})\sqrt{(q-1)^2+4p(1+r)}} - \frac{(1+r)(q-r\bar{y})}{(1+\bar{y}+r\bar{y})^2\sqrt{(q-1)^2+4p(1+r)}}\right)\left(-3\bar{\lambda}^3 - 2\frac{\bar{y}}{1+\bar{y}+r\bar{y}}\bar{\lambda}^2\right)}{\left(-3\lambda^3 - 2\frac{\bar{y}}{1+\bar{y}+r\bar{y}}\lambda^2\right)\left(-3\bar{\lambda}^3 - 2\frac{\bar{y}}{1+\bar{y}+r\bar{y}}\bar{\lambda}^2\right)}\right)$$

$$+\left(\frac{\left(-\frac{1}{(1+\bar{y}+r\bar{y})^2\sqrt{(q-1)^2+4p(1+r)}}\bar{\lambda}^2 - \frac{r}{(1+\bar{y}+r\bar{y})\sqrt{(q-1)^2+4p(1+r)}} - \frac{(1+r)(q-r\bar{y})}{(1+\bar{y}+r\bar{y})^2\sqrt{(q-1)^2+4p(1+r)}}\right)\left(-3\lambda^3 - 2\frac{\bar{y}}{1+\bar{y}+r\bar{y}}\lambda^2\right)}{\left(-3\lambda^3 - 2\frac{\bar{y}}{1+\bar{y}+r\bar{y}}\lambda^2\right)\left(-3\bar{\lambda}^3 - 2\frac{\bar{y}}{1+\bar{y}+r\bar{y}}\bar{\lambda}^2\right)}\right).$$

The denominator is non zero term since

$$(-3\lambda^3-2\frac{\bar{y}}{1+\bar{y}+r\bar{y}}\lambda^2)(-3\bar{\lambda}^3-2\frac{\bar{y}}{1+\bar{y}+r\bar{y}}\bar{\lambda}^2)=9+6\frac{\bar{y}}{1+\bar{y}+r\bar{y}}(\lambda+\bar{\lambda})+4(\frac{\bar{y}}{1+\bar{y}+r\bar{y}})^2.$$

At p^* $\lambda+\bar{\lambda}=-\frac{q-r\bar{y}+\bar{y}}{1+\bar{y}+r\bar{y}}$, so the denominator becomes

$$9-6\frac{\bar{y}(q-r\bar{y}+\bar{y})}{(1+\bar{y}+r\bar{y})^2}+4(\frac{\bar{y}}{1+\bar{y}+r\bar{y}})^2=9-6\frac{\bar{y}(q-r\bar{y})}{(1+\bar{y}+r\bar{y})^2}-2(\frac{\bar{y}}{1+\bar{y}+r\bar{y}})^2.$$

Note that $\frac{\bar{y}}{1+\bar{y}+r\bar{y}}<1$ so $-(\frac{\bar{y}}{1+\bar{y}+r\bar{y}})^2>-1$ and $-\frac{\bar{y}(q-r\bar{y})}{(1+\bar{y}+r\bar{y})^2}>-\frac{q-r\bar{y}}{1+\bar{y}+r\bar{y}}$.
So,

$$9-6\frac{\bar{y}(q-r\bar{y})}{(1+\bar{y}+r\bar{y})^2}-2(\frac{\bar{y}}{1+\bar{y}+r\bar{y}})^2>9-6\frac{q-r\bar{y}}{1+\bar{y}+r\bar{y}}-2$$

and since at p^* $\frac{q-r\bar{y}}{1+\bar{y}+r\bar{y}}<1$,

$$9-6\frac{q-r\bar{y}}{1+\bar{y}+r\bar{y}}-2>9-6-2=1>0.$$

It remains to show that the numerator is non zero term.
The numerator is
$\Big(-\frac{1}{(1+\bar{y}+r\bar{y})^2\sqrt{(q-1)^2+4p(1+r)}}\lambda^2-\frac{r}{(1+\bar{y}+r\bar{y})\sqrt{(q-1)^2+4p(1+r)}}-\frac{(1+r)(q-r\bar{y})}{(1+\bar{y}+r\bar{y})^2\sqrt{(q-1)^2+4p(1+r)}}\Big)\Big(-3\bar{\lambda}^3-2\frac{\bar{y}}{1+\bar{y}+r\bar{y}}\bar{\lambda}^2\Big)+\Big(-\frac{1}{(1+\bar{y}+r\bar{y})^2\sqrt{(q-1)^2+4p(1+r)}}\bar{\lambda}^2-\frac{r}{(1+\bar{y}+r\bar{y})\sqrt{(q-1)^2+4p(1+r)}}-\frac{(1+r)(q-r\bar{y})}{(1+\bar{y}+r\bar{y})^2\sqrt{(q-1)^2+4p(1+r)}}\Big)\Big(-3\lambda^3-2\frac{\bar{y}}{1+\bar{y}+r\bar{y}}\lambda^2\Big)$
$=\frac{3}{(1+\bar{y}+r\bar{y})^2\sqrt{(q-1)^2+4p(1+r)}}(\lambda+\bar{\lambda})+\Big(\frac{3r}{(1+\bar{y}+r\bar{y})\sqrt{(q-1)^2+4p(1+r)}}+\frac{3(1+r)(q-ry)}{(1+\bar{y}+r\bar{y})^2\sqrt{(q-1)^2+4p(1+r)}}\Big)$
$(\lambda^3+\bar{\lambda}^3)+\Big(\frac{2r\bar{y}}{(1+\bar{y}+r\bar{y})^2\sqrt{(q-1)^2+4p(1+r)}}+\frac{2(1+r)(q-ry)y}{(1+\bar{y}+r\bar{y})^3\sqrt{(q-1)^2+4p(1+r)}}\Big)(\lambda^2+\bar{\lambda}^2)+\frac{4\bar{y}}{(1+\bar{y}+r\bar{y})^3\sqrt{(q-1)^2+4p(1+r)}}.$

Recall that at p^* $\frac{q-r\bar{y}}{1+\bar{y}+r\bar{y}}=\frac{1+\bar{y}+r\bar{y}}{q-r\bar{y}+\bar{y}}$. Also, at p^* $\lambda+\bar{\lambda}=2\cos\theta_0$, $\lambda^2+\bar{\lambda}^2=4\cos^2\theta_0-2$ and $\lambda^3+\bar{\lambda}^3=8\cos^3\theta_0-6\cos\theta_0$ where $\cos\theta_0=-\frac{1}{2}(\frac{q-r\bar{y}+\bar{y}}{1+\bar{y}+r\bar{y}})$.
The numerator at p^* is

$$-\frac{3(q-r\bar{y}+\bar{y})}{(1+\bar{y}+r\bar{y})^3\sqrt{(q-1)^2+4p(1+r)}}-\frac{3r(q-r\bar{y}+\bar{y})^3}{(1+\bar{y}+r\bar{y})^4\sqrt{(q-1)^2+4p(1+r)}}-\frac{3(1+r)(q-r\bar{y}+\bar{y})^2}{(1+\bar{y}+r\bar{y})^4\sqrt{(q-1)^2+4p(1+r)}}$$
$$+\frac{9r(q-r\bar{y}+\bar{y})}{(1+\bar{y}+r\bar{y})^2\sqrt{(q-1)^2+4p(1+r)}}+\frac{9(1+r)}{(1+\bar{y}+r\bar{y})^2\sqrt{(q-1)^2+4p(1+r)}}+\frac{2r\bar{y}(q-r\bar{y}+\bar{y})^2}{(1+\bar{y}+r\bar{y})^4\sqrt{(q-1)^2+4p(1+r)}}$$
$$+\frac{2(1+r)(q-r\bar{y}+\bar{y})\bar{y}}{(1+\bar{y}+r\bar{y})^4\sqrt{(q-1)^2+4p(1+r)}}-\frac{4r\bar{y}}{(1+\bar{y}+r\bar{y})^2\sqrt{(q-1)^2+4p(1+r)}}-\frac{4(1+r)\bar{y}}{(1+\bar{y}+r\bar{y})^2(q-r\bar{y}+\bar{y})\sqrt{(q-1)^2+4p(1+r)}}+\frac{4\bar{y}}{(1+\bar{y}+r\bar{y})^3\sqrt{(q-1)^2+4p(1+r)}}.$$

Note that $-1<\cos\theta^*<-\frac{1}{2}$ which implies that $1<\frac{q-r\bar{y}+\bar{y}}{1+\bar{y}+r\bar{y}}<2$ and $-\frac{1}{q-r\bar{y}+\bar{y}}>-\frac{1}{1+\bar{y}+r\bar{y}}$.
The numerator is greater than

$$-\frac{6}{(1+\bar{y}+r\bar{y})^2\sqrt{(q-1)^2+4p(1+r)}}-\frac{12(1+r)}{(1+\bar{y}+r\bar{y})^2\sqrt{(q-1)^2+4p(1+r)}}+\frac{9r}{(1+\bar{y}+r\bar{y})\sqrt{(q-1)^2+4p(1+r)}}+\frac{9(1+r)}{(1+\bar{y}+r\bar{y})^2\sqrt{(q-1)^2+4p(1+r)}}+\frac{2r\bar{y}}{(1+\bar{y}+r\bar{y})^2\sqrt{(q-1)^2+4p(1+r)}}+$$
$$\frac{2(1+r)\bar{y}}{(1+\bar{y}+r\bar{y})^3\sqrt{(q-1)^2+4p(1+r)}}-\frac{4r\bar{y}}{(1+\bar{y}+r\bar{y})^2\sqrt{(q-1)^2+4p(1+r)}}-\frac{4(1+r)\bar{y}}{(1+\bar{y}+r\bar{y})^3\sqrt{(q-1)^2+4p(1+r)}}+\frac{4\bar{y}}{(1+\bar{y}+r\bar{y})^3\sqrt{(q-1)^2+4p(1+r)}}$$
$$=\frac{2(1-r)\bar{y}}{(1+\bar{y}+r\bar{y})^3\sqrt{(q-1)^2+4p(1+r)}}-\frac{6+3(1+r)+2r\bar{y}}{(1+\bar{y}+r\bar{y})^2\sqrt{(q-1)^2+4p(1+r)}}$$

$$+\frac{9r}{(1+\bar{y}+r\bar{y})\sqrt{(q-1)^2+4p(1+r)}}. \tag{3.13}$$

Term (3.13) is positive if $2(1-r)\bar{y}-(6+3(1+r)+2r\bar{y})(1+\bar{y}+r\bar{y})+9r(1+\bar{y}+r\bar{y})^2>0$.
That is equivalent to $(9r^3+16r^2+7r)\bar{y}^2+(13r^2+16r-7)\bar{y}+6r-9>0$
or

$$\bar{y}>\frac{-(13r^2+16r-7)+\sqrt{(13r^2+16r-7)^2+4(6r-9)(9r^3+16r^2+7r)}}{2(9r^3+16r^2+7r)}.$$

Substitute the value of $\bar{y}$, we get

$$\frac{q-1+\sqrt{(q-1)^2+4p^*(1+r)}}{2(1+r)}>\frac{-(13r^2+16r-7)+\sqrt{(13r^2+16r-7)^2+4(6r-9)(9r^3+16r^2+7r)}}{2(9r^3+16r^2+7r)}$$

multiply both sides by $2(1+r)$ and then add $-(q-1)$ for both sides, we get

$$\sqrt{(q-1)^2+4p^*(1+r)}>2(1+r)\Big(\frac{-(13r^2+16r-7)+\sqrt{(13r^2+16r-7)^2+4(6r-9)(9r^3+16r^2+7r)}}{2(9r^3+16r^2+7r)}\Big)-(q-1)$$

take the square of both sides, we obtain

$$(q-1)^2+4p^*(1+r)>\Big(2(1+r)(\frac{-(13r^2+16r-7)+\sqrt{(13r^2+16r-7)^2+4(6r-9)(9r^3+16r^2+7r)}}{2(9r^3+16r^2+7r)})-(q-1)\Big)^2$$

add $-(q-1)^2$ for the both sides and then multiply by $\frac{1}{4(1+r)}$, we get

$$p^* > \frac{\left(2(1+r)\left(\frac{-(13r^2+16r-7)+\sqrt{(13r^2+16r-7)^2+4(6r-9)(9r^3+16r^2+7r)}}{2(9r^3+16r^2+7r)}\right)-(q-1)\right)^2-(q-1)^2}{4(1+r)}$$

If term (3.13) is grater than zero, then $\frac{d|\lambda|^2}{dp}\mid_{p=p^*} > 0$, and then Neimark-Sacker bifurcation conditions are satisfied.

4. Direction of Neimark-Sacker bifurcation

In this section we will use the normal form theory of discrete systems to determine the direction and the stability of the invariant closed curve bifurcating from the positive fixed point (see [9]). System (2.3) can be written as

$$Y_{n+1} = JY_n + G(Y_n) \tag{4.1}$$

where, $J = \begin{pmatrix} -\frac{q-r\bar{y}}{1+\bar{y}+r\bar{y}} & 0 & \frac{\bar{y}}{1+\bar{y}+r\bar{y}} \\ 1 & 0 & 0 \\ 0 & 1 & 0 \end{pmatrix}$ and, $Y_n = \begin{pmatrix} w_n \\ v_n \\ u_n \end{pmatrix}$

$G(Y) = \frac{1}{2}B(Y,Y) + \frac{1}{6}C(Y,Y,Y) + O(\| Y \|^3)$

$B(Y,Y) = \begin{pmatrix} B_1(Y,Y) \\ 0 \\ 0 \end{pmatrix}$ and, $C(Y,Y,Y) = \begin{pmatrix} C_1(Y,Y,Y) \\ 0 \\ 0 \end{pmatrix}$

$B_i(x,y) = \sum_{j,k=1}^{n} \frac{\partial^2 X_i(\xi)}{\partial\xi_j\partial\xi_k}\mid_{\xi=0} (x_j y_k)$ and $C_i(x,y,z) = \sum_{j,k,l=1}^{n} \frac{\partial^3 X_i(\xi)}{\partial\xi_j\partial\xi_k}\mid_{\xi=0} (x_j y_k z_l)$

$B_1(\phi,\psi) = \frac{2(q-r\bar{y})}{(1+\bar{y}+r\bar{y})^2}\phi_1\psi_1 - \frac{2r\bar{y}}{(1+\bar{y}+r\bar{y})^2}\phi_3\psi_3 + \frac{qr-(r^2+1)\bar{y}}{(1+\bar{y}+r\bar{y})^2}[\phi_3\psi_1+\phi_1\psi_3]$,

$C_1(\phi,\psi,\eta) = -\frac{6(q-r\bar{y})}{(1+\bar{y}+r\bar{y})^3}\phi_1\psi_1\eta_1 + \frac{2\bar{y}-4r(q-r\bar{y})}{(1+\bar{y}+r\bar{y})^3}\left(\phi_1\psi_1\eta_3+\phi_3\psi_1\eta_1+\phi_1+\psi_3\eta_1\right) + \frac{2r^3\bar{y}+4r\bar{y}-2r^2q}{(1+\bar{y}+r\bar{y})^3}\left(\phi_1\psi_3\eta_3+\phi_3\psi_1\eta_3+\phi_3\psi_3\eta_1\right) + \frac{6r^2\bar{y}}{(1+\bar{y}+r\bar{y})^3}\phi_3\psi_3\eta_3$,

Recall that $\theta_0 = \cos^{-1}(-\frac{q-r\bar{y}+\bar{y}}{2(1+\bar{y}+r\bar{y})})$. Let q and p^* be the eigenvectors corresponding to the eigenvalues $\lambda = \cos\theta_0 + i\sin\theta_0 = e^{i\theta_0}$ and $\bar{\lambda} = \cos\theta_0 - i\sin\theta_0 = e^{-i\theta_0}$, respectively, where $q \sim \begin{pmatrix} e^{i\theta_0} \\ 1 \\ e^{-i\theta_0} \end{pmatrix}$ and $p^* \sim \begin{pmatrix} \frac{1+\bar{y}+r\bar{y}}{\bar{y}}e^{-i\theta_0} \\ e^{i\theta_0} \\ 1 \end{pmatrix}$. Note that $\sim$ means that the vector can differ from that given by a non-zero complex multiplier. To normalize q and p^*, we must find ζ such that $< \zeta p^*, q >= 1$, where $< .,. >$ is the standard scalar product in $\mathbb{C}^3$.

$$< \zeta p^*, q >= \zeta \sum_{i=1}^{3} \bar{p_i^*} q_i = \zeta\left(\frac{1+\bar{y}+r\bar{y}}{\bar{y}}e^{-i\theta_0} + 2e^{-i\theta_0}\right)$$

Set $\zeta = \frac{1}{\frac{1+\bar{y}+r\bar{y}}{\bar{y}}e^{2i\theta_0}+2e^{-i\theta_0}}$. So take $p = \zeta * p^*$. We have $< p,q >= 1$.

The critical real eigenspace T^c corresponding to $\lambda_{1,2}$ is two-dimensional and is spanned by $\{Re(q), Im(q)\}$. The real eigenspace T^s corresponding to the real eigenvalues of J is one-dimensional. Any vector $x \in \mathbb{R}^3$ can be decomposed as

$$x = zq + \bar{z}\bar{q} + y$$

where, $z \in \mathbb{C}^1$, $\bar{z}\bar{q} \in T^c$ and $y \in T^s$. The complex variable z is a coordinate on T^c. We have

$$z =< p, x >,$$

$$y = x - < p,x > q - < \bar{p},x > \bar{q}.$$

In these coordinates, the map (4.1) takes the form

$$\tilde{z} = e^{i\theta_0}z + < p, G(zq+\bar{z}\bar{q}+y) >,$$

$$\tilde{y} = Jy + G(zq+\bar{z}\bar{q}+y) - < p, G(zq+\bar{z}\bar{q}+y) > q - < \bar{p}, G(zq+\bar{z}\bar{q}+y) > \bar{q}.$$

The previous system can be written as

$$\tilde{z} = e^{i\theta_0}z + \frac{1}{2}G_{20}z^2 + G_{11}z\bar{z} + \frac{1}{2}G_{02}\bar{z}^2 + \frac{1}{2}G_{21}z^2\bar{z} + < G_{10}, y > z + < G_{01}, y > \bar{z},$$

$$\tilde{y} = Jy + \frac{1}{2}H_{20}z^2 + H_{11}z\bar{z} + \frac{1}{2}H_{02}\bar{z}^2 + \frac{1}{2}H_{21}z^2\bar{z}$$

where,

$$G_{20} =< p, B(q,q) >, G_{11} =< p, B(q,\bar{q} >, G_{02} =< p, B(\bar{q},\bar{q}) >, G_{21} =< p, C(q,q,\bar{q}) >$$

and

$$H_{20} = B(q,q) - < p, B(q,q) > q - < \bar{p}, B(q,q) > \bar{q},$$

$$H_{11} = B(q,\bar{q}) - < p, B(q,\bar{q}) > q - < \bar{p}, B(q,\bar{q}) > \bar{q}$$

and

$$< G_{10}, y >=< p, B(q,y) >, < G_{01}, y >=< p, B(\bar{q}, y) >$$

where the scaler product is in $\mathbb{C}^3$.
From the center manifold theorem, there exists a center manifold W^c which can be approximated as

$$Y = V(z,\bar{z}) = \frac{1}{2}w_{20}z^2 + w_{11}z\bar{z} + \frac{1}{2}w_{02}\bar{z}^2$$

where $< q, w_{ij} >= 0$. The vectors $w_{ij} \in \mathbb{C}^3$ can be found from the linear equations

$$(e^{2i\theta_0}I_3 - J)w_{20} = H_{20},$$

$$(I_3 - J)w_{11} = H_{11},$$

$$(e^{-2i\theta_0}I_3 - J)w_{02} = H_{02}.$$

These equations has unique solutions. Note that the matrices $(I_3 - J)$ and $(e^{\pm 2i\theta_0}I_3 - J)$ are invertible in $\mathbb{C}^3$ since 1 and $e^{\pm 2i\theta_0}$ are not eigenvalues of J. Recall that $e^{i\theta_0} \neq 1$. So, z can be written as
$\tilde{z} = e^{i\theta_0}\bar{z} + \frac{1}{2}G_{20}z^2 + G_{11}z\bar{z} + \frac{1}{2}G_{02}\bar{z}^2 + \frac{1}{2}[G_{21} + 2 < p, B(q, (I-J)^{-1}H_{11}) > + < p, B(\bar{q}, (e^{2i\theta_0}I - J)^{-1}H_{20}) >]z^2\bar{z} + \ldots$.
Taking into account the identities

$$(I-J)^{-1}q = \frac{1}{1-e^{i\theta_0}}q,\ (e^{2i\theta_0}I - J)^{-1}q = \frac{e^{-i\theta_0}}{e^{i\theta_0}-1}q,\ (i-j)^{-1}\bar{q} = \frac{1}{1-e^{i\theta_0}}\bar{q}$$

and

$$(e^{2i\theta_0}I - J)^{-1}\bar{q} = \frac{e^{-i\theta_0}}{e^{i\theta_0}-1}\bar{q}.$$

Also, z can be written using the map

$$\tilde{z} = e^{i\theta_0}z + \sum_{k,l\geq 2}\frac{1}{k!j!}g_{kj}z^k\bar{z}^j \tag{4.2}$$

where, $g_{20} =< p, B(q,q) >$, $g_{11} =< p, B(q,\bar{q}) >$, $g_{02} =< p, B(\bar{q},\bar{q}) >$
and $g_{21} =< p, C(q,q,\bar{q}) > +2 < p, B(q, (I-J)^{-1}B(q,\bar{q})) > + < p, B(\bar{q}, (e^{2i\theta_0}I-J)^{-1}B(q,q)) > + \frac{e^{-i\theta_0}(1-2e^{i\theta_0})}{1-e^{i\theta_0}} < p, B(q,q) >< p, B(q,\bar{q}) > - \frac{2}{1-e^{-i\theta_0}} |< p, B(q,\bar{q}) >|^2 - \frac{e^{i\theta_0}}{e^{3i\theta_0}-1} |< p, B(\bar{q},\bar{q}) >|^2$.
The map (4.2) can be transformed into the form

$$\tilde{z} = e^{i\theta_0}z(1 + d(p^*)) \mid z^2 \mid$$

where, p^* is the value of the bifurcation parameter p where the Neimark-Sacker bifurcation exists and the real number $a(p^*) = Re(d(p^*))$, that determines the direction of bifurcation of the closed invariant curve, can be computed by the following formula

$$a(p^*) = Re\Big(\frac{e^{-i\theta_0}g_{21}}{2}\Big) - Re\Big(\frac{(1-2e^{i\theta_0})e^{-2i\theta_0}}{2(1-e^{i\theta_0})}g_{20}g_{11}\Big) - \frac{1}{2} \mid g_{11} \mid^2 - \frac{1}{4} \mid g_{02} \mid^2 .$$

Now, we compute $a(p^*)$. Recall that $g_{20} =< p, B(q,q) >$

where, $B(q,q) = \begin{pmatrix} \frac{2\left(q-r\bar{y}\right)e^{2i\theta_0} - 2r\bar{y}e^{-2i\theta_0} + 2qr - 2\left(r^2+1\right)\bar{y}}{(1+\bar{y}+r\bar{y})^2} \\ 0 \\ 0 \end{pmatrix}$.

$$g_{20} = \frac{1}{e^{3i\theta_0} + 2\frac{\bar{y}}{1+\bar{y}+r\bar{y}}}\Big(\frac{2qe^{2i\theta_0} + 2qr - 2(r^2+1)\bar{y} - 4r\bar{y}\cos 2\theta_0}{(1+\bar{y}+r\bar{y})^2}\Big).$$

$g_{11} =< p, B(q,\bar{q}) >$, where $B(q,\bar{q}) = \begin{pmatrix} \frac{2\left(q-r\bar{y}\right) - 2r\bar{y} + 2\left(qr - (r^2+1)\bar{y}\right)\cos 2\theta_0}{(1+\bar{y}+r\bar{y})^2} \\ 0 \\ 0 \end{pmatrix}$

so,

$$g_{11} = \frac{1}{e^{3i\theta_0} + 2\frac{\bar{y}}{1+\bar{y}+r\bar{y}}}\Big(\frac{2(q-r\bar{y}) - 2r\bar{y} + 2(qr - (r^2+1)\bar{y})\cos 2\theta_0}{(1+\bar{y}+r\bar{y})^2}\Big).$$

$g_{02} =< p, B(\bar{q},\bar{q}) >$ where $B(\bar{q},\bar{q}) = \begin{pmatrix} \frac{2qe^{-2i\theta_0} - 4r\bar{y}\cos 2\theta + 2\left(qr - (r^2+1)\right)}{(1+\bar{y}+r\bar{y})^2} \\ 0 \\ 0 \end{pmatrix}$.

So,

$$g_{02} = \zeta\frac{1+\bar{y}+r\bar{y}}{\bar{y}}e^{-i\theta_0}\Big(\frac{2qe^{-2i\theta_0} - 4r\bar{y}\cos 2\theta + 2(qr - (r^2+1))}{(1+\bar{y}+r\bar{y})^2}\Big)$$

or

$$g_{02} = \frac{1}{e^{3i\theta_0} + 2\frac{\bar{y}}{1+\bar{y}+r\bar{y}}}\Big(\frac{2qe^{-2i\theta_0} - 4r\bar{y}\cos 2\theta + 2(qr-(r^2+1))}{(1+\bar{y}+r\bar{y})^2}\Big).$$

$g_{21} =< p,C(q,q,\bar{q}) > +2 < p,B(q,(I-J)^{-1}B(q,\bar{q})) > + < p,B(\bar{q},(e^{2i\theta_0}I-J)^{-1}B(q,q)) > + \frac{e^{-i\theta_0}(1-2e^{i\theta_0})}{1-e^{i\theta_0}} < p,B(q,q) >< p,B(q,\bar{q}) > - \frac{2}{1-e^{-i\theta_0}} |< p,B(q,\bar{q}) >|^2 - \frac{e^{i\theta_0}}{e^{3i\theta_0}-1} |< p,B(\bar{q},\bar{q}) >|^2.$

$$C(q,q,\bar{q}) = \begin{pmatrix} \frac{(-6(q-r\bar{y})-4r^2(q-r\bar{y})+8r\bar{y})e^{i\theta_0}+(4\bar{y}-8r(q-r\bar{y})+6r^2\bar{y})e^{-i\theta_0}+(2\bar{y}-4r(q-r\bar{y}))e^{3i\theta_0}+(4r\bar{y}-2r^2(q-r\bar{y}))e^{-i\theta_0}}{(1+\bar{y}+r\bar{y})^3} \\ 0 \\ 0 \end{pmatrix}$$

$$< p,C(q,q,\bar{q}) >= \frac{1}{e^{3i\theta_0} + 2\frac{\bar{y}}{1+\bar{y}+r\bar{y}}}\Bigg(\frac{\Big(-6(q-r\bar{y})-4r^2(q-r\bar{y})+8r\bar{y}\Big)e^{i\theta_0}}{(1+\bar{y}+r\bar{y})^3} + \frac{\Big(4\bar{y}-8r(q-r\bar{y})+6r^2\bar{y}\Big)e^{-i\theta_0}+\Big(2\bar{y}-4r(q-r\bar{y})\Big)e^{3i\theta_0}+\Big(4r\bar{y}-2r^2(q-r\bar{y})\Big)e^{-i\theta_0}}{(1+\bar{y}+r\bar{y})^3}\Bigg).$$

The second term in g_{21} is $< p,B(q,(I-J)^{-1}B(q,\bar{q})) >$

$$(I-J)^{-1} = \begin{pmatrix} \frac{1+q+\bar{y}}{1+\bar{y}+r\bar{y}} & 0 & -\frac{\bar{y}}{1+\bar{y}+r\bar{y}} \\ -1 & 1 & 0 \\ 0 & -1 & 1 \end{pmatrix}^{-1} = \begin{pmatrix} \frac{1+\bar{y}+r\bar{y}}{q+1} & \frac{\bar{y}}{q+1} & \frac{\bar{y}}{q+1} \\ \frac{1+\bar{y}+r\bar{y}}{q+1} & \frac{1+q+\bar{y}}{q+1} & \frac{\bar{y}}{q+1} \\ \frac{1+\bar{y}+r\bar{y}}{q+1} & \frac{1+q+\bar{y}}{q+1} & \frac{1+q+\bar{y}}{q+1} \end{pmatrix}$$

$$(I-J)^{-1}B(q,\bar{q}) = \begin{pmatrix} \frac{1}{q+1}\Big(\frac{2(q-r\bar{y})-2r\bar{y}-2(qr-(r^2+1)\bar{y})\cos 2\theta_0}{1+\bar{y}+r\bar{y}}\Big) \\ \frac{1}{q+1}\Big(\frac{2(q-r\bar{y})-2r\bar{y}-2(qr-(r^2+1)\bar{y})\cos 2\theta_0}{1+\bar{y}+r\bar{y}}\Big) \\ \frac{1}{q+1}\Big(\frac{2(q-r\bar{y})-2r\bar{y}-2(qr-(r^2+1)\bar{y})\cos 2\theta_0}{1+\bar{y}+r\bar{y}}\Big) \end{pmatrix} = \begin{pmatrix} S \\ S \\ S \end{pmatrix}$$

$$B(q,(I-J)^{-1}B(q,\bar{q})) = \begin{pmatrix} \frac{2\Big(q-r\bar{y}\Big)Se^{i\theta}-2r\bar{y}Se^{-i\theta}+2\Big(qr-(r^2+1)\bar{y}\Big)S\cos 2\theta_0}{(1+\bar{y}+r\bar{y})^2} \\ 0 \\ 0 \end{pmatrix}$$

$$< p,B(q,(I-J)^{-1}B(q,\bar{q})) >= \frac{1}{e^{3i\theta_0} + 2\frac{\bar{y}}{1+\bar{y}+r\bar{y}}}\Bigg(\frac{2(q-r\bar{y})Se^{i\theta} - 2r\bar{y}Se^{-i\theta}}{(1+\bar{y}+r\bar{y})^2} + \frac{2\Big(qr-(r^2+1)\bar{y}\Big)S\cos 2\theta_0}{(1+\bar{y}+r\bar{y})^2}\Bigg)$$

$$(e^{2i\theta_0}I-J)^{-1} = \begin{pmatrix} e^{2i\theta_0}+\frac{q-r\bar{y}}{1+\bar{y}+r\bar{y}} & 0 & -\frac{\bar{y}}{1+\bar{y}+r\bar{y}} \\ -1 & e^{2i\theta_0} & 0 \\ 0 & -1 & e^{2i\theta_0} \end{pmatrix}^{-1}$$

$$= \frac{1}{D}\begin{pmatrix} e^{4i\theta_0} & \frac{\bar{y}}{1+\bar{y}+r\bar{y}} & \frac{\bar{y}}{1+\bar{y}+r\bar{y}}e^{2i\theta_0} \\ e^{2i\theta_0} & e^{4i\theta_0}+\frac{q-r\bar{y}}{1+\bar{y}+r\bar{y}}e^{2i\theta_0} & \frac{\bar{y}}{1+\bar{y}+r\bar{y}} \\ 1 & e^{2i\theta_0}+\frac{q-r\bar{y}}{1+\bar{y}+r\bar{y}} & e^{4i\theta_0}+\frac{q-r\bar{y}}{1+\bar{y}+r\bar{y}}e^{2i\theta_0} \end{pmatrix}$$

where D is the determinant of the matrix $(e^{2i\theta_0}I-J)$ such that $D = e^{4i\theta_0}(e^{2i\theta_0}+\frac{q-r\bar{y}}{1+\bar{y}+r\bar{y}}) - \frac{\bar{y}}{1+\bar{y}+r\bar{y}}$.

$$(e^{2i\theta_0}I-J)^{-1}B(q,q) = \begin{pmatrix} \frac{L}{D}e^{4i\theta_0} \\ \frac{L}{D}e^{2i\theta_0} \\ \frac{L}{D} \end{pmatrix}$$

where, $L = \frac{2\Big(q-r\bar{y}\Big)e^{2i\theta_0}-2r\bar{y}e^{-2i\theta_0}+2\Big(qr-(r^2+1)\bar{y}\Big)}{(1+\bar{y}+r\bar{y})^2}$.

$$B(\bar{q},(e^{2i\theta_0}I-J)^{-1}B(q,q) = \begin{pmatrix} \frac{L}{D}\Big(\frac{2(q-r\bar{y})e^{3i\theta_0}-2r\bar{y}e^{i\theta_0}+(qr-(r^2+1)\bar{y})(e^{5i\theta_0}+e^{-i\theta_0})}{(1+\bar{y}+r\bar{y})^2}\Big) \\ 0 \\ 0 \end{pmatrix}.$$

$$< p,B(\bar{q},(e^{2i\theta_0}I-J)^{-1}B(q,q)) >= \frac{L}{D}\Big(\frac{1}{e^{3i\theta_0}+2\frac{\bar{y}}{1+\bar{y}+r\bar{y}}}\Big)\Big(\frac{2(q-r\bar{y})e^{3i\theta_0}-2r\bar{y}e^{i\theta_0}+(qr-(r^2+1)\bar{y})(e^{5i\theta_0}+e^{-i\theta_0})}{(1+\bar{y}+r\bar{y})^2}\Big).$$

$a(p^*) = Re(\frac{e^{-i\theta_0}}{2} < p,c(q,q,\bar{q}) >) + Re(e^{-i\theta_0} < p,B(q,(I-J)^{-1}B(q,\bar{q})) >) + Re(\frac{e^{-i\theta_0}}{2} < p,B(\bar{q},(e^{2i\theta_0}I-J)^{-1}B(q,q))) >).$

Theorem 4.1. *If $a(p^*) < 0$ (respectively, > 0), then Neimark-Saker bifurcation of system (2.3) at $p = p^*$ is supercritical (respectively, subcritical) and there exists a unique invariant closed curve bifurcates from the positive fixed point $\bar{y}$ which is asymptotically stable (respectively, unstable).*

5. Numerical examples

In this section we give numerical examples which support our results in the previous sections.

Example 5.1. *Take*

$$y_{n+1} = \frac{p + 4y_{n-2}}{1 + y_n + 0.3y_{n-2}} \tag{5.1}$$

with the initial conditions $y_{-2} = y_{-1} = y_0 = 1$.

$$\bar{y} = \frac{3 + \sqrt{9 + 5.2p}}{2.6}.$$

Note that for $p < \frac{q}{1+r} = 3.0769$, the bifurcation point p^* is satisfy

$$\frac{1 + \frac{3+\sqrt{9+5.2p^*}}{2}}{4 + .7(\frac{3+\sqrt{9+5.2p^*}}{2.6})} = \frac{4 - .3(\frac{3+\sqrt{9+5.2p^*}}{2.6})}{1 + \frac{3+\sqrt{9+5.2p^*}}{2}}$$

$$(.25 + \frac{.21}{(2.6)^2})(3 + \sqrt{9+5.2p^*})^2 + (1 + \frac{1.2}{2.6} - \frac{2.8}{2.6})(3 + \sqrt{9+5.2p^*}) - 15 = 0$$

$$3 + \sqrt{9+5.2p^*} = \frac{-(1 + \frac{1.2}{2.6} - \frac{2.8}{2.6}) + \sqrt{(1 + \frac{1.2}{2.6} - \frac{2.8}{2.6})^2 + 4 \times 15 \times (0.25 + \frac{0.21}{(2.6)^2})}}{2(0.25 + \frac{0.21}{(2.6)^2})}$$

$$p^* = \frac{([\frac{-(1+\frac{1.2}{2.6}-\frac{2.8}{2.6}) + \sqrt{(1+\frac{1.2}{2.6}-\frac{2.8}{2.6})^2 + 4\times 15\times(0.25+\frac{0.21}{(2.6)^2})}}{2(0.25+\frac{0.21}{(2.6)^2})}] - 3)^2 - 9}{5.2}$$

$$p^* = 0.83564585$$

Now, we will check if Neimark-Sacker bifurcation conditions hold. By theorem (3.2), it is enough to check if

$$p^* > \frac{\left(2(1+r)\left(\frac{-(13r^2+16r-7) + \sqrt{(13r^2+16r-7)^2 + 4(6r-9)(9r^3+16r^2+7r)}}{2(9r^3+16r^2+7r)}\right) - (q-1)\right)^2 - (q-1)^2}{4(1+r)}.$$

Note that at $p = p^*$, $\bar{y} = 2.55889613$ and

$$\frac{1 + \bar{y} + r\bar{y}}{q - r\bar{y} + \bar{y}} = \frac{1 + .3 \times 2.55889613 + 2.55889613}{4 - .3 \times 2.55889613 + 2.55889613} = .74708948,$$

and

$$\frac{\left(2(1+r)\left(\frac{-(13r^2+16r-7) + \sqrt{(13r^2+16r-7)^2 + 4(6r-9)(9r^3+16r^2+7r)}}{2(9r^3+16r^2+7r)}\right) - (q-1)\right)^2 - (q-1)^2}{4(1+r)}$$

$$= \frac{\left(2(1.3)(\frac{-(-13(0.3)^2+16\times 0.3-7) + \sqrt{(13(0.3)^2 16\times 0.3-7)^2 + 4(6\times 0.3-9)(9(0.3)^3+16(0.3)^2+7\times 0.3)}}{2(9(0.3)^3+16(0.3)^2+7\times 0.3)}) - 3\right)^2 - (3)^2}{4(1.3)}$$

$$= -1.1334411 < 0.83564585 = p^*.$$

So the condition of Theorem 3.2 is satisfied. That implies equation (5.1) undergoes a Neimark-Sacker bifurcation at $p = p^* = 0.83564585$. The bifurcation diagram of equation (5.1) is shown in Figure 5.1. Figure 5.1 shows that the positive fixed point $\bar{y}$ is asymptotically stable for $p > p^*$ and change its stability at Neimark-Sacker bifurcation value p^* and an invariant simple closed curve appears on the plane $(x(n), x(n-2))$ for $p < p^*$. Figure 5.2 and Figure 5.3 shows the phase portraits associated with Figure 5.2 for $p = p^*$ and $p = 0.95$, respectively.

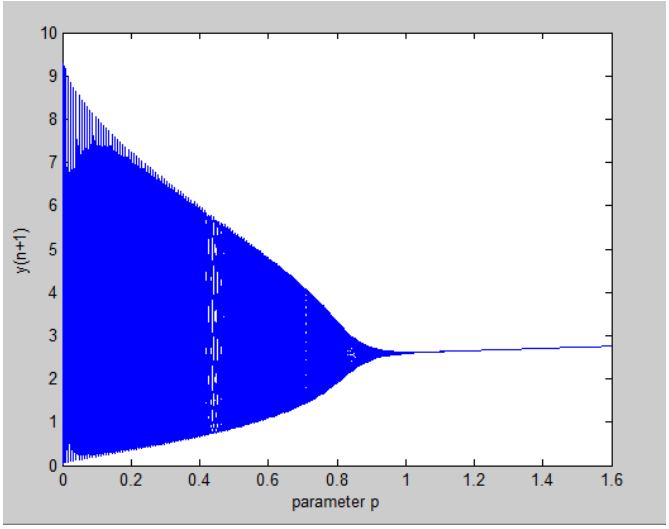

Figure 5.1: Neimark-Sacker bifurcation of the map $y_{n+1} = \frac{p+4y_{n-2}}{1+y_n+0.3yn-2}$, p is a parameter.

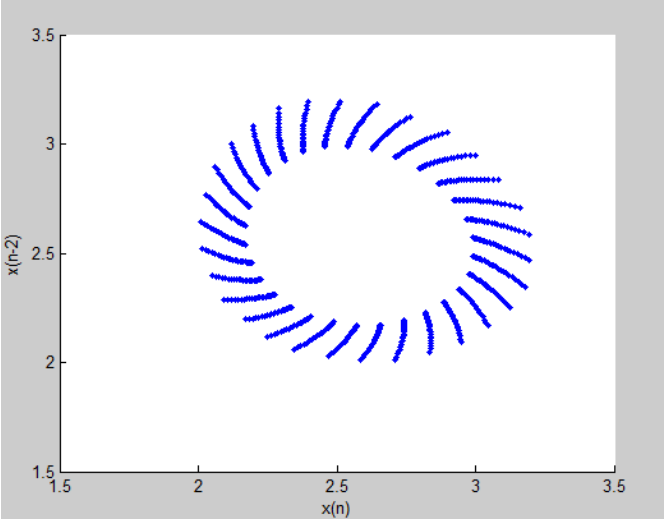

Figure 5.2: Phase portraits of the map $y_{n+1} = \frac{p+4y_{n-2}}{1+y_n+0.3yn-2}$ for $p = p^*$.

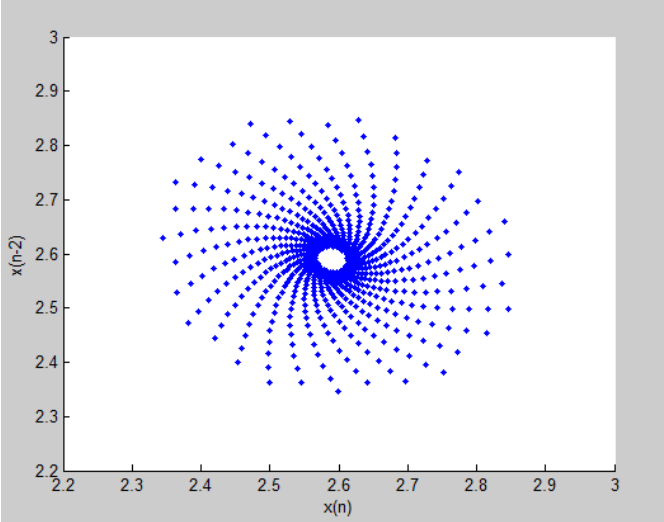

Figure 5.3: Phase portraits of the map $y_{n+1} = \frac{p+4y_{n-2}}{1+y_n+0.3yn-2}$ for $p = 0.95$.

References

[1] G.-M. Tang, L.-X. Hu, G. Ma, *Global Stability of a Rational Difference Equation*, Discrete Dynamics in Nature and Society, Volume 2010.

[2] E. Camouzis, G. Ladas, *Dynamics of Third-Order Rational Difference Equations With Open Problems And Conjectures*, Chapman. Hall/CRC, Boca Raton, 2008.

[3] M. Saleh, N. Alkoumi, A. Farhat, *On the dynamics of a rational difference equation* $x_{n+1} = \frac{\alpha+\beta x_n+\gamma x_{n-k}}{Bx_n+Cx_{n-k}}$, Chaos Soliton, (2017), 76-84.

[4] M. Saleh, A. Farhat, *Global asymptotic stability of the higher order equation* $x_{n+1} = \frac{ax_n+bx_{n-k}}{A+Bx_{n-k}}$, J. Appl. Math. Comput, (2017), 135-148, doi: 10.1007/s12190-016-1029-4.

[5] M. Saleh, A.Asad, *Dynamics of kth order rational difference equation*, J. Appl. Nonlinear Dyn., (2021), 125-149, doi: 10.5890/JAND.2021.03.008.

[6] M. Saleh, S.Hirzallah, *Dynamics and bifurcation of a second order rational difference equation with quadratic terms*, J. Appl. Nonlinear Dyn., (to appear).

[7] M. Saleh, S.Hirzallah, *Dynamics and bifurcation of a second order quadratic rational difference equation*, J. Math. Sci. Model., **3**(3) (2020), 102-119.

[8] S. Elaydi, *An Introduction to Difference Equations,* 3rd Edition, Springer, 2000.

[9] A. Y. Kuznetsov, *Elements of Applied Bifurcation Theory*, 2nd Ed., Springer-Verlag, 1998.

Journal of Mathematical Sciences and Modelling, 4 (1) (2021) 38-50
Research Article

Journal of Mathematical Sciences and Modelling

Journal Homepage: www.dergipark.gov.tr/jmsm
ISSN 2636-8692
DOI: http://dx.doi.org/10.33187/jmsm.885876

Transmission of Time and Position Variable Cryptology in Fibonacci and Lucas Number Series with Music

Cemil Karaçam[1*], Firdevs Nur Algül[1] and Daniel Tavit[1]

[1] *Beşiktaş Bilim ve Sanat Merkezi, Beşiktaş, İstanbul, Turkey*
[*] *Corresponding author*

Article Info

Keywords: *ASCII Code, Cryptology, Fibonacci Numbers, Lucas Numbers, Music.*
2010 AMS: *00A65, 11B39, 94A60, 97M80.*
Received: *24 February 2021*
Accepted: *28 April 2021*
Available online: *30 April 2021*

Abstract

Since people existed, they have prioritized confidentiality in information sharing and communication. Although there are independent studies on encryption and music in literature, no study is seen on encryption methods that are created by using the properties of mathematical number strings and can be expressed with musical instruments. The purpose in this research is to develop ideas for an effective encryption method and to create a time and location variable encryption method considering this deficiency in the literature by getting advantage of the additive feature in Fibonacci and Lucas number sequences and moving from here to develop new perspectives on encryption science. In the research letters in alphabet, numbers and 10 of the most used symbols were selected and ASCII codes were determined. The objects to be encrypted are divided into 6 main groups (uppercase vowel, uppercase consonant, lowercase vowel, lowercase consonant letters, numbers, and symbols). ASCII codes are written with the additive property of the Fibonacci and Lucas numbers (Zeckendorf's Theorem) and matched with the corresponding notes. In addition to the first method in the study, the encryption system is encrypted by shifting depending on time. In addition to this method, the encryption system was encrypted by shifting depending on the location. In the last method, the text to be encrypted was encrypted by shifting depending on both location and time. The software of the first stage of the encryption system has been created. The encryption method we have created can be transmitted in both audio and text. Since encryption can be applied with various instruments, it offers variety in terms of data privacy. In the encryption system, people who have a musical ear can audibly decipher the password regardless of the written source. In the research, the same text differs as time and location change. This method allows multiple transformations of a character in a text. With these features, it differs from the encryption methods made until now.

1. Introduction

People have given importance to confidentiality in their communication since the moment they existed and they have constantly developed new methods in this field. Encoding and encrypting information is a method developed thousands of years ago by empires and states to prevent the information they wanted to be kept secret from falling into the hands of the enemy [1]. These times, when much more primitive encryption methods were used and we have come a long way with the introduction of mechanics and technology into our lives.
Encryption (cryptology), which is one of the sub-branches of mathematics is the science of coding (cryptography), as well as code analysis (cryptanalysis). While code science refers to the creation part of the encryption, code analysis refers to the decryption of the generated code. Its encryption is expressed in the TDK (Turkish Dictionary) as secret texts, encrypted documents science, or analysis. Encryption is the process of making the content of plain text unreadable [1]. Cryptology is mathematics like number theory, that is, it is the application of formulas and algorithms that form the basis of cryptography and encryption analysis [2]. The number of information added to the literature is increasing day by day as a result of increasing discoveries and inventions. Protecting this information is getting more difficult. One of the important methods of protecting information is encryption. The importance of cryptography has increased with the transfer of private,

***Email address and ORCID number*: cemil-karacam@hotmail.com, 0000-0001-7186-5114 (C. Karaçam), firdevs_nur_algul@hotmail.com, 0000-0002-3027-7946 (F. N. Algül), danieltavit1@gmail.com, 0000-0003-4089-8508 (D. Tavit)**

commercial, political, and military data of critical privacy in electronic environments [3]. Many different encryption methods have been used from the past to the present. According to the information obtained, the first cryptologist (code scientist) is an Egyptian scribe who lived in BC. 1900s. He created the inscriptions he wrote by encrypted hieroglyphs and used some hieroglyphs that were never used before [1]. One of the first encryption methods that emerged in history was Caesar encryption. In Caesar encryption, instead of every letter seen in the Roman alphabet, the text is encrypted by writing the letter after the corresponding letter in the alphabet. The Enigma machine invented by German scientist Scherbius and Jefferson disks used by the US army can be shown as examples of encryption methods used throughout history.
Music has come to these days by continuously developing since its emergence. Music has a great place and importance in our lives, we are continuously listening to music at home, at school, on trips, and when we go out for walking. The relationship between mathematics and music dates back to the sixth century BC by the ancient Greek philosopher Pythagoras (570-495 BC) [4]. It is known that the mathematical scientist Pythagoras was also very interested in music and found octave and even thin-thick sounds by dividing a wire in the middle. It is seen that they progress in parallel with each other during their development [5]. Other people interested in music and mathematics are J. S. Bach and W. A. Mozart can be shown as examples. It is known that both famous composers have high mathematical intelligence and especially Bach's biggest hobby is mathematics [5]. When the education programs in the middle ages are examined, it is seen that music, mathematics, and astronomy are in the same group.
Art and aesthetics have always been an integral part of mathematics. Many musical instrument producers carry the sound graphics of their instruments to graphics suitable for instruments. Electronic music records are also closely related to graphics. It is essential that mathematicians and musicians collaborate when producing even a piece of music [6].
Studies on music, which can be taught from an early age, emphasize that rhythm studies are associated with mathematics, music experiences are very important in spatial relations and shape comprehension, and that music is based on mathematical thinking and mathematical relations [7]. The Fibonacci number sequence, is the number sequence that first appeared with the "Rabbit Problem", which was discussed in the book "Liber Abaci" published in 1202 by Leonardo of Pisa, known as Fibonacci [8]. The number sequence continues as 1, 1, 2, 3, 5, 8, 13, 21, 34, 55, 89, 144, 233,.... Each number is the sum of the two numbers preceding it. A similar number sequence is the Lucas number sequence created by French mathematician Edward Lucas. Unlike the Fibonacci number sequence, the Lucas number sequence was continued by starting with the numbers 2 and 1. Lucas number sequence continues as 2, 1, 3, 4, 7, 11, 18, 29, 47, ... [9]. Gül Karadeniz has proved in her research [10] that positive and negative integers can be expressed by Fibonacci numbers and used the Zeckendorf Theorem in her proof.

Theorem 1.1 (The Zeckendorf Theorem[10])**.** *Each N positive integer can be shown as the sum of different positive index Fibonacci numbers. This representation is one way definite. It can be clearly expressed as:*

$$k_{i+1} \quad \leq k_i - 2 \quad (i = 1,2,\ldots,r-1)$$

$$k_i \geq 2$$

It is a theorem that states that each positive integer N can be written as

$$N = F_{k_1} + F_{k_2} + \cdots + F_{k_r}$$

Proof. The proof is clear if the integer N is itself a Fibonacci number. Assume that the theorem is true for all integers less than or equal to F_n and $F_{n+1} > N > F_{n:}$.

$$N = F_n + (N - F_n); N - F_n < F_n$$

Thus, it is proven that every positive integer can be represented as the sum of positive Fibonacci numbers [10]. It becomes and from our assumption, it is seen that $N - F_n$ can be defined as to comply with the terms of Table 1. □

There are many studies in the literature on the science of encryption and music. It is possible to collect these studies under the following titles:

- Cryptology techniques and usage areas,
- Concepts used and necessary information in cryptology,
- Encryption systems,
- Relationships between mathematics and encryption,
- The relationship between musical education and mathematical thinking,
- The effect of music on people and their development,
- The relationship between mathematics and music,
- Fibonacci and Lucas numbers.

Çağla Özyılmaz [1] has mentioned the history of cryptology, related basic concepts, and done symmetric encryption applications in her master thesis. In the following parts of the thesis, she talked about Fibonacci numbers and mentioned the codes of various number strings. Zainab Hashim Obaıd [3], on the other hand, gave information about the basic concepts and gave information about the structure of various algorithms, and made an application and performance analysis on the text and images of different sizes and compared the results in his research. Musa Aghayev [2] talked about basic encryption methods and made determinations about their weaknesses and strengths by performing performance analyzes of encryption methods. Shahin Nasıbov [11] made suggestions to increase the security of the RSA encryption system against the Fermat Factorization Method and presented many methods based on this method in his master thesis. Cihan Orhan [6] spoke about the relationship between mathematics and music and their need for each other in his article. He stated that mathematics and music are intertwined and their developments affect each other. Ayperi Dikici [7] investigated the effect of music education on mathematics ability. In his book 'A Geometry of Music: Harmony and Counterpoint' in the Extended Common Practice [12] written by Dmitri Tymoczko, he emphasized the relationship between geometry and music and explained many musical expressions. While Ayten Esi [5] observed the link between mathematics and music in her research, she tried to explain with various examples that one is an integral part

	2	3	4	5	6	7	8	9	10		2	3	4	5	6	7	8	9	10
1	1									**29**					1		1		
2		1								**30**	1				1		1		
3			1							**31**		1			1		1		
4	1		1							**32**			1		1		1		
5				1						**33**	1		1		1		1		
6	1			1						**34**								1	
7		1		1						**35**	1							1	
8					1					**36**		1						1	
9	1				1					**37**			1					1	
10		1			1					**38**			1					1	
11			1		1					**39**				1				1	
12	1		1		1					**40**				1				1	
13						1				**41**				1				1	
14	1					1				**42**					1			1	
15		1				1				**43**					1			1	
16			1			1				**44**					1			1	
17	1		1			1				**45**			1		1			1	
18				1		1				**46**	1		1		1			1	
19	1			1		1				**47**						1		1	
20		1		1		1				**48**	1					1		1	
21							1			**49**		1				1		1	
22	1						1			**50**			1			1		1	
23		1					1			**51**	1		1			1		1	
24			1				1			**52**				1		1		1	
25	1		1				1			**53**	1			1		1		1	
26				1			1			**54**		1		1		1		1	
27	1			1			1			**55**									1
28		1		1			1												

Table 1: Zeckendorf Representation of Positive Integers with Fibonacci Numbers

of the other and emphasized that mathematics is intertwined with music. As a result, she emphasizes the interweaving of science and art, as it was noticed in Ancient Greece, by taking the relationship of mathematics and music as an example. Uzay Bora [13] in his article on "A Basic Point Where Science and Art Cross: The Relationship Between Mathematics and Music", examines the relationship between musical elements and mathematics. The article includes mathematical explanations of various concepts such as pitch, timbre, intervals, Pythagorean coma, equal regular system, and examples suitable for thematic transformations and harmonic distance calculations. Eric Riedel's [14] research is a study conducted to compare musical education and mathematics on 6th-grade students of a school in Atlanta. As a result of the study, it was determined that students who received music education had higher mathematics application grades than students who did not. Gülay Göğüş [15] investigated the effect of music education on mathematics lesson scores in her study and states that music education has a positive effect on mathematics lessons. Kaya [16] mentioned the importance of scientific methods in his/her study and investigated the interactions of arithmetic and music in ancient times. Selen Beytekin [17] explained the fundamentals of music and fracture geometry and explained the interactions of jazz music and geometry to explain jazz and its theoretical foundations. Ufuk Bıçak [18] focused on explaining the harmony theory based on the relationship between music and mathematics in his/her master's thesis. Firstly, he/she examined Pythagoras' works in the field of music, and then explained the New Harmony theory and the applications of the theory. İlhami Kaya [19] conducted various studies on the instrument named monochord designed by Pythagoras, and also included the following expressions for the relationship between music and mathematics in the past: "Before history, musical sounds were expressed in numbers and proportions rather than notes.". Gareth Roberts [20] mentioned the relationship between music and mathematics disciplines in his published book. Book; covers topics such as simple proportions and the Pythagorean theory of musical scales and harmonic consonant and harmony series, musical symmetries, and group theory. Sümeyye Bakım [4] first mentioned mathematics as the basis of music. She explained mathematical expressions corresponding to some musical concepts, examined the relationship between mathematics and music. The studies conducted on the use of the Fibonacci Sequence and the Golden Ratio in instrument making and whether some polyphonic music composers take this ratio into account during the process of composing their works have been examined and their accuracy has been discussed. Cennet Bolat [9] used the Binet formula and matrix algebra, which generalized some properties of k-Fibonacci and k-Lucas numbers and are a generalization of Fibonacci and Lucas numbers. Gökhan Kuzuoğlu [8] stated the characteristics of Fibonacci and Lucas number sequences in his thesis. In the 'Fabulous Fibonacci Numbers' written by Alfred S. Posamentier and Ingmar Lehmann [21], the history of the Fibonacci number sequence, where it is used, its interactions with various disciplines, and the properties of the Fibonacci-Lucas number sequences are mentioned in detail. Gül Karadeniz [10] prepared a thesis on Fibonacci and Pell numbers and Zeckendorf proof. In her thesis, she determined that all numbers (positive and negative indexes) can be expressed with Fibonacci numbers and created an algorithm on this subject.

Although there are studies in the literature that have dealt with the science of encryption from various aspects with various methods, there is no study on the time-variant encryption method using the additive property in Fibonacci and Lucas number sequences.

1.1. Purpose of the research

Although there are independent researches on the science of encryption, there is no study in the literature on encryption methods that are created using the properties of mathematical number strings that can be expressed with musical instruments. The purpose of this research is to create a time and location variable encryption method by taking advantage of the additive feature of the Fibonacci and Lucas number sequences, considering this deficiency in the literature, and to develop ideas for an effective encryption method by creating new perspectives on the science of encryption.

Hypothesis: Fibonacci and Lucas number-based and mathematics related to music

1. Encryption algorithm,
2. Time data based on the encryption algorithm,
3. Encryption algorithm based on location information,
4. Can a double-layer encryption algorithm be created based on time and location information?

2. Method

In the research mainly, literature review, content analysis, and field scanning method were used. In the first stage of the research, 10 of the most used letters, numbers, and symbols in the alphabet were selected and ASCII codes were determined. ASCII codes are written with the additive property of the Fibonacci numbers in the largest and shortest form that can be written and matched with the corresponding notes. In overlapping encodings, the last Fibonacci number is split once again.

1	2	3	4	5	6	7	8
C	D	E	F	G	A	B	C

Table 2: Note Matches (C major tone sequence example)

1	2	3	4	5	6	7	8
G	A	B	C	D	E	F	G

Table 3: Note Matches (G major tone sequence example)

1	2	3	4	5	6	7	8
D	E	F	G	A	B	C	D

Table 4: Note Matches (D major tone sequence example)

1	2	3	4	5	6	7	8
B	C	D	E	F	G	A	B

Table 5: Note Matches (B major tone sequence example)

The numbers in the expansions written with Fibonacci numbers are matched to the relevant note of the number remaining from the division of 7 (mod7) as in Table 2.

Groups	*Number Sequences Used*	*Music Tone Used*
Uppercase Vowels	Fibonacci Number Sequence	C Major
Uppercase Consonants	Fibonacci Number Sequence	C Major
Lowercase Vowels	Fibonacci Number Sequence	G Major
Lowercase Consonants	Fibonacci Number Sequence	G Major
Numbers	Lucas Number Sequence	D Major
Symbols	Fibonacci and Lucas Number Sequences	B Major

Table 6: Number Sequences and Tones Used

We created our method by giving ASCII code for letters in the Turkish alphabet but not existing in the English alphabet. We matched the codes in uppercase letters as İ-91, Ş-92, Ü-93, Ç-94, Ğ-95 and lower case letters as ı-123, ö-124, ü-125, ç-126, ğ-126, ş-128.

2.1. Encryption of letters

We divided the letters in our alphabet into 4 parts. These are:

Code	*Letter*	*Code*	*Letter*
065	A	066	B
067	C	068	D
069	E	070	F
071	G	072	H
073	I	074	J
075	K	076	L
078	N	077	M
080	P	079	O
082	R	081	Q
084	T	083	S
086	V	085	U
088	X	087	W
090	Z	089	Y

Table 7: ASCII Codes – Uppercase Letter (Gökhan, 2013)

Code	*Letter*	*Code*	*Letter*
097	A	098	b
099	C	100	d
101	E	102	f
103	G	104	h
105	I	106	J
107	K	108	l
109	M	110	n
111	O	112	p
113	Q	114	r
115	S	116	t
117	U	118	v
119	W	120	x
121	Y	122	z

Table 8: ASCII Codes - Lowercase Letter [22]

A	55+8+2	A C D
E	55+13+1	A A C
I	55+13+5	A A G
İ	(55+34+2) 55+21+13+2	A B A D
O	55+21+3	A B E
Ö	55+34+3	A A E
U	55+21+8+1	A B C C
Ü	55+34+3+1	A A E C

Table 9: Encryption of Uppercase Vowels

2.1.1. Uppercase letters

As seen in Table 9, the eight uppercase vowel letters in our alphabet are encoded with Fibonacci numbers and matched with notes given to the numbers in the sequence. Only the number 34 was opened as 21 + 13 as a result of the overlapping in the letter İ.
For example, let's encrypt the letter E. The ASCII code of the letter E is 69. It opens in Fibonacci numbers with a total of 69 and the number is expressed as 55 + 13 + 1. These numbers are converted into notes by matching the remaining digits after dividing from the 7th parts (mod7) with the strings of notes.

$$55 \equiv 6 \pmod 7 \quad 13 \equiv 6 \pmod 7 \quad 1 \equiv 1 \pmod 7$$

Since the sequence of C major is used in the encoding of the uppercase vowels, the rest are matched with the appropriate notes as in Table 2.

$$6 \equiv A \quad 6 \equiv A \quad 1 \equiv C$$

2.1.2. Uppercase consonants

As seen in Table 13, 22 uppercase consonants are encrypted. Only because of the inner conflicts in the letters T, Y and Z, 8 for the letter T is defined and the number 34 in the letters Y and Z were once again opened.
Let's encrypt the letter S for example. ASCII code of the letter S is 83. The number 83 is expressed in its shortest form with Fibonacci numbers. The expansion is $55+21+5+2$. These numbers are converted into notes by matching with the remaining numbers from the division of 7th parts (mod7) and so matched with the strings of notes.

B	55+8+3	A C E
C	55+8+3+1	A C E C
Ç	55+34+5	A A G
D	55+13	A A
F	55+13+2	A A D
G	55+13+3	A A E
Ğ	55+34+5+1	A A G C
H	55+13+3+1	A A E C
J	55+13+5+1	A A G C
K	55+13+5+2	A A G D
L	55+21	A B
M	55+21+1	A B C
N	55+21+2	A B D
P	55+21+3+1	A B E C
Q	55+21+5	A B G
R	55+21+5+1	A B G C
S	55+21+5+2	A B G D
Ş	55+34+5+2	A G D
T	(55+21+8) 55+21+5+3	A B G E
V	55+21+8+2	A B C D
W	55+21+8+3	A B C E
X	55+21+8+3+1	A B C E C
Y	(55+34) 55+21+13	A B A
Z	(55+34+1) 55+21+13+1	A B A C

Table 10: Encryption of Uppercase Consonants

$$55 \equiv 6 \pmod 7 \quad 21 \equiv 0 \pmod 7 \quad 5 \equiv 5 \pmod 7 \quad 2 \equiv 2 \pmod 7$$

Since the sequence of C major is used in the encoding of the uppercase vowels, the rest are matched with the appropriate notes as in Table 2.

$$6 \equiv A \quad 0 \equiv B \quad 5 \equiv G \quad 2 \equiv D$$

2.1.3. Lowercase vowels

a	89+8	D G
e	89+8+3+1	D G B G
ı	(89+34) 89+21+13	D F E
i	89+13+3	D E B
o	89+21+1	D F G
ö	(89+34+1) 89+21+13+1	D F E G
u	89+21+5+2	D F D A
ü	(89+34+2) 89+21+13+2	D F E A

Table 11: Encryption of Lowercase Vowels

As can be seen in Table 11, 8 lowercase consonants in the alphabet are encrypted. Due to the overlaps in the letters ı, ö, and ü, the number 34 has been opened as $21+13$.
For example, let's encrypt the letter i. The ASCII code of letter i is 105. The number 105 is expressed in shortest form with Fibonacci numbers. The expansion will be as $89+13+3$. These numbers are converted into notes by matching the remaining numbers from the 7th parts (mod7) with the strings of notes.

$$89 \equiv 5 \pmod 7 \quad 13 \equiv 6 \pmod 7 \quad 3 \equiv 3 \pmod 7$$

Since G major is used in the encoding of small vowels, the rest are matched with the appropriate notes as in Table 3.

$$5 \equiv D \quad 6 \equiv E \quad 3 \equiv B$$

2.1.4. Lowercase consonants

As seen in Table 15, 22 small consonants are encrypted. The numbers 34 and 8 are opened once again due to the overlap in the letters ğ and y. For example, let's encrypt the letter k. The ASCII code of the letter k is 107. The number 107 is expressed as shortest in Fibonacci numbers. Expansion will be $89+13+5$ and every number is matched with the notes. These numbers are converted into notes by matching the remaining numbers from the 7th parts (mod7) with the strings of notes.

b	89+8+1	D G G
c	89+8+2	D G A
ç	89+34+3	D E B
d	89+8+3	D G B
f	89+13	D E
g	89+13+1	D E G
ğ	(89+34+3+1) 89+21+13+3+1	D F E B G
h	89+13+2	D E A
j	89+13+3+1	D E B G
k	89+13+5	D E D
l	89+13+5+1	D E D G
m	89+13+5+2	D E D A
n	89+21	D FA
p	89+21+2	D F A
q	89+21+3	D F B
r	89+21+3+1	D F B G
s	89+21+5	D F D
ş	89+34+5	D E D
t	89+21+5+1	D F D G
v	(89+21+8) 89+21+5+3	D F D B
w	89+21+8+1	D F G G
x	89+21+8+2	D F G A
y	89+21+8+3	D F G B
z	89+21+8+3+1	D F G B G

Table 12: Encryption of Lowercase Consonants

$$89 \equiv 5 \pmod 7 \quad 13 \equiv 6 \pmod 7 \quad 5 \equiv 5 \pmod 7$$

Since G major is used in the encoding of small consonants, the rest are matched with the appropriate notes as in Table 3.

$$5 \equiv D \quad 6 \equiv E$$

2.2. Encryption of symbols and numbers

	Simge1	**S2**	**S3**	**S4**	**S5**	**S6**	**S7**	**S8**	**S9**	**S10**
Fibonacci	1	1	2	3	5	8	13	21	34	55
Lucas	2	1	3	4	7	11	18	29	47	76

Table 13: Encryption of Lowercase Consonants

As seen in Table 13, each symbol is expressed as the sum of the relevant Fibonacci and Lucas numbers, respectively.

(simge 1) .	1+2	B C
(simge 2) ,	1+1	B B
(simge 3) ?	2+3	C D
(simge 4) !	3+4	D E
(simge 5) -	5+7	F A
(simge 6) +	8+11	B E
(simge 7) :	13+8	G B
(simge 8) “ ”	21+29	A B A B
(simge 9) ( )	34+47	G F
(simge 10) @	55+76	G G

Table 14: Encryption of Symbols

In Table 14, the 10 most used symbols and their corresponding notes are determined. The symbol “ ” is inverted because it coincides with the number 6. Fibonacci and Lucas numbers are used in the encryption of symbols.
The “ ” (quotation mark) symbol matches the same notes as the letter L, so encrypted as repeating the same notes.
For example, let’s encrypt the () symbol. The Fibonacci and Lucas numbers to which this symbol (S9) is paired are 34 and 47, respectively. These numbers are divided into 7 with the method mentioned before and the rest are encrypted by matching the notes.
The difficulty is faced in using the Fibonacci sequence of numbers when encrypting numbers. Therefore, the Lucas number sequence is used when encrypting the numbers. 10 digits are encrypted as seen in Table 14. The Lucas numbers to which the numbers are matched are

0	1+1	D D
1	1	D
2	2+1	E D
3	3+1	F D
4	5+2	A E
5	8+3	D F
6	13+5	B A
7	21+8	C D
8	34+13	B B B B
9	55+21	B C

Table 15: Encryption of Numbers

expressed in the shortest form using the additive expressibility feature of the Fibonacci numbers, these additive expressions are converted to notes over mode 7.
Since the number 8 and the symbol,(comma) correspond to the same notes as 8, B notes are repeated.
For example, let's encrypt the number 9. This number matches Lucas number 10, which is 76. The additive expression of this number with Fibonacci numbers is $55 + 21$. This additive expression is converted into notes over mode 7 and encrypted.

2.3. Music terms used and transitions in encoding

- Stacatto: Intermittent playing or singing
- Silencio: Waiting without playing or singing
- Vibrato: Musical effect consisting of regular change of pitch
- Tone: It is a concept that is based on a series of majors and minors.

When we start the sentence, we added a different feature to each section to understand which group the original note that the sequence belongs to.

- By doing staccato in numbers.
- Making vibrato on the violin in symbols,
- Playing normally in letters

We also used different wait times when switching between the two groups (e.g. symbols and numbers) to indicate which groups were switched between.
Between the same groups $\rightarrow$ 1-beat of silence,
Letter – Number $\rightarrow$ 2 beats of silence,
Number – Symbol $\rightarrow$ 3 beats of silence,
Letter – Symbol $\rightarrow$ 4 beats of silence are used.

2.4. Time, location, and time-location variable encryption

The time structure that we will use in encryption is divided into 6 main sections in accordance with our main structure as can be seen in Table 18.

Day	**Month**	**Year**	**Hour**	**Minute**	**Second**

Table 16: Time Structure Used

1. 6 different elements of our alphabet are matched with the components of time.
2. Components of time are determined.
3. The numerical equivalents of the units of time are divided by the mode value and the remainder are determined.
4. Units are shifted according to the remaining values.
5. For encryption, the remainder is negatively shifted.

The location structure that we will use in encryption is firstly divided into 2 parts as parallel and meridian, as seen in Table 8. After that, both are divided into their 3 components.

Parallel			**Meridian**		
Degree	**Minute**	**Second**	**Degree**	**Minute**	**Second**

Table 17: Used Location Structure

2.5. Application

1. For our research to be more understandable, let's explain the simplest application with an example.

   Example 2.1. *Let's turn the TüBitAK2020 word to notes.*

   T = A B G E (Table 10)
   ü = D F E A (Table 11)
   B = A C E (Table 10)
   i = A B A D (Table 11)
   t = D F D G (Table 12)
   A = A C D E (Table 9)
   K = A A G D (Table 10)
   2 = E D (Table 15)
   0 = D D (Table 15)
   2 = E D (Table 15)
   0 = D D (Table 15)
   . = B C (Table 14)

2. Time-Based Application
   (a) Time information is received.
   (b) The number written with 6-digit (1, 2, 3, 4, 5, 6) elements is taken.
   (c) The received number is matched with groups and time information.

   Let's match the 6 main elements of time with the 6 main structures that will create our text.

1st Group	
1	UPP.VOWEL
2	UPP.CONSONANT
3	LOW.VOWEL
4	LOW.CONSONANT
5	NUMBER
6	SYMBOL

2nd Group	
1	DAY
2	MONTH
3	YEAR
4	HOUR
5	MINUTE
6	SECOND

Example 2.2. *Let's take the number 356124. Let our time be 09.01.2020 / 17.48.53.*

In this case:

Uppercase vowels $\leftrightarrow$ *Year*
Uppercase consonants $\leftrightarrow$ *Minute*
Lowercase vowels $\leftrightarrow$ *Second*
Lowercase consonants $\leftrightarrow$ *Day*
Number $\leftrightarrow$ *Month*
Symbol $\leftrightarrow$ *Hour*

As a result of this match, transactions are done and the remainder is calculated one by one, each group is shifted as much as the remainder, our text is then encrypted.

Day $\leftrightarrow$ $(\bmod 24)$
Month $\leftrightarrow$ $(\bmod 10)$
Year $\leftrightarrow$ (*mod8*)
Hour $\leftrightarrow$ $(\bmod 10)$
Minute $\leftrightarrow$ $(\bmod 24)$
Second $\leftrightarrow$ *(mod8)*

	Uppercase Vowel	Uppercase Consonant	Lowercase Vowel	Lowercase Consonant	Number	Symbol
MODE	8	24	8	24	10	10
MATCH	3	5	6	1	2	4
TIME	2020	48	53	09	01	17
REMAINDER/SHIFT	4	0	5	9	1	7

Table 18: Time Based Application (Shift Determination)

The shift is calculated by dividing the time values according to the relevant mode and taking the remainder.

Uppercase vowels : $2020 \equiv 4 (\bmod 8)$
Uppercase consonants : $48 \equiv 0 (\bmod 24)$
Lowercase vowels : $53 \equiv 5 (\bmod 8)$
Lowercase consonants : $09 \equiv 9 (\bmod 24)$
Number : $01 \equiv 1 (\bmod 10)$
Symbol : $17 \equiv 7 (\bmod 10)$

Example 2.3. *For example : The letter ü is 24 as seen in Table 8. When it matches, its value is 09. When the number 09 is divided into mod24, the remainder is 9. Therefore, the letter ü is shifted by 9 letters and becomes the letter o.*

T → *T* → *A B G E (Table 10)*
ü → *o* → *D F G (Table 11)*
B → *B* → *A C E (Table 10)*
i → *a* → *D G (Table 11)*
t → *t* → *D G B (Table 12)*
A → *O* → *A B E (Table 9)*
K → *K* → *A A G D (Table 10)*
2 → *3* → *F D (Table 15)*
0 → *1* → *D (Table 15)*
2 → *3* → *F D (Table 15)*
0 → *1* → *D (Table 15)*
. → *“”* → *A B A B (Table 14)*

Encryption can be done by repeating the same transactions in reverse.

3. Location-Based Application

(a) Location information is received.
(b) The number written with 6-digit (1, 2, 3, 4, 5, 6) elements is taken.
(c) The received number is matched with groups and location information.

Let’s match the 6 main elements of the position with the 6 main structures that will form our text.

1st Group	
1	UPP.VOWEL
2	UPP.CONSONANT
3	LOW.VOWEL
4	LOW.CONSONANT
5	NUMBER
6	SYMBOL

2nd Group	
1	Degree
2	Minute
3	Second
4	Degree
5	Minute
6	Second

Example 2.4. *Let’s take the number 654231 and let’s choose the location as* $49^\circ 3' 49'' North\ 29^\circ 0' 36'' East$.

Uppercase vowels ↔ *Second (East)*
Uppercase consonants ↔ *Minute (East)*
Lowercase vowels ↔ *Degree (East)*
Lowercase consonants ↔ *Minute (North)*
Number ↔ *Second (North)*
Symbol ↔ *Degree (North)*

As a result of this match, transactions are done and the remainder is calculated one by one, each group is shifted as much as the remainder, our text is then encrypted.

Degree ↔ *(mod10)*
Minute ↔ *(mod24)*
Second ↔ *(mod10)*
Degree ↔ *(mod8)*
Minute ↔ *(mod24)*
Seconds ↔ *(mod8)*

	Uppercase Vowel	Uppercase Consonant	Lowercase Vowel	Lowercase Consonant	Number
MODE	8	24	8	24	10
MATCH	6	5	4	2	3
TIME	36	0	29	3	49
REMAINDER/SHIFT	4	0	5	0	9

T → *T* → *A B G E (Table 10)*
ü → *o* → *D F G (Table 11)*
B → *B* → *A C E (Table 10)*
i → *a* → *D G (Table 11)*
t → *t* → *D F D G (Table 12)*
A → *O* → *A B E (Table 9)*
K → *K* → *A A G D (Table 10)*
2 → *1* → *D (Table 15)*
0 → *9* → *B C (Table 15)*
2 → *1* → *D (Table 15)*
0 → *9* → *B C (Table 15)*
. → *,* → *B B (Table 14)*

4. Location and Time-Based Application In the location and time-based application, encryption is performed firstly by location. This application will continue through the example depending on the location. The new text created as a result of the 3rd phase is XoBatAK1919. Time-dependent re-encryption is done through this text. Application3 + Application 2 = Application 4.
   (a) Time information is taken.
   (b) The number written with 6-digit (1, 2, 3, 4, 5, 6) elements is taken..
   (c) The number taken is matched with groups and time information.

   Let's match the 6 main elements of time with the 6 main structures that will create our text.

1st Group	
1	UPP.VOWEL
2	UPP.CONSONANT
3	LOW.VOWEL
4	LOW.CONSONANT
5	NUMBER
6	SYMBOL

2nd Group	
1	DAY
2	MONTH
3	YEAR
4	HOUR
5	MINUTE
6	SECOND

Example 2.5. *Let's take the number 312546. Let's our time be 09.01.2020/19.44.01.*
In this case:

Uppercase vowels ↔ *Year*
Uppercase consonants ↔ *Day*
Lowercase vowels ↔ *Month*
Lowercase consonants ↔ *Minute*
Number ↔ *Hour*
Symbol ↔ *Secinds*

As a result of this match, transactions are done and the remainder is calculated one by one, each group is shifted as much as the remainder, our text then becomes encrypted.

Day ↔ *(mod24)*
Month ↔ *(mod8)*
Year ↔ *(mod8)*
Time ↔ *(mod10)*
Month ↔ *(mod24)*
Seconds ↔ *(mod10)*

	Uppercase Vowel	Uppercase Consonant	Lowercase Vowel	Lowercase Consonant	Number	Symbol
MODE	8	24	8	24	10	10
MATCH	3	1	2	5	4	6
TIME	2020	09	01	44	19	01
REMAINDER/SHIFT	4	9	1	20	9	1

X → *C* → *A C E*
o → *o* → *D F E G*
B → *K* → *A A G D*
a → *e* → *D G B G*
t → *q* → *D F B*
O → *A* → *A C D*
K → *K* → *A B C D*
1 → 0 → *D D*
9 → 8 → *B B*
1 → 0 → *D D*
9 → 8 → *B B*
, → ? → *C D*

Our last encryption becomes: CöKeqAK0808?

3. Findings

Our encryption method can be expressed in 4 different ways:

1. Our first model is based on mathematics and music, expressing ASCII numbers with the additive property of Fibonacci and Lucas numbers and converting them into notes.
2. In addition to our first model, a time variable encryption program is created.
3. In addition to our first model, a location variable encryption program is created.
4. In addition to our first model, a time and location variable encryption program is created.

An algorithm containing English characters is created with the software of the first encryption method.

4. Conclusion and discussion

As a result of the literature review, it was realized that there was no encryption method made using the properties of mathematical number strings and musical instruments. In the study, 6 main titles are determined for letters, numbers, and symbols. Then ASCII codes of letters, numbers, and symbols are assigned. Being expressed by Fibonacci and Lucas number sequences, these codes are encoded with 4 different variables: time, location, and time-location. The codes were matched with the notes to be played with the violin. It is found that the hypothesis that is the basis of the research is feasible.

- Most of the encryption methods are made with a certain logic over a single main text. Our main text components are divided into 6 main groups and encryption diversity is created and a program that is difficult to encrypt is done. It has been determined that other encryption programs do not have lowercase-uppercase, vowel-consonant, number-symbol distinctions. In encryption, various transition methods have been determined to avoid confusion between the 6 main groups.
- 4 different one on the basis, encryption moves from easy to difficult:
    1. ASCII codes → Fibonacci and Lucas numbers → Note
    2. ASCII codes → Fibonacci and Lucas numbers → Time variable → Note
    3. ASCII codes → Fibonacci and Lucas numbers → Location variable → Note
    4. ASCII codes → Fibonacci and Lucas numbers → Time and Location variable → Note

Encryption systems have been established. It is seen that it differs from other encryption programs as the richness of application.

- The encryption system we have created can be transmitted both in audio and text. At the same time, it offers diversity in terms of data privacy as it can be applied with various instruments (piano-violin-viola-cello, etc.).
- The encryption method in the research is suitable for people who have musical knowledge. People having a good musical ear can audibly encrypt the password regardless of any written source. Due to these features, it differs from the encryption methods made so far. In addition, the data transfer can be transferred as solo and choral.
- The encryption method created is a difficult method to be encrypted because it contains many details between Fibonacci and Lucas number sequences, ASCII codes, and notes.
- The most common encryption method is the solution of objects through the possibilities of using them in a text according to languages. In this research, it is seen that the same object (2, 3, 4) applications create a richness of being transferred in different ways in different locations / times / locations and times.
- In other encryption methods, it has been determined that encrypting an object is one step. But in this study, the same text differs as time changes and location changes. This allows the same object to be encoded differently in a text.
- One of the disadvantages of our study is that communication between any two people who do not have sufficient musical knowledge is not healthy. Environmental conditions (noise, etc.) can affect the efficiency of the audio transmission.
- Since it is applied manually in terms of application, time and personal errors are possible, even if small. This disadvantage has been removed by transforming the method into a software program to create ease of application and speed.
- The encryption method being created is based on the Turkish alphabet.
- It can be done in accordance with other alphabets. The number of symbols used can be increased to increase the variety of applications.
- In the research, simple translation encryption is done based on the remaining. Application with the asymmetric encryption method can make it a very difficult system to be encrypted.
- Fibonacci and Lucas number sequences were used in the research. Different encryption methods can be developed by changing the number of strings used. If software that detects notes can be created, the program can also be used commercially (military-data security-banking, etc.). Encryption can be implemented in a music piece with the help of a melody, which is more difficult, complex, and secret to be decoded.

References

[1] Ç. Özyılmaz, *Introduction to Cryptology*, Master Thesis, Karabuk University, 2014.
[2] M. Aghayev, *On Cryptology and Data Encryption Techniques*, Master Thesis, Ege University, 2017.
[3] Z. H. Obaıd, *Comparison of Cryptology Methods*, Master Thesis, Erciyes University, 2016.
[4] S. Bakım, *Investigation of the Use of Fibonacci Sequence and Golden Ratio in Music*, Master Thesis, Selçuk University, 2014.
[5] A. Esi, *Mathematics and music*, J. Awareness, **2**(3S) (2017), 631–642.
[6] C. Orhan, *Matematik ve müzik*, Matematik Dünyası, **6**(1995), 6–7.
[7] A. Dikici, *Investigation of the Effect of Music Education Provided with Orff Technique on Mathematical Ability*, Ph.D. Thesis, Ankara University, 2002.
[8] G. Kuzuoğlu, *Divisibility Properties of Some Sequences Related to Fibonacci Numbers*, Master Thesis, Kocaeli University, 2019.

[9] C. Bolat, *Properties and Applications of K-Fibonacci, K-Lucas Numbers*, Master Thesis, Selcuk University, 2008.
[10] G.Karadeniz, *Zeckendorf Representation of Fibonacci and Pell Numbers and Integers*, Master Thesis, Gazi University, 2006.
[11] S. Nasıbov, *On Cryptology Systems and Applications*, Master Thesis, Ege University, 2015.
[12] D. Tymoczko, *A Geometry of Music: Harmony and Counterpoint in the Extended Common Practice*, Oxford University Press, New York, 2011.
[13] U. Bora, *A key point where science and art cross: Mathematics and music relationship*, J. Uludağ Univ. Fac. Educ., **15**(1) (2002), 53–68.
[14] E. Riedel, *The Relationship Between Music Instruction and Academic Achievement in Mathematics by Nechelle Nipper Sharpe*, Walden University, USA, 2013.
[15] G. Göğüş, *The relation between musical and mathematical learning success*, J. Uludağ Univ. Fac. Educ., **21**(1) (2008), 79-89.
[16] İ. Kaya, *Contributions of Pythagoras and Archytas to the Mathematical Music Theory*, Master Thesis, Mimar Sinan Fine Arts University, 2009.
[17] S. Beytekin, *Mathematical Analysis of Jazz on Piano and Analysis of Its Relationship with Fractal Geometry*, Master Thesis, 2015.
[18] U. Bıçak, *A New Harmony Theory With Solar Voyage For Orchestra In the Context of the Relationship Between Music and Mathematics*, Master Thesis, Mimar Sinan Fine Arts University, 2018.
[19] İ. Kaya, *The relation between monochord string splits and harmonics*, Electron. J. Soc. Sci., **16**(61) (2017), 636–646.
[20] G. E. Roberts, *From Music to Mathematics: Exploring the Connections*, Johns Hoplinks University Press, Baltimore, 2016.
[21] I. Lehmann, A. Posamentier, *The Fabulous Fibonacci Numbers*, Prometheus Books, New York, 2007.
[22] A. Gökhan, *ASCII Codes of Lowercase & Uppercase Letters*, Accessed Date: 12.10.2019, available at http://www.phpservisi.com/kucuk-buyuk-harflerin-ascii-kodlari/.